

BIOMEDICAL PHOTONICS

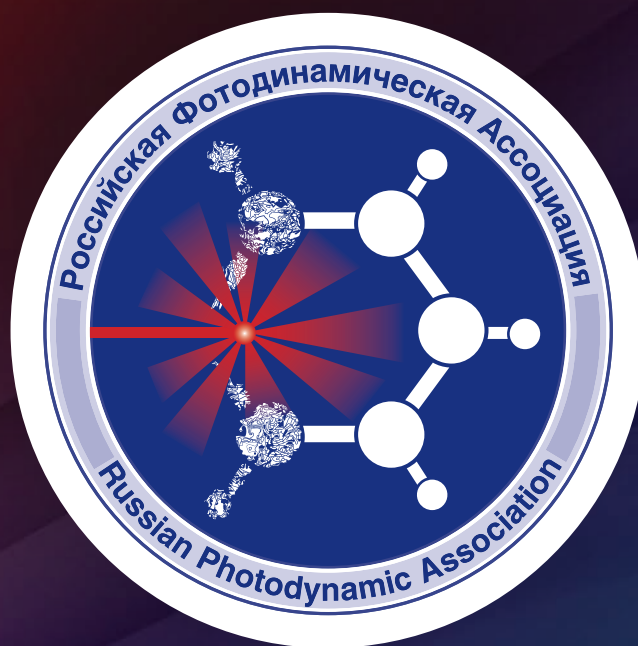
Volume 13, # 3, 2024

In the issue:

- Effect of photobiomodulation therapy with low level laser on gingival in post-curettage patients
- New cationic chlorin as potential agent for antimicrobial photodynamic therapy
- Results of microsurgical resection of glioblastomas under endoscopic and fluorescent control
- Morphological evaluation of the effectiveness of treating infected wounds with high-intensity pulsed broadband irradiation
- Photodynamic therapy in the prevention of HPV-induced recurrences of precancer and initial cancer of the cervix

BMP

Российская Фотодинамическая Ассоциация



www.pdt-association.com

BIOMEDICAL PHOTONICS

FOUNDERS:

Russian Photodynamic Association
P.A. Herzen Moscow Cancer Research Institute

EDITOR-IN-CHIEF:

Filonenko E.V., Dr. Sci. (Med.), professor, head of the Centre of laser and photodynamic diagnosis and therapy of tumors in P.A. Herzen Moscow Cancer Research Institute (Moscow, Russia)

DEPUTY CHIEF EDITOR:

Grin M.A., Dr. Sci. (Chem.), professor, chief of department of Chemistry and technology of biological active substances named after Preobragenskiy N.A. in Moscow Technological University (Moscow, Russia)

Loschenov V.B., Dr. Sci. (Phys and Math), professor, chief of laboratory of laser biospectroscopy in the Natural Sciences Center of General Physics Institute of the Russian Academy of Sciences (Moscow, Russia)

EDITORIAL BOARD:

Kaprin A.D., Academician of the Russian Academy of Sciences, Dr. Sci. (Med.), professor, general director of National Medical Research Radiological Centre of the Ministry of Health of the Russian Federation (Moscow, Russia)

Romanko Yu.S., Dr. Sci. (Med.), professor of the department of Oncology, radiotherapy and plastic surgery named after L.L. Lyovshina in I.M. Sechenov First Moscow State Medical University (Moscow, Russia)

Stranadko E.Ph., Dr. Sci. (Med.), professor, chief of department of laser oncology and photodynamic therapy of State Research and Clinical Center of Laser Medicine named by O.K. Skobelcin of FMBA of Russia (Moscow, Russia)

Blondel V., PhD, professor at University of Lorraine, joint-Head of the Health-Biology-Signal Department (SBS) (Nancy, France)

Bolotine L., PhD, professor of Research Center for Automatic Control of Nancy (Nancy, France)

Douplik A., PhD, professor in Ryerson University (Toronto, Canada)

Steiner R., PhD, professor, the honorary director of Institute of Laser Technologies in Medicine and Metrology at Ulm University (Ulm, Germany)

BIOMEDICAL PHOTONICS –

research and practice, peer-reviewed, multidisciplinary journal.

The journal is issued 4 times per year.

The circulation – 1000 copies., on a quarterly basis.

The journal is included into the List of peer-reviewed science press of the State Commission for Academic Degrees and Titles of Russian Federation
The journal is indexed in the international abstract and citation database – Scopus.

The publisher «Agentstvo MORE».
Moscow, Khokhlovskiy lane., 9

Editorial staff:

Chief of the editorial staff	Ivanova-Radkevich V.I.
Science editor professor	Mamontov A.S.
Literary editor	Moiseeva R.N.
Translators	Kalyagina N.A.
Computer design	Kreneva E.I.
Desktop publishing	Shalimova N.M.

The Address of Editorial Office:

Russia, Moscow, 2nd Botkinskiy proezd, 3
Tel. 8 (495) 945–86–60
www: PDT-journal.com
E-mail: PDT-journal@mail.ru

Corresponding to:

125284, Moscow, p/o box 13

Registration certificate ПИ № ФС 77–51995, issued on 29.11.2012 by the Federal Service for Supervision of Communications, Information Technology, and Mass Media of Russia

The subscription index

of «Rospechat» agency – 70249

The editorial staff is not responsible for the content of promotional material. Articles represent the authors' point of view, which may be not consistent with view of the journal's editorial board. Editorial Board admits for publication only the articles prepared in strict accordance with guidelines for authors. Whole or partial presentation of the material published in the Journal is acceptable only with written permission of the Editorial board.

BIOMEDICAL PHOTONICS

BIOMEDICAL PHOTONICS –

научно-практический, рецензируемый,
мультидисциплинарный журнал.
Выходит 4 раза в год.
Тираж – 1000 экз., ежеквартально.

Входит в Перечень ведущих рецензируемых
научных журналов ВАК РФ.
Индексируется в международной
реферативной базе данных Scopus.

Издательство «Агентство МОРЕ».
Москва, Хохловский пер., д. 9

Редакция:

Зав. редакцией	Иванова-Радкевич В.И.
Научный редактор	проф. Мамонтов А.С.
Литературный редактор	Моисеева Р.Н.
Переводчики	Калягина Н.А.
Компьютерный дизайн	Кренева Е.И.
Компьютерная верстка	Шалимова Н.М.

Адрес редакции:

Россия, Москва, 2-й Боткинский пр., д. 3
Тел. 8 (495) 945–86–60
www: PDT-journal.com
E-mail: PDT-journal@mail.ru

Адрес для корреспонденции:

125284, Москва, а/я 13

Свидетельство о регистрации ПИ
№ ФС 77–51995, выдано 29.11.2012 г.
Федеральной службой по надзору в сфере
связи, информационных технологий
и массовых коммуникаций (Роскомнадзор)

Индекс по каталогу агентства
«Роспечать» – 70249

Редакция не несет ответственности за содержа-
ние рекламных материалов.

В статьях представлена точка зрения авторов,
которая может не совпадать с мнением редак-
ции журнала.

К публикации принимаются только статьи, под-
готовленные в соответствии с правилами для
авторов, размещенными на сайте журнала.

Полное или частичное воспроизведение матери-
алов, опубликованных в журнале, допускается
только с письменного разрешения редакции.

УЧРЕДИТЕЛИ:

Российская Фотодинамическая Ассоциация
Московский научно-исследовательский онкологический институт
им. П.А. Герцена

ГЛАВНЫЙ РЕДАКТОР:

Филоненко Е.В., доктор медицинских наук, профессор, руководитель
Центра лазерной и фотодинамической диагностики и терапии опухолей
Московского научно-исследовательского онкологического института
им. П.А. Герцена (Москва, Россия)

ЗАМ. ГЛАВНОГО РЕДАКТОРА:

Грин М.А., доктор химических наук, профессор, заведующий
кафедрой химии и технологии биологически активных соединений
им. Н.А. Преображенского Московского технологического университета
(Москва, Россия)

Лощенов В.Б., доктор физико-математических наук, профессор,
заведующий лабораторией лазерной биоспектроскопии в Центре
естественно-научных исследований Института общей физики
им. А.М. Прохорова РАН (Москва, Россия)

РЕДАКЦИОННАЯ КОЛЛЕГИЯ:

Каприн А.Д., академик РАН, доктор медицинских наук, профессор,
генеральный директор Национального медицинского исследовательского
центра радиологии Минздрава России (Москва, Россия)

Романко Ю.С., доктор медицинских наук, профессор кафедры онкологии,
радиотерапии и пластической хирургии им. Л.Л. Лёвшина Первого Москов-
ского государственного медицинского университета имени И.М. Сеченова
(Москва, Россия)

Странадко Е.Ф., доктор медицинских наук, профессор, руководитель Отде-
ления лазерной онкологии и фотодинамической терапии ФГБУ «Государствен-
ный научный центр лазерной медицины им. О.К.Скобелкина ФМБА России»

Blondel V., профессор Университета Лотарингии, руководитель отделения
Здравоохранение-Биология-Сигналы (SBS) (Нанси, Франция)

Bolotine L., профессор научно-исследовательского центра автоматики
и управления Нанси (Нанси, Франция)

Douplik A., профессор Университета Райерсона (Торонто, Канада)

Steiner R., профессор, почетный директор Института лазерных технологий
в медицине и измерительной технике Университета Ульма (Ульм, Германия)

ORIGINAL ARTICLES

Effect of photobiomodulation therapy with low level laser on gingival in post-curettage patients

Wahyuningtya D.T., Astuti S.D., Widiyanti P., Setiawatie E.M., Guspiari K., Amir M.S., Arifianto D., Yaqubi A.K., Apsari A., Susilo Y., Syahrom A.

4

New cationic chlorin as potential agent for antimicrobial photodynamic therapy

Suvorov N.V., Shchelkova V.V., Rysanova E.V., Bagatelia Z.T., Diachenko D.A., Afaniutin A.P., Vasil'ev Yu.L., Diachkova E.Yu., Santana Santos I.C., Grin M.A.

14

Results of microsurgical resection of glioblastomas under endoscopic and fluorescent control

Rynda A.Yu., Olyushin V.E., Rostovtsev D.M., Zabrodskaya Yu.M., Papayan G.V.

20

Morphological evaluation of the effectiveness of treating infected wounds with high-intensity pulsed broadband irradiation

Egorov V.S., Filimonov A.Yu., Chudnykh S.M., Abduvosidov Kh.A., Chekmareva I.A., Paklina O.V., Baranchugova L.M., Kondrat'ev A.V.

31

Photodynamic therapy in the prevention of HPV-induced recurrences of precancer and initial cancer of the cervix

Trushina O.I., Filonenko E.V., Novikova E.G., Mukhtarulina S.V.

42

ОРИГИНАЛЬНЫЕ СТАТЬИ

Влияние фотобиомодуляционной терапии с использованием лазера (650 нм) на состояние десен после кюретажа

D.T. Wahyuningtya, S.D. Astuti, P. Widiyanti, E.M. Setiawatie, M.S. Amir, D. Arifianto, A.K. Yaqubi, A. Apsari, Y. Susilo, A. Syahrom

4

Новый катионный хлорин как потенциальный агент для антимикробной фотодинамической терапии

Н.В. Суворов, В.В. Щелкова, Е.В. Русанова, З.Т. Багателия, Д.А. Дьяченко, А.П. Афаниутин, Ю.Л. Васильев, Е.Ю. Дьячкова, И.К. Сантана Сантос, Грин М.А.

14

Результаты микрохирургической резекции глиобластом под эндоскопическим и флуоресцентным контролем

А.Ю. Рында, В.Е. Олюшин, Д.М. Ростовцев, Ю.М. Забродская, Г.В. Папаян

20

Морфологическая оценка эффективности лечения инфицированных ран высокоинтенсивным импульсным широкополосным облучением

В.С. Егоров, А.Ю. Филимонов, С.М. Чудных, Х.А. Абдувосидов, И.А. Чекмарева, О.В. Паклина, Л.М. Баранчугова, А.В. Кондратьев

31

Фотодинамическая терапия в профилактике ВПЧ-индуцированных рецидивов предрака и начального рака шейки матки

О.И. Трушина, Е.В. Филоненко, Е.Г. Новикова, С.В. Мухтарулина

42

EFFECT OF PHOTOBIMODULATION THERAPY WITH LOW LEVEL LASER ON GINGIVAL IN POST-CURETTAGE PATIENTS

Wahyuningtya D.T.¹, Astuti S.D.¹, Widiyanti P.¹, Setiawatie E.M.¹, Guspiari K.¹, Amir M.S.¹,
 Arifianto D.¹, Yaqubi A.K.¹, Apsari A.², Susilo Y.³, Syahrom A.⁴

¹Airlangga University, Surabaya, Indonesia

²Hang Tuah University, Surabaya, Indonesia

³Soetomo University, Surabaya, Indonesia

⁴Universiti Teknologi Malaysia, Johor Bahru, Malaysia

Abstract

This research investigate how red laser treatment affects individuals who have had chemotherapy's ability to heal their wounds. The sixty individuals were split up into groups for treatment and control. On the third and fifth days, the treatment group had reduced signs of inflammation and enhanced recovery. The results point to possible advantages of red laser treatment for recovery after a cure. 60 patients were divided into 30 therapy groups and 30 control groups to investigate the role of photo biomodulation therapy in wound healing. The therapy groups had 60 seconds of light biomodulation therapy utilizing a 650 nm red laser at a dose of 3,5 J/cm². The gingival index, prostaglandin E2, human defensin 2, and interleukin-1 β levels in the laser-treated and control groups' saliva were measured. The level of significance was set at $p < 0.05$. The result of this study on day zero after curettage showed that subjects treated with 650 nm laser levels of prostaglandin E2, human defensin 2, and interleukin-1 β remained essentially the same as the control group subjects without therapy. On the third and fifth days after curettage, subjects treated with 650 nm laser showed lower levels of prostaglandin E2, human defensin 2, and interleukin-1 β . They exhibited substantial differences from the control group subjects without therapy. The gingival index on post-curettage patients showed no significant differences between laser therapy and control groups on day zero but significantly differed on the third and fifth days. Photobiomodulation therapy with a red laser can help the healing of post-curettage subjects according to the analysis' findings of the gingival index, prostaglandin E2, human defensin 2, and interleukin-1 β .

Key words: post curettage wound healing, 650 nm red laser, photo biomodulation, pro-inflammatory mediator.

For citations: Wahyuningtya D.T., Astuti S.D., Widiyanti P., Setiawatie E.M., Guspiari K., Amir M.S., Arifianto D., Yaqubi A.K., Apsari A., Susilo Y., Syahrom A. Effect of photobiomodulation therapy with low level laser on gingival in post-curettage patients, *Biomedical Photonics*, 2024, vol. 13, no. 3, pp. 4–13. doi: 10.24931/2413-9432-2024-13-3-4-13

Contacts: Astuti S.D., e-mail: suryanidyah@fst.unair.ac.id

ВЛИЯНИЕ ФОТОБИОМОДУЛЯЦИОННОЙ ТЕРАПИИ С ИСПОЛЬЗОВАНИЕМ ЛАЗЕРА (650 НМ) НА СОСТОЯНИЕ ДЕСЕН ПОСЛЕ КЮРЕТАЖА

D.T. Wahyuningtya¹, S.D. Astuti¹, P. Widiyanti¹, E.M. Setiawatie¹, K. Guspiari¹, M.S. Amir¹,
 D. Arifianto¹, A.K. Yaqubi¹, A. Apsari², Y. Susilo³, A. Syahrom⁴

¹Airlangga University, Surabaya, Indonesia

²Hang Tuah University, Surabaya, Indonesia

³Soetomo University, Surabaya, Indonesia

⁴Universiti Teknologi Malaysia, Johor Bahru, Malaysia

Резюме

Изучено влияние лазера, излучающего в красной области спектра, на способность к заживлению ран после химиотерапии. В исследовании участвовали 60 человек, которые были разделены на две группы: лечения и контрольная. Пациенты из группы лечения получали 60-секундную световую биомодуляционную терапию с использованием красного лазера с длиной волны 650 нм и световой дозой 3,5 Дж/см². Были измерены десневой индекс, уровни простагландина E2, человеческого дефензина 2 и интерлейкина-1 β в слюне пациентов из обеих групп. Принятый уровень значимости $p < 0,05$. Результаты исследования после кюретажа показали, что у пациентов, получивших воздействие лазером с длиной волны 650 нм, уровни простагландина E2, человеческого дефензина 2 и интерлейкина-1 β оставались практически такими же, как и у пациентов контрольной группы без терапии. На 3-й и 5-й дни после

кюретажа у пациентов группы лечения наблюдались более низкие уровни простагландина E2, человеческого дефензина 2 и интерлейкина-1 β , чем в контрольной группе. Десневой индекс у пациентов после кюретажа не выявил существенных различий между группами лечения и контрольной группой в день лечения, но значительно отличался на 3-й и 5-й дни. В эти сроки в группе лечения наблюдалось уменьшение признаков воспаления и ускорение выздоровления. Результаты указывают на возможные преимущества лечения лазером, излучающим в красной области спектра, для восстановления после химиотерапии. Фотобиомодуляционная терапия красным лазером может способствовать процессам заживления у пациентов после кюретажа согласно результатам анализа десневого индекса, простагландина E2, человеческого дефензина 2 и интерлейкина-1 β .

Ключевые слова: заживление ран после кюретажа, лазер 650 нм, фотобиомодуляция, провоспалительный медиатор.

Для цитирования: Wahyuningtya D.T., Astuti S.D., Widiyanti P., Setiawatie E.M., Guspiari K., Amir M.S., Arifianto D., Yaqubi A.K., Apsari A., Susilo Y., Syahrom A. Влияние фотобиомодуляционной терапии с использованием лазера (650 нм) на состояние десен после кюретажа // Biomedical Photonics. – 2024. – Т. 13, № 3. – С. 4–13. doi: 10.24931/2413-9432-2024-13-3-4-13

Contacts: Astuti S.D., e-mail: suryanidyah@fst.unair.ac.id

Introduction

Curettage is a type of periodontal therapy that makes use of a tool or hand instrument to remove plaque, classified deposits, and smooth cementum around degenerated teeth. This is because plaque and deposits combined with bacteria cause periodontal tissue damage and stimulate the inflammatory process in the gingival tissue, which can damage the alveolar bone and cause tooth mobility in severe cases. After curettage, the healing process is a series of natural processes that occur in body cells damaged by trauma or anatomical traces. This process begins somewhere between the second and fifth days after curettage therapy. A healthy vascular system will hasten to heal. If there is a bacterial infection in the process, the process will be delayed or will not occur at all. The increased dentistry using lasers over the last few decades has led to amazing technological advancements that can be used in dental care. The CO₂, Neodymium: Yttrium-Aluminum-Garnet (Nd: YAG), and Erbium: Yttrium-Aluminum-Garnet (EYAG) lasers are the ones most frequently used to treat peri-dental illness (Er: YAG) [1]. During treatments like gingivectomy, curettage, and the elimination of melanin pigmentation, it is frequently utilized to remove calculus, simplify bone surgery, and lessen soft tissue injury [2]. In addition to providing an antiseptic effect on non-vascularized tissues (such as bone and dentin) and overcoming antibiotic resistance in subgingival biofilms, lasers are hypothesized to enhance decontamination during treatment [3,4].

Oral disorders like tooth decay, periodontitis, and gingivitis affect 3.47 billion people worldwide, causing non-fatal impairment. Patient assessment of treatment requirements and clinical results is crucial for maintaining oral health. Healthy living, including dental health, improves the quality of life, labour productivity, and learning capacity [5]. The absence of clinically detectable inflammation determines periodontal health and bacterial plaque plays a role in the development and maintenance of inflammation. Risk factors like diabetes,

smoking, and hereditary variables can affect periodontal disease progression. Compliance with oral hygiene practices and periodontal maintenance can impact local bacterial infections [6].

The wound healing process consists of several phases from hemostasis, inflammation, cell movement, matrix-forming, and remodeling [7]. The wound healing process caused by periodontitis will differ from person to person, as many factors will influence the healing of wounds, including aging and medication use, tobacco use, and bacterial illnesses in which endotoxins can cause an extended rise of pro-inflammatory cytokines, interleukins-1 β (IL-1 β) and TNF-, thereby prolonging the inflammatory phase and other factors that can inhibit the wound healing process. Antibiotics are quite effective in the treatment of infections and can also prevent the onset of pain due to the wound healing process, even though the optimal dose has yet to be discovered [8].

Photo-biomodulation therapy (PBM) is a low-intensity light irradiation therapy used for medical and dermatological conditions [9]. It involves ingestion of photon energy by body tissues' natural chromophores. Near-infrared and red light are used for therapy in animals and patients, as haemoglobin and melanin absorb blue light at specific wavelengths [10].

Recent media interest has focused on photodynamic therapy (PDT), a minimally invasive therapeutic method, as a novel cancer treatment option. When a photosensitizer is exposed to certain light wavelengths, it combines with molecular oxygen to produce reactive oxygen species, which cause cell death in the target tissue [11]. Longer wavelengths of light (red and infrared) penetrate the tissue more effectively because the amount of light that is absorbed by the tissue reduces as the wavelength increases. The «network optical window» is the term for the 600 to 1200 nm wavelength range. The skin is more sensitive to light because the shorter wavelength (600 nm) penetrates less tissue and absorbs more energy. Longer wavelengths (850 nm) lack the energy to sufficiently create reactive oxygen species

and excite oxygen in the singlet state. The highest tissue permeability consequently occurs between 600 and 850 nm [12].

The 405 nm and 649 nm diode laser has been demonstrated in aPDT15 and PBM investigations to expedite the proliferative process of wound healing following molar extraction based on the results of histological and immunohistochemical testing [1]. In a different study, 'bio stimulators' were low-level lasers and light-emitting diodes (LEDs) with less power than surgical lasers. A sort of light therapy called photo-biomodulation therapy (PBMT) encourages the growth of epithelial cells, an anti-inflammatory response, pain alleviation, and the prevention of scarring, all of which are necessary for wound healing [13]. Laser is a non-invasive, effective, safe, and inexpensive medical device based on aPDT and PBMT therapy for response accelerators for healing dental and oral diseases. Laser parameters and dose influence therapy results. Low-level laser therapy (LLLT) has short-term advantages in lowering pocket depth, but medium-term effects are not significant. Long-term benefits are unknown due to methodological weaknesses and a lack of studies [14]. Research on LLLT for wound healing continues [15].

Wound healing in the oral cavity involves repairing palate and gingival tissue without scar tissue, influenced by early inflammation, reduced immune mediators, fewer blood vessels, bone marrow-derived cells, quick re-epithelialization, and fibroblast proliferation [16, 17]. Microbial infection of the oral cavity is a common risk factor for periodontal disease, which can lead to gingival inflammation and if not treated promptly, may affect the periodontium in general [18]. Bacteria that cause gingival inflammation are *Streptococcus*, *Haemophilus* and *Neisseria species* [8]. *Aggregatibacter actinomycetemcomitans*, *Tannerella forsythia*, *Porphyromonas gingivalis*, *Campylobacter rectus*, *Prevotella intermedia*, and *Selenomonas species* are among the most prevalent subgingival bacterial species [11,19]. The duration of the natural wound healing process is mainly caused by both local and systemic disorders [20].

Local and systemic factors, such as poor blood flow, infection, and foreign substances, affect wound healing. To accelerate healing, therapeutic mechanisms like photo-biomodulation laser therapy and non-invasive approaches are needed. This study aims to determine the method of laser diode therapy and the irradiation time in root canal treatment.

Materials and Methods

Ethical Approval

The Ethics Committee of the Faculty of Dentistry at Airlangga University has accepted this study with the ethical number [551/HRECC.FODM/IX/2021].

Light Source

LLLT is a therapeutic advance that uses low-level infrared light spectrum lasers. The effect is related to tissue bio-stimulation, with photoelectric, photo energetic, and photochemical reactions eliciting a therapeutic response [21]. Photo biomodulation, on the other hand, uses a 650 nm-wavelength diode laser to induce a quicker healing process, as well as to reduce pain and inflammation by stimulating the cell's response to light. The diode laser spectrum and power were tested with the Jasco CT-10 and Thorlabs S140C chromate detectors. The results of laser characterization showed that the laser spectrum was 650 ± 0.05 nm, the power value was stable at 12.02 ± 0.01 mW, and the beam area was 0.20 ± 0.03 with a stable temperature of 32 °C during therapy. Therapy was carried out at a distance of 1 cm from the wound with an energy density of 3.5 J/cm² and a long exposure time of 60 seconds.

Treatments

The study involved 60 patients from the Dental and Oral Hospital's Periodontology section, divided into 30 therapy and control groups. The therapy group received a 650-nm red laser photo biomodulation therapy for 60 seconds, followed by curettage. Saliva samples were collected and transferred to ELISA plates. The samples were then blocked with 10% ovalbumin and 100 mL of hBD-1 mouse monoclonal antibody. The study aimed to understand the effects of laser therapy on gingival and salivary index in patients with periodontal cancer.

The study focuses on the characterization of a 650 nm diode laser used for photo biomodulation therapy, with the control group not receiving any treatment. The second phase is an experimental study examining the impact of specific factors on other variables. This study looked at gingival index and pro-inflammatory mediators in response to different types of therapy, specifically the administration of 650 nm diode laser photo biomodulation therapy and wound healing with antibiotics, in order to assess the level of effectiveness of the red-light diode laser or its effect on the tissue wound healing process in post-curettage patients. The test group patients underwent conventional non-surgical treatment associated with a laser irradiation session to eliminate the bacterial biofilm from the root surface and stop the inflammatory process. Prostaglandin E2 (PGE2), interleukin-1 β (IL1 β), and human beta defensin 2 (HBD2) concentrations were evaluated using the enymed-linked immunosorbent assay and the gingival index.

Enzyme-Linked Immunosorbent Assay (ELISA) Testing

By dilution, 120 l of Standard Solution into 120 l of standard diluent was used to create the standard and wash buffer. In deionized or distilled water, the wash buffer was diluted with 15 ml of the wash buffer concentrate before being mixed with 300 ml of water.

The sample well plate and standard well (not the blank, control well) each received 50 l of the standard, 40 l of the sample, 10 l of anti-PGE2 antibody (or anti-IL1 β antibody or anti-Human antibody defensins 2), and 50 l of streptavidin-HRP. The wells were sealed with sealer and incubated for 60 minutes at 37 °C before being rinsed three times with wash buffer. The next step is to add 50 l of each of the following solutions to each well: 50 liters each of the substrate solutions A and B, 10 minutes of incubation at 37°C, and 50 l of stop solution (blue color will turn yellow). An Elisa reader operating at a wavelength of 450 nm was used to measure the optical density (OD) following the addition of the Stop Solution. Fig. 1 shows the diluting procedure for the sample.

Measurement of Gingival Index

Starting points included the third and fifth days after curettage, as well as the zero-day before and after, for dental index testing. A gingival index score of post-curettage research subjects on day zero, third and fifth following laser therapy is how the gingival index examination was done. The gingival index (GI), a metric developed by Leo and Stillness, is employed to evaluate the presence and degree of gingivitis in a community, group, or person. The following criteria were used to determine the gingival state and the gingival index score: 0 indicates normal gingiva, 1 indicates a mild inflammation with mild discoloration and mild edoema but no bleeding on probing, and 2 indicates a significant inflammation with redness, edoema, and glossy skin; bleeding on probing. 3 = significant redness, edoema, ulceration, and a propensity for spontaneous bleeding; severe inflammation.

Data Analysis

This study gathered information on the gingival index, proinflammatory markers such as PGE2, IL 1 β , and HBD-2, as well as instrumentation tests using a diode laser. The Kolmogorov-Smirnov test was used to determine whether the data were normally distributed. Individual sample T-Test can be used to do statistical analyses if the data are regularly distributed. The interval/ratio data scale, unpaired independent data groups, normal distribution of group data, and the absence of outliers in group data are necessary preconditions for using the independent sample T-Test.

Results

IL 1 β protein testing was conducted to monitor inflammation during the wound healing process, both before extraction (day 0) and after extraction (day three and day five post-wound occurrence). In general, the observation results indicated a decrease in the levels of IL 1 β . The normality test, performed using Kolmogorov-Smirnov, demonstrated that the data exhibited a normal distribution for the control group (without photobiomodulation therapy) with a significance level

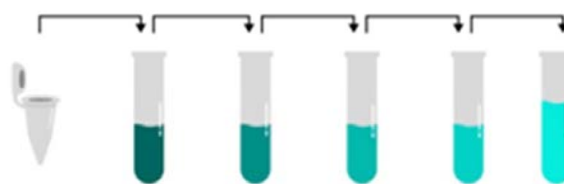


Рис. 1. Методика стандартного разведения.
Fig. 1. Standard dilution.

(a) of 0.300, while for the photobiomodulation therapy group, it was 0.115. Table 1 shows that post-extraction on day 1, day 3, and day five significantly impacted IL 1 β levels ($p < 0.05$). All control group subjects exhibited higher IL 1 β levels when compared to the photobiomodulation therapy group.

Enzyme-linked immunosorbent assay PGE2 test results

PGE2 protein levels fell from day zero to day five, which are significant mediators in the etiology of periodontitis and indications of inflammation in the healing phase of wounds. The independent T-Test was used to compare the PGE2 levels in the control and treatment groups to see if there were any variations in the mean values between the two unrelated sample groups. On the first, third, and fifth days, T-Tests were performed on all data collected in the control and treatment groups. On the first, third, and fifth post-curettage days, the mean PGE2 values in the control and treatment groups are displayed in Table 1.

PGE2 levels were measured in post-curettage subjects using the expression test, and the results showed greater levels in the laser therapy group but no statistically significant difference from the control group. The levels of PGE2 were lower in the laser therapy group on the first, third-, and fifth days following curettage, which was substantially different from the levels in the control group. Figure 2 shows visually the amounts of prostaglandin E2 at the zero, first, third-, and fifth-days post-curettage in patients.

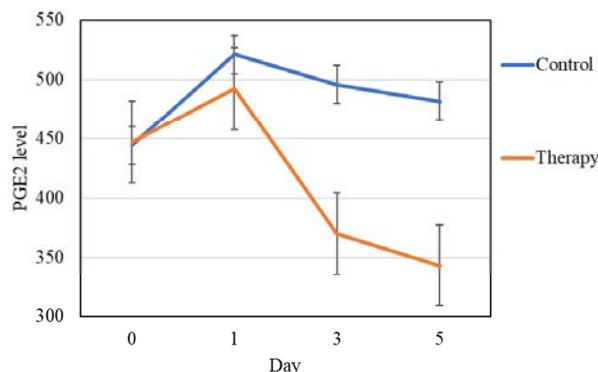


Рис. 2. Уровни простагландина E2 в контрольной группе и группе лечения.
Fig. 2. Prostaglandin E2 levels against the control and therapy groups.

Таблица 1

Работа тока у больных с признаками воспаления кист поджелудочной железы и без признаков воспаления кист поджелудочной железы

Table 1

Electric current work in patients with signs of inflammation of pancreatic cysts and without signs of inflammation of pancreatic cysts

Дни Days	Группа Group	N	Значение Average	SD	Независимый Т-тест Independent T Test
0	Контроль Control	30	444.17	10.54	p = 0.277
	Лечение Therapy	30	447.20	10.85	
1	Контроль Control	30	521.13	36.79	p = 0.030*
	Лечение Therapy	30	492.20	26.86	
3	Контроль Control	30	495.93	36.78	p = 0.031*
	Лечение Therapy	30	369.77	36.90	
5	Контроль Control	30	481.73	40.02	p = 0.001*
	Лечение Therapy	30	343.13	22.33	

*Различия статистически значимы

*There is a different meaning

Enzyme-Linked Immunosorbent assay test results in Human defensin 2

Human defensin 2 protein levels, crucial for wound healing, decreased from day zero to day five, indicating a decline in pathogenic bacteria colonization in the oral cavity. The amount of human defensin 2 proteins in the control and therapy groups were compared using the Independent T-Test to determine the average difference between the two groups of unrelated samples. T-Tests were run for the control and treatment groups on the first, third, and fifth days. Table 2 shows the distribution of the mean values of human defensin 2 in the control and treatment groups in post-curettage patients on the zero, first, third, and fifth days after curettage.

Based on the test results, the therapy group's expression of Human Defensin 2 had higher levels on day zero of the wound-healing process in post-curettage individuals, but it was not statistically different from the control group. On the first, third, and fifth days, there was a substantially different expression of defensin 2 in the 650 nm red laser therapy group compared to the control group. Human Defensin 2 levels in post-curettage patients are depicted graphically in Figure 3 at zero, first, third-, and fifth days following curettage.

Enzyme-Linked Immunosorbent assay test results Interleukin-1 β

Measurements of interleukin-1 β levels revealed a decrease from day zero to day fifth. Then the results of assessing interleukin-1 β protein levels in the control and therapy groups were compared using the Independent

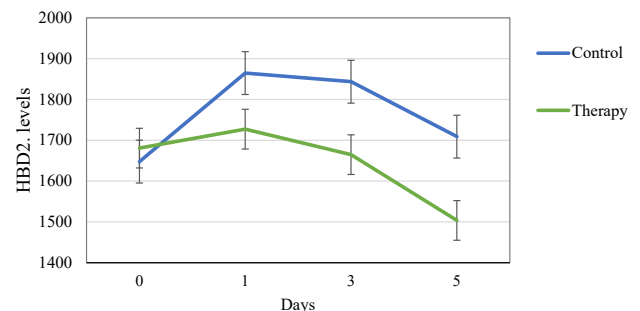


Рис. 3. Сравнение уровней дефензина 2 человека в контрольной группе и группе лечения в период с 0-го по 5-й дни.

Fig. 3. Comparison of Human defensin 2 levels against the control and therapy groups on zero-day to the fifth day.

T-Test to determine the average difference between the two groups of unrelated samples. T-Tests for the control and treatment groups were run on the first, third, and fifth days. Table 3 displays the distribution of interleukin-1 β in the control and treatment groups for post-curettage patients on the zero, first, third, and fifth days after curettage.

According to the test results, the therapy group's post-curettage subjects had greater levels of interleukin-1 β at day zero of the wound healing process than the control group, although this difference was not significant ($p=0.127$). On day first ($p=0.043$), third ($p=0.029$), and fifth ($p=0.027$), interleukin-1 β expression in the 650 nm red laser treatment group was substantially different from that of the control group. Human Defensin 2 levels in post-curettage patients are depicted graphically in Figure 4 at zero, first, third-, and fifth days following curettage.

Gingival Index Test Results
The gingival index examination was conducted on day zero, with further assessments after three days. The condition index was calculated using measurements of

fluid discharge, color, shape alterations, acute bleeding, and bleeding time. The study found that the control and therapy groups had mildly inflammatory gingival health on day zero, with the treatment group experiencing

Таблица 2
Сравнение результатов независимого выборочного Т-теста для уровней человеческого дефенсина 2 с контрольной группой и группой лечения в 1-й, 3-й и 5-й день после кюретажа

Table 2
Comparison of the results of the Independent Sample T-Test for levels of Human defensin 2 against the control group and the therapy group on day first, day third, and day fifth after curettage

Дни Days	Группа Group	N	Значение Average	SD	Независимый Т-тест Independent T Test
0	Контроль Control	30	1647.70	38.60	p = 0.687
	Лечение Therapy	30	1680.83	73.58	
1	Контроль Control	30	1864.77	32.51	p = 0.000*
	Лечение Therapy	30	1727.30	85.09	
3	Контроль Control	30	1843.60	38.79	p = 0.018*
	Лечение Therapy	30	1664.80	32.62	
5	Контроль Control	30	1709.00	43.12	p = 0.001*
	Лечение Therapy	30	1503.63	88.49	

*Различия статистически значимы
*There is a different meaning

Таблица 3
Сравнение результатов независимого выборочного Т-теста уровней интерлейкина-1β с контрольной группой и группой терапии на 0-й, 1-й, 3-й и 5-й дни после кюретажа

Table 3
Comparison of the results of the Independent Sample T-Test of interleukin-1β levels against the control group and the therapy group on the zero, first, third, and fifth days after curettage

Дни Days	Группа Group	N	Значение Average	SD	Независимый Т-тест Independent T Test
0	Контроль Control	30	1822.20	41.38	p = 0.127
	Лечение Therapy	30	1811.53	51.00	
1	Контроль Control	30	2223.97	88.53	p = 0.043*
	Лечение Therapy	30	1904.20	60.66	
3	Контроль Control	30	2086.90	91.59	p = 0.029*
	Лечение Therapy	30	1801.83	53.29	
5	Контроль Control	30	2000.30	87.03	p = 0.027*
	Лечение Therapy	30	1774.07	48.65	

*Различия статистически значимы
*There is a different meaning

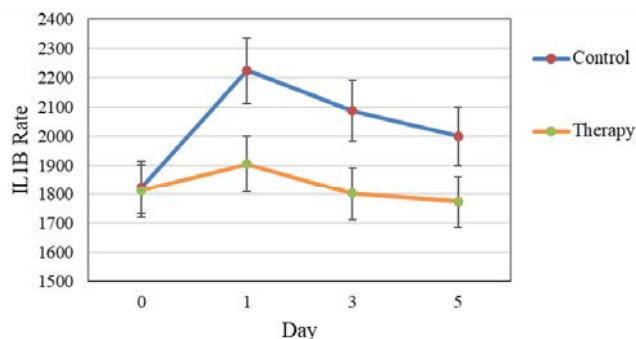


Рис. 4. Сравнение уровней интерлейкина-1 β в контрольной группе и группе лечения в период с 0-го по 5-й дни.

Fig. 4. Comparison of interleukin-1 β levels against the control and treatment groups on zero-day to the fifth day.

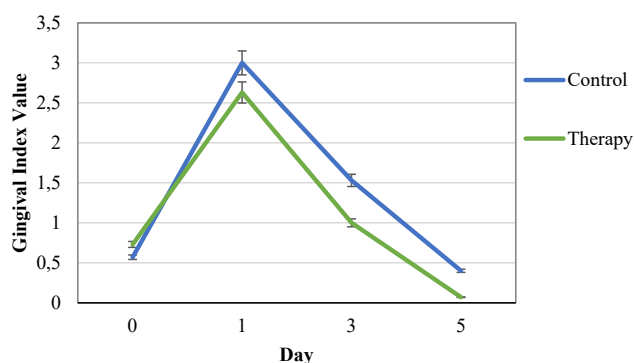


Рис. 5. Сравнение показателей десневого индекса в контрольной группе и группе лечения.

Fig. 5. Comparison of gingival index scores in the control group and the therapy group.

Таблица 4

Результаты U-теста Манна-Уитни на 0-й, 1-й, 3-й и 5-й дни после кюретажа

Table 4

Mann-Whitney U test results on zero, first, third, and fifth days after curettage

Дни Days	Группа Group	N	Значение Average	Критерий Манна-Уитни Mann-Whitney U
0	Контроль Control	30	0.57	p = 0.573
	Лечение Therapy	30	0.73	
1	Контроль Control	30	3.00	p = 0.000*
	Лечение Therapy	30	2.63	
3	Контроль Control	30	1.53	p = 0.001*
	Лечение Therapy	30	1.00	
5	Контроль Control	30	0.40	p = 0.002*
	Лечение Therapy	30	0.07	

*Различия статистически значимы

*There is a different meaning

severe inflammatory health. On day 3, the control group deteriorated, while the treatment group showed moderately inflammatory health, with an average score of 1. The treatment group had a lower gingival index score of 0.07 on the fifth day, compared to the control group's average gingival score of 0.4, which showed that both groups were in good health. Figure 5 depicts the evaluation of the gingival index in the laser treatment and control groups on the first, second, third-, and fifth days following curettage.

The average number of gingival indices varies, as seen in Figure 9, but the shape and distribution of the data are the same. The median difference's significance is not evident. Since the Gingiva Index measurement in the control and therapy groups contains interval data, the Mann-Whitney U method is utilized for the Non-Parametric Test. The findings of the Mann-Whitney U test in Table 4 indicate that there is a different interpretation of the gingival index on the zero, first, third-, and fifth days following curettage in the control group compared to the treatment group in post-curettage patients ($p < 0.05$).

Discussion

Photobiomodulation therapy (PBMT) is a therapeutic approach using low-level infrared light spectrum lasers to stimulate tissue [22]. It works by absorbing photons by molecular photo acceptors or chromophores [23]. Effective tissue penetration occurs between 650 and 1200 nanometers, with absorption and scattering stronger in the blue section [24]. Most LLLT in animals and patients uses red light and near-infrared [25].

This study aims to expedite healing and reduce pain and inflammation using photo biomodulation therapy using a diode laser with a characterization wavelength of 649 ± 0.05 . The red laser light's energy and wavelength are 12.02 ± 0.01 mW at 650 nm [26]. The low-power dose of 3.5 J/cm^2 is crucial for the therapy, and the laser diode power characteristic test ensures maximum power stability at 60 seconds. The therapy is suitable for patients with various conditions [27]. Periodontal disease, causing tooth loss in adults, is primarily caused by bacterial buildup near teeth. Gingivitis and periodontitis are two types. Root planning and scaling are interconnected processes [28].

Curettage is a periodontal treatment that involves a change in microbiota and decreased inflammation. If inflammation persists, curettage can be performed. The depth of periodontal pockets can be significantly increased, depending on the damage. With proper care and maintenance, most patients can regain a 4 mm to 5 mm pocket depth. The study involved 60 patients, with 30 in the therapeutic group and 30 in the control group. After curettage treatment, the therapeutic group received red laser irradiation on the first day, followed by the control group on the third and fifth days. Samples were collected at each visit.

The collected samples were then tested for PGE2, IL-1 β , and HBD-2 levels using an ELISA kit with 96 well plates. The ELISA kit used in this study has a sensitivity of 1.28 ng/L for PGE2, 10.07 pg/mL for IL-1 β , and 5.31 ng/L for HBD-2. One of the immunological techniques that aim to determine or measure levels of protein expression activity/response and immune reaction status from individual reactions/immune responses is the ELISA technique [30].

Wound healing involves fibrosis and regeneration, with fibrosis replacing damaged tissue with connective tissue [11, 31]. Laser biomodulation therapy enhances phagocytosis and lysosomal activity, activating Cytochrome Oxidase C and triggering downstream signaling cascades that promote protein synthesis, anti-inflammatory reactions, antioxidants, and cell proliferation [32].

Prostaglandin E2, a pro-inflammatory mediator, promotes the synthesis of inflammatory substances, particularly in periodontitis, particularly IL-1 β [33]. Periodontitis patients have higher PGE2 levels, which can be blocked with anti-inflammatory medications to slow disease progression and reduce bone resorption, with faster decline in therapy groups [34]. Then the levels of PGE2, IL-1 β , and HBD-2 in the samples were assessed using an ELISA kit with 96 well plates. The ELISA kit used in this study has a sensitivity of 1.28 ng/L for PGE2, 10.07 pg/mL for IL-1 β , and 5.31 ng/L for HBD-2.

The ELISA technique assesses immune response status and protein expression activity. The study found that IL-1 β concentration in gingival crevicular fluid (GCF) decreased after non-surgical periodontal therapy [35]. Laser phototherapy inhibited IL-1 β production, affecting

wound healing [36]. The study found differences in IL-1 β protein levels during post-curettage wound healing using red laser photo biomodulation therapy at a 650 nm wavelength. The therapy group showed a faster decline than the control group [37].

The study shows that red laser photo biomodulation therapy significantly enhances wound healing in post-curettage patients, with a lower gingival index and faster decline in inflammation compared to the control group, indicating a positive healing effect [38]. Laser therapy wavelengths, particularly 600-700 nm, can stimulate cell proliferation and differentiation, regenerate tissue, reduce inflammation, and alleviate pain in chromophore cells [39]. The study demonstrates that red laser photo biomodulation therapy at 650 nm can accelerate wound healing in post-curettage patients, with significant reductions in test parameters [40]. This therapy accelerates fibroblast proliferation, which produces collagen and influences the epithelialization process, ultimately determining the outcome of wound healing [41].

According to the findings of statistical tests, there was a difference in post-curettage wound healing time between patients receiving photo biomodulation therapy and patients who did not receive photo biomodulation therapy with a probability value (p-value) of 0.05 in each pro-inflammatory mediator test (IL-1 β , PGE2, and hB-2) and gingival index studies. If the P value is less than 0.05, the result is considered statistically significant. This value indicates that there is substantial evidence against the null hypothesis. As a result, the researcher discards the alternative hypothesis in favor of the null hypothesis. In comparison to patients who didn't get laser therapy, post-curettage patients who received a 650 nm diode laser showed faster-wound healing, according to the null hypothesis.

Conclusion

The findings of this study showed that levels of prostaglandin E2, human defensin 2, and interleukin-1 β in participants treated with a 650 nm laser on the first day after curettage were not statistically different from those in the control group of subjects who received no therapy. On the third and fifth day after curettage, subjects treated with 650 nm laser showed lower levels of Prostaglandin E2, Human Defensin 2, and interleukin-1 β and were distinct from the control group subjects without therapy. The results of the measurement of the gingival index on post-curettage patients on day zero showed that there was no significant difference between the control group and the laser therapy group, while on the third and fifth days there was a significant difference in the gingival index. Based on the examination of the gingival index, prostaglandin E2, human defensin 2, and interleukin-1 β , photo biomodulation therapy with a red laser can aid in the healing of post-curettage individuals.

REFERENCES

1. Astuti S. D. et al. An in-vivo study of photobiomodulation using 403 nm and 649 nm diode lasers for molar tooth extraction wound healing in wistar rats. *Odontology*, 2022, vol. 110 (2), pp. 240-253. doi: <https://doi.org/10.1007/s10266-021-00653-w>
2. Sağlam M. et al. Combined application of Er: YAG and Nd: YAG lasers in treatment of chronic periodontitis. A split-mouth, single-blind, randomized controlled trial. *Journal of periodontal research*, 2017, vol 52(5), pp. 853-862. doi: <https://doi.org/10.1111/jre.12454>
3. Astuti S.D. et al. The efficacy of photodynamic inactivation with laser diode on *Staphylococcus aureus* biofilm with various ages of biofilm. *Infectious disease reports*, 2020, vol. 12(S1), pp. 68-74. doi: <https://doi.org/10.4081/idr.2020.8736>
4. Astuti S.D. et al. Chlorophyll mediated photodynamic inactivation of blue laser on *Streptococcus mutans*. In *AIP Conference Proceedings*, 2016, vol. 1718(1), pp. 120001.
5. Daigo Y. et al. Wound healing and cell dynamics including mesenchymal and dental pulp stem cells induced by photobiomodulation therapy: an example of socket-preserving effects after tooth extraction in rats and a literature review. *International Journal of Molecular Sciences*, 2020, vol. 21(18), pp. 6850. doi: <https://doi.org/10.3390/ijms21186850>
6. de Paula Eduardo C. et al. Laser phototherapy in the treatment of periodontal disease. A review. *Lasers in medical science*, 2010, vol. 25 (6), pp. 781-792. doi: DOI 10.1007/s10103-010-0812-y
7. Erming S.A. et al. Wound repair and regeneration: mechanisms, signaling, and translation. *Science translational medicine*, 2014, vol. 6 (265), pp. 265sr6-265sr6. doi: DOI: 10.1126/scitranslmed.3009337
8. Mardianto A.I. et al. Photodynamic Inactivation of *Streptococcus mutans* Bacteri with Photosensitizer *Moringa oleifera* Activated by Light Emitting Diode (LED). In *Journal of Physics: Conference Series*, 2020, vol. 1505 (1), pp. 012061
9. Sutherland J.C. et al. Biological Effects of Polychromatic Light. *Photochemistry and photobiology*, 2002, vol. 76 (2), pp. 164-170. doi: [https://doi.org/10.1562/0031-8655\(2002\)0760164BEOPL2.0.CO2](https://doi.org/10.1562/0031-8655(2002)0760164BEOPL2.0.CO2)
10. Astuti S.D. et al. Photodynamic effectiveness of laser diode combined with ozone to reduce *Staphylococcus aureus* biofilm with exogenous chlorophyll of *Dracaena angustifolia* leaves. *Biomedical Photonics*, 2019, vol. 8 (2), pp. 4-13.
11. Correia J.H. et al. Photodynamic therapy review: Principles, photosensitizers, applications, and future directions. *Pharmaceutics*, 2021, vol. 13 (9), pp. 1332. doi: <https://doi.org/10.3390/pharmaceutics13091332>
12. Astuti S.D. et al. Combination effect of laser diode for photodynamic therapy with doxycycline on a wistar rat model of periodontitis. *BMC oral health*, 2021, vol. 21(1), pp. 1-15.
13. Hung C.M. et al. Gingyo-san enhances immunity and potentiates infectious bursal disease vaccination. Evid. *Based Complementary Altern Med*, 2011. doi: <https://doi.org/10.1093/ecam/nep021>
14. Plaetzer K. et al. Photophysics and photochemistry of photodynamic therapy: fundamental aspects. *J Lasers Med Sci*, 2009, vol. 24 (2), pp. 259-268.
15. Ren C. et al. The effectiveness of low-level laser therapy as an adjunct to non-surgical periodontal treatment: a meta-analysis. *J. Periodontal Res*, 2017, vol. 52 (1), pp. 8-20. doi: <https://doi.org/10.1111/jre.12361>
16. Gilowski L. et al. Amount of interleukin-1 β and interleukin-1 receptor antagonist in periodontitis and healthy patients. *Arch. Oral Biol*, 2014, vol. 59 (7), pp. 729-734. doi: <https://doi.org/10.1016/j.archoralbio.2014.04.007>
17. Harvey J.D. et al. Periodontal microbiology. *Dent. Clin*, 2017, vol. 61 (2), pp. 253-269. doi: <https://doi.org/10.1016/j.cden.2016.11.005>
18. Iglesias-Bartolome R. et al. Transcriptional signature primes human oral mucosa for rapid wound healing. *Sci. Transl. Med*, 2018, Vol. 10 (451), pp. eaap8798. doi: 10.1126/scitranslmed.aap8798
19. Savitt E.D. et al. Distribution of certain subgingival microbial species in selected periodontal conditions. *J Periodontal Res*, 1984, vol. 19 (2), pp. 111-23. doi: <https://doi.org/10.1111/j.1600-0765.1984.tb00800.x>
20. Ismiyatin K. et al. Different 650 nm laser diode irradiation times affect the viability and proliferation of human periodontal ligament fibroblast cells. *Dent. J (Majalah Kedokteran Gigi)*, 2019, vol. 52 (3), pp. 142-142.

ЛИТЕРАТУРА

1. Astuti S. D. et al. An in-vivo study of photobiomodulation using 403 nm and 649 nm diode lasers for molar tooth extraction wound healing in wistar rats // *Odontology*. – 2022. – Vol. 110 (2). – P. 240-253. doi: <https://doi.org/10.1007/s10266-021-00653-w>
2. Sağlam M. et al. Combined application of Er: YAG and Nd: YAG lasers in treatment of chronic periodontitis. A split-mouth, single-blind, randomized controlled trial // *Journal of periodontal research*. – 2017. – Vol 52(5). – P. 853-862. doi: <https://doi.org/10.1111/jre.12454>
3. Astuti S.D. et al. The efficacy of photodynamic inactivation with laser diode on *Staphylococcus aureus* biofilm with various ages of biofilm // *Infectious disease reports*. – 2020. – Vol. 12(S1). – P. 68-74. doi: <https://doi.org/10.4081/idr.2020.8736>
4. Astuti S.D. et al. Chlorophyll mediated photodynamic inactivation of blue laser on *Streptococcus mutans* // In *AIP Conference Proceedings*. – 2016. – Vol. 1718(1). – P. 120001.
5. Daigo Y. et al. Wound healing and cell dynamics including mesenchymal and dental pulp stem cells induced by photobiomodulation therapy: an example of socket-preserving effects after tooth extraction in rats and a literature review // *International Journal of Molecular Sciences*. – 2020. – Vol. 21(18). – P. 6850. doi: <https://doi.org/10.3390/ijms21186850>
6. de Paula Eduardo C. et al. Laser phototherapy in the treatment of periodontal disease. A review // *Lasers in medical science*. – 2010. – Vol. 25 (6). – P. 781-792. doi: DOI 10.1007/s10103-010-0812-y
7. Erming S.A. et al. Wound repair and regeneration: mechanisms, signaling, and translation // *Science translational medicine*. – 2014. – Vol. 6 (265). – P. 265sr6-265sr6. doi: DOI: 10.1126/scitranslmed.3009337
8. Mardianto A.I. et al. Photodynamic Inactivation of *Streptococcus mutans* Bacteri with Photosensitizer *Moringa oleifera* Activated by Light Emitting Diode (LED) // In *Journal of Physics: Conference Series*. – 2020. – Vol. 1505 (1). – P. 012061
9. Sutherland J.C. et al. Biological Effects of Polychromatic Light // *Photochemistry and photobiology*. – 2002. – Vol. 76 (2). – P. 164-170. doi: [https://doi.org/10.1562/0031-8655\(2002\)0760164BEOPL2.0.CO2](https://doi.org/10.1562/0031-8655(2002)0760164BEOPL2.0.CO2)
10. Astuti S.D. et al. Photodynamic effectiveness of laser diode combined with ozone to reduce *Staphylococcus aureus* biofilm with exogenous chlorophyll of *Dracaena angustifolia* leaves // *Biomedical Photonics*. – 2019. – Vol. 8 (2). – P. 4-13.
11. Correia J.H. et al. Photodynamic therapy review: Principles, photosensitizers, applications, and future directions // *Pharmaceutics*. – 2021. – Vol. 13 (9). – P. 1332. doi: <https://doi.org/10.3390/pharmaceutics13091332>
12. Astuti S.D. et al. Combination effect of laser diode for photodynamic therapy with doxycycline on a wistar rat model of periodontitis // *BMC oral health*. – 2021. – Vol. 21(1). – P. 1-15.
13. Hung C.M. et al. Gingyo-san enhances immunity and potentiates infectious bursal disease vaccination. Evid // *Based Complementary Altern Med*. – 2011. doi: <https://doi.org/10.1093/ecam/nep021>
14. Plaetzer K. et al. Photophysics and photochemistry of photodynamic therapy: fundamental aspects // *J Lasers Med Sci*. – 2009. – Vol. 24 (2). – P. 259-268.
15. Ren C. et al. The effectiveness of low-level laser therapy as an adjunct to non-surgical periodontal treatment: a meta-analysis // *J. Periodontal Res*. – 2017. – Vol. 52 (1). – P. 8-20. doi: <https://doi.org/10.1111/jre.12361>
16. Gilowski L. et al. Amount of interleukin-1 β and interleukin-1 receptor antagonist in periodontitis and healthy patients // *Arch. Oral Biol*. – 2014. – Vol. 59 (7). – P. 729-734. doi: <https://doi.org/10.1016/j.archoralbio.2014.04.007>
17. Harvey J.D. et al. Periodontal microbiology // *Dent. Clin*. – 2017. – Vol. 61 (2). – P. 253-269. doi: <https://doi.org/10.1016/j.cden.2016.11.005>
18. Iglesias-Bartolome R. et al. Transcriptional signature primes human oral mucosa for rapid wound healing // *Sci. Transl. Med*. – 2018. – Vol. 10 (451). – P. eaap8798. doi: 10.1126/scitranslmed.aap8798
19. Savitt E.D. et al. Distribution of certain subgingival microbial species in selected periodontal conditions // *J Periodontal Res*. – 1984. – Vol. 19 (2). – P. 111-23. doi: <https://doi.org/10.1111/j.1600-0765.1984.tb00800.x>
20. Ismiyatin K. et al. Different 650 nm laser diode irradiation times affect the viability and proliferation of human periodontal ligament fibroblast cells // *Dent. J (Majalah Kedokteran Gigi)*. – 2019. – Vol. 52 (3). – P. 142-142.

21. Politis C. et al. Wound healing problems in the mouth // *Front. Physiol.* 2016, vol. 7, pp. 507. doi: <https://doi.org/10.3389/fphys.2016.00507>
22. Popova C. et al. Correlation Between Healing Parameters and PGE2 Expression Levels in Non-Surgical Therapy of Chronic Periodontitis. *J of IMAB – Annual Proceeding Scientific Papers*, 2017, vol. 23 (4), pp. 1758-1764. doi: 10.5272/jimab.2017234.1758
23. Arjmand B. et al. Low-Level Laser Therapy: Potential and Complications. *J Lasers Med Sci*, 2021, vol. 12. doi: 10.34172/jlms.2021.42
24. Rosso M.P.D.O. et al. Photobiomodulation therapy (PBMT) in peripheral nerve regeneration: a systematic review. *J. Biomed. Eng.*, 2018, vol. 5 (2), pp. 44. doi: <https://doi.org/10.3390/bioengineering5020044>
25. Farivar S. et al. Biological effects of low-level laser therapy. *J Lasers Med Sci*, 2014, vol. 5 (2), pp. 58.
26. Suhariningsih D. et al. The effect of electric field, magnetic field, and infrared ray combination to reduce HOMA-IR index and GLUT 4 in diabetic model of Mus musculus. *Lasers in Medical Science*, 2020, vol. 35 (6), pp. 1315-1321.
27. Astuti S.D. et al. Effectiveness Photodynamic Inactivation with Wide Spectrum Range of Diode Laser to Staphylococcus aureus Bacteria with Endogenous Photosensitizer: An in vitro Study. *Journal of International Dental and Medical Research*, 2019, vol. 12 (2), pp. 481-486.
28. Ren C. et al. The effectiveness of low-level laser therapy as an adjunct to non-surgical periodontal treatment: a meta-analysis. *J. Periodontal Res*, 2017, vol. 52 (1), pp. 8-20. doi: <https://doi.org/10.1111/jre.12361>
29. Setiawatie E.M. et al. An in vitro Anti-microbial Photodynamic Therapy (APDT) with Blue LEDs to activate chlorophylls of Alfalfa Medicago Sativa L on Aggregatibacter actinomycetemcomitans. *J. Int. Dent. Medical Res*, 2016, vol. 9 (2), pp. 118-125.
30. Sidharthan S. et al. Gingival crevicular fluid levels of Interleukin-22 (IL-22) and human β Defensin-2 (hBD-2) in periodontal health and disease: A correlative study. *J Oral Biol Craniofac Res*, 2020, vol. 10 (4), pp. 498-503. doi: <https://doi.org/10.1016/j.jobcr.2020.07.021>
31. Tang E. et al. Laser-activated transforming growth factor- β 1 induces human β -defensin 2: implications for laser therapies for periodontitis and peri-implantitis. *J. Periodontal Res*, 2017, vol. 52 (3), pp. 360-367. doi: <https://doi.org/10.1111/jre.12399>
32. Muliani Izat W.O.A. et al. The Effectiveness of Sea Cucumber Extract (Holothuroidea Sp) on Interleukin-1 β (IL-1 β) Expression in Periodontitis (Research on Wistar Rats). (Doctoral dissertation, Hasanuddin University), 2020.
33. Genco R.J. et al. Periodontal disease and overall health: a clinician's guide. *Yardley, Pennsylvania, USA: Professional Audience Communications Inc.*, 2010, pp. 254-263.
34. Santosa B. et al. Elisa Method for Measurement of Metallothionein Protein in Rice. *Leaves Ir Bagendit*, 2020.
35. Sakurai Y. et al. Inhibitory effect of low-level laser irradiation on LPS stimulated prostaglandin E2 production and cyclooxygenase 2 in human gingival fibroblasts. *Eur. J. Oral Sci.*, 2000, vol. 108 (1), pp. 29-34. doi: <https://doi.org/10.1034/j.1600-0722.2000.00783.x>
36. Hanna R. et al. Phototherapy as a rational antioxidant treatment modality in COVID-19 management; new concept and strategic approach: a critical review. *Antioxidants*, 2020, vol. 9 (9), pp. 875. doi: <https://doi.org/10.3390/antiox9090875>
37. Ebrahimi P. et al. Effect of photobiomodulation in secondary intention gingival wound healing a systematic review and meta-analysis. *BMC Oral Health*, 2021, vol. 21 (1), pp. 1-16.
38. Astuti S.D. et al. Effectiveness of 650 nm red laser photobiomodulation therapy to accelerate wound healing post tooth extraction. *Biomedical Photonics*, 2024, vol. 13 (1), pp. 4-15. <https://doi.org/10.24931/2413-9432-2024-13-1-4-15>
39. Genco R.J. et al. Periodontal disease and overall health: a clinician's guide. *Yardley, Pennsylvania, USA: Professional Audience Communications Inc.*, 2010, pp. 254-263.
40. Avci P. et al. Low-level laser (light) therapy (LLLT) in skin: stimulating, healing, restoring. *Semin Cutan Med Surg*, 2013, vol. 32 (1), pp. 41.
41. Rasouli M. et al. The interplay between extracellular matrix and progenitor/stem cells during wound healing: Opportunities and future directions. *Acta Histochemica*, 2021, Vol. 123 (7), pp. 151785. doi: <https://doi.org/10.1016/j.acthis.2021.151785>
21. Politis C. et al. Wound healing problems in the mouth // *Front. Physiol.* – 2016. – Vol. 7. – P. 507. doi: <https://doi.org/10.3389/fphys.2016.00507>
22. Popova C. et al. Correlation Between Healing Parameters and PGE2 Expression Levels in Non-Surgical Therapy of Chronic Periodontitis // *J of IMAB – Annual Proceeding Scientific Papers*. – 2017. – Vol. 23 (4). – P. 1758-1764. doi: 10.5272/jimab.2017234.1758
23. Arjmand B. et al. Low-Level Laser Therapy: Potential and Complications // *J Lasers Med Sci*. – 2021. – Vol. 12. doi: 10.34172/jlms.2021.42
24. Rosso M.P.D.O. et al. Photobiomodulation therapy (PBMT) in peripheral nerve regeneration: a systematic review // *J. Biomed. Eng.* – 2018. – Vol. 5 (2). – P. 44. doi: <https://doi.org/10.3390/bioengineering5020044>
25. Farivar S. et al. Biological effects of low-level laser therapy // *J Lasers Med Sci*. – 2014. – Vol. 5 (2). – P. 58.
26. Suhariningsih D. et al. The effect of electric field, magnetic field, and infrared ray combination to reduce HOMA-IR index and GLUT 4 in diabetic model of Mus musculus // *Lasers in Medical Science*. – 2020. – Vol. 35 (6). – P. 1315-1321.
27. Astuti S.D. et al. Effectiveness Photodynamic Inactivation with Wide Spectrum Range of Diode Laser to Staphylococcus aureus Bacteria with Endogenous Photosensitizer: An in vitro Study // *Journal of International Dental and Medical Research*. – 2019. – Vol. 12 (2). – P. 481-486.
28. Ren C. et al. The effectiveness of low-level laser therapy as an adjunct to non-surgical periodontal treatment: a meta-analysis // *J. Periodontal Res*. – 2017. – Vol. 52 (1). – P. 8-20. doi: <https://doi.org/10.1111/jre.12361>
29. Setiawatie E.M. et al. An in vitro Anti-microbial Photodynamic Therapy (APDT) with Blue LEDs to activate chlorophylls of Alfalfa Medicago Sativa L on Aggregatibacter actinomycetemcomitans // *J. Int. Dent. Medical Res*. – 2016. – Vol. 9 (2). – P. 118-125.
30. Sidharthan S. et al. Gingival crevicular fluid levels of Interleukin-22 (IL-22) and human β Defensin-2 (hBD-2) in periodontal health and disease: A correlative study // *J Oral Biol Craniofac Res*. – 2020. – Vol. 10 (4). – P. 498-503. doi: <https://doi.org/10.1016/j.jobcr.2020.07.021>
31. Tang E. et al. Laser-activated transforming growth factor- β 1 induces human β -defensin 2: implications for laser therapies for periodontitis and peri-implantitis // *J. Periodontal Res*. – 2017. – Vol. 52 (3). – P. 360-367. doi: <https://doi.org/10.1111/jre.12399>
32. Muliani Izat W.O.A. et al. The Effectiveness of Sea Cucumber Extract (Holothuroidea Sp) on Interleukin-1 β (IL-1 β) Expression in Periodontitis (Research on Wistar Rats) // (Doctoral dissertation, Hasanuddin University). – 2020.
33. Genco R.J. et al. Periodontal disease and overall health: a clinician's guide // *Yardley, Pennsylvania, USA: Professional Audience Communications Inc.* – 2010. – P. 254-263.
34. Santosa B. et al. Elisa Method for Measurement of Metallothionein Protein in Rice // *Leaves Ir Bagendit*. – 2020.
35. Sakurai Y. et al. Inhibitory effect of low-level laser irradiation on LPS stimulated prostaglandin E2 production and cyclooxygenase 2 in human gingival fibroblasts // *Eur. J. Oral Sci.* – 2000. – Vol. 108 (1). – P. 29-34. doi: <https://doi.org/10.1034/j.1600-0722.2000.00783.x>
36. Hanna R. et al. Phototherapy as a rational antioxidant treatment modality in COVID-19 management; new concept and strategic approach: a critical review // *Antioxidants*. – 2020. – Vol. 9 (9). – P. 875. doi: <https://doi.org/10.3390/antiox9090875>
37. Ebrahimi P. et al. Effect of photobiomodulation in secondary intention gingival wound healing a systematic review and meta-analysis // *BMC Oral Health*. – 2021. – Vol. 21 (1). – P. 1-16.
38. Astuti S.D. et al. Effectiveness of 650 nm red laser photobiomodulation therapy to accelerate wound healing post tooth extraction // *Biomedical Photonics*. – 2024. – Vol. 13 (1). – P. 4-15. <https://doi.org/10.24931/2413-9432-2024-13-1-4-15>
39. Genco R.J. et al. Periodontal disease and overall health: a clinician's guide // *Yardley, Pennsylvania, USA: Professional Audience Communications Inc.* – 2010. – P. 254-263.
40. Avci P. et al. Low-level laser (light) therapy (LLLT) in skin: stimulating, healing, restoring // *Semin Cutan Med Surg*. – 2013. – Vol. 32 (1). – P. 41.
41. Rasouli M. et al. The interplay between extracellular matrix and progenitor/stem cells during wound healing: Opportunities and future directions // *Acta Histochemica*. – 2021. – Vol. 123 (7). – P. 151785. doi: <https://doi.org/10.1016/j.acthis.2021.151785>

NEW CATIONIC CHLORIN AS POTENTIAL AGENT FOR ANTIMICROBIAL PHOTODYNAMIC THERAPY

Suvorov N.V.¹, Shchelkova V.V.^{2,3}, Rysanova E.V.², Bagatelia Z.T.⁴, Diachenko D.A.⁴, Afaniutin A.P.⁵, Vasil'ev Yu.L.^{1,4}, Diachkova E.Yu.⁴, Santana Santos I.C.⁶, Grin M.A.¹

¹Institute of Fine Chemical Technologies, MIREA-Russian Technological University, Moscow, Russia

²Moscow Regional Research and Clinical Institute, Moscow, Russia

³N. Kosygin Russian State University, Moscow, Russia

⁴I.M. Sechenov First Moscow State Medical University (Sechenov University), Moscow, Russia

⁵AveDent, Dental Clinic, Orel, Russia

⁶São Carlos School of Engineering, University of São Paulo, São Paulo, Brazil

Abstract

Multiple drug resistance is a major global health security risk. Increasing resistance of bacteria to existing drugs puts on the agenda the search for alternative ways to combat antibiotic-resistant pathogens. One of these innovative methods is antimicrobial photodynamic therapy (APDT), which is equally effective against antibiotic-sensitive and antibiotic-resistant pathogens. The most effective photosensitizers (PS) for APDT are molecules containing positively charged groups in their composition. In this work, we have obtained a new cationic derivative of natural chlorin containing a pyridazine group in its composition, the introduction of which occurs using click chemistry approaches. The antimicrobial photoinduced cytotoxicity of the proposed cationic PS, as well as its uncharged precursor, was assessed against a number of gram-positive and gram-negative bacteria: *S. aureus*, *K. pneumoniae*, *E. faecalis*, *P. aeruginosa*. It has been shown that cationic chlorin exhibits an increased bactericidal effect when irradiated with light ($\lambda = 660$ nm, $P_s = 70.73$ mW/cm²) compared to its base form. When microbial suspensions were incubated with 24 μ M cationic PS and subsequently irradiated, a significant bactericidal effect was observed against all of the aforementioned bacteria. As a result of microbiological studies, it was demonstrated that the proposed cationic PS exhibits high photoinduced antimicrobial activity.

Key words: antimicrobial PDT, antibiotic resistance, antimicrobial activity, chlorophyll, chlorin e6.

For citations: Suvorov N.V., Shchelkova V.V., Rysanova E.V., Bagatelia Z.T., Diachenko D.A., Afaniutin A.P., Vasil'ev Yu.L., Diachkova E.Yu., Santana Santos I.C., Grin M.A. New cationic chlorin as potential agent for antimicrobial photodynamic therapy, *Biomedical Photonics*, 2024, vol. 13, no. 3, pp. 14–19. doi: 10.24931/2413–9432–2024–13–3–14–19

Contacts: Suvorov N.V., e-mail: suvorov.nv@gmail.com

НОВЫЙ КАТИОННЫЙ ХЛОРИН КАК ПОТЕНЦИАЛЬНЫЙ АГЕНТ ДЛЯ АНТИМИКРОБНОЙ ФОТОДИНАМИЧЕСКОЙ ТЕРАПИИ

Н.В. Суворов¹, В.В. Щелкова^{2,3}, Е.В. Русанова², З.Т. Багателия⁴, Д.А. Дьяченко⁴, А.П. Афанютин⁵, Ю.Л. Васильев^{1,4}, Е.Ю. Дьячкова⁴, И.К. Сантана Сантос⁶, Грин М.А.¹

¹Институт тонких химических технологий, РТУ МИРЭА, Москва, Россия

²Московский областной научно-исследовательский клинический институт им. М.Ф. Владимирского, Москва, Россия

³Российский государственный университет им. А.Н. Косыгина, Москва, Россия

⁴Первый МГМУ им. И.М. Сеченова (Сеченовский Университет), Москва, Россия

⁵Стоматологическая клиника АвеДент, Оре́л, Россия

⁶Инженерная школа Сан-Карлоса, Университет Сан-Паулу, Сан-Паулу, Бразилия

Резюме

Множественная устойчивость микроорганизмов к антибиотикам является одним из основных рисков для безопасности в области глобального здравоохранения. Нарастание резистентности бактерий к уже имеющимся препаратам поставили на повестку дня поиск альтернативных способов борьбы с антибиотикорезистентными возбудителями инфекций. Одним из таких инновационных методов

является антимикробная фотодинамическая терапия (АФДТ) одинаково эффективная против антибиотикочувствительных и антибиотикорезистентных возбудителей. Наиболее эффективными фотосенсибилизаторами (ФС) для АФДТ являются молекулы, содержащие положительно-заряженные группы в своем составе. В настоящей работе нами было получено новое катионное производное природного хлорина, содержащее пиридазиновую группу в своем составе, введение которой происходит с использованием подходов click-химии. Противомикробную фотоиндуцированную цитотоксичность предлагаемого катионного ФС, а также его незаряженного предшественника, оценивали в отношении ряда грамположительных и грамотрицательных бактерий: *S. aureus*, *K. pneumoniae*, *E. faecalis*, *P. aeruginosa*. Показано, что катионный хлорин обладает повышенным бактерицидным действием при облучении светом ($\lambda = 660$ нм, $P_s = 70,73$ мВт/см²) по сравнению со своей основной формой. При инкубировании микробных суспензий с раствором катионного ФС в концентрации 24 мкМ и последующим облучением наблюдался заметный бактерицидный эффект в отношении всех вышеперечисленных бактерий. В результате проведенных микробиологических исследований показано, что предлагаемый катионный ФС обладает высокой фотоиндуцированной антимикробной активностью.

Ключевые слова: антимикробная ФДТ, антибиотикорезистентность, противомикробная активность, хлорофилл, хлорин еб.

Для цитирования: Суворов Н.В., Щелкова В.В., Русанова Е.В., Багателья З.Т., Дьяченко Д.А., Афанютин А.П., Васильев Ю.Л., Дьячкова Е.Ю., Сантана Сантос И.К., Грин М.А. Новый катионный хлорин как потенциальный агент для антимикробной фотодинамической терапии // Biomedical Photonics. – 2024. – Т. 13, № 3. – С. 14–19. doi: 10.24931/2413–9432–2024–13–3–14–19

Контакты: Суворов Н.В., e-mail: suvorov.nv@gmail.com

Introduction

Multiple antibiotic resistance is a major global health security risk. According to the WHO, already in 2019, 1.27 million deaths worldwide were directly related to drug-resistant infections. If this problem is not addressed, it is predicted that by 2050 the number of such deaths will increase to 10 million annually [1, 2]. According to the Central Research Institute of Epidemiology of Rospotrebnadzor, the number of nosocomial infections in Russia annually affects 2-2.5 million (1.5% of the population). The increasing bacterial resistance to existing drugs, coupled with poor bioavailability and lack of structures that could potentially form the basis of new antibiotics, have put the search for alternative ways to combat antibiotic-resistant pathogens on the agenda.

One such innovative method is antimicrobial photodynamic therapy (APDT) for localized infections [3-6], equally effective against antibiotic-sensitive and antibiotic-resistant pathogens. Antimicrobial photodynamic therapy (APDT) is based on the use of a photosensitizer (PS) drug and harmless visible light. Photosensitizers are capable, when exposed to light of a certain wavelength corresponding to their maximum absorption, to cause the formation of cytotoxic agents, in particular singlet oxygen, stimulating oxidative destruction of the main components (unsaturated lipids, protein channels and enzymes) of cell membranes – the life-supporting structures of microbial cells [7]. Photo-oxidative processes in the lipid bilayer of cell membranes lead to the formation of pores and disruption of cellular permeability barriers. The death of a microbial cell occurs as a result of the leakage of cellular metabolites, primarily potassium ions and protons, and dissipation of the membrane potential.

One of the main advantages of antimicrobial photodynamic therapy is the multiple nature of the

oxidative destruction of microbial target cells, which prevents the development of resistance to subsequent cycles of photodynamic effects. In addition, since the bactericidal effect of APDT is local in nature, it does not have a systemic detrimental effect on the saprophytic flora of the body. The use of APDT thus solves two main problems of modern antibiotic therapy: high resistance of pathogenic microorganisms to antibiotics and systemic toxicity [8-10].

To date, many PS have been synthesized for antimicrobial PDT, both based on tetrapyrrole compounds and using other dyes. Unlike synthetic dyes, derivatives of natural chlorins have a number of advantages. The main sources of such compounds are plants and algae containing chlorophyll. Such raw materials are easily accessible and cheap, and methods for extracting pigment from them are not labor-intensive. Thanks to the reduced pyrrole ring, chlorophyll A derivatives exhibit absorption in the near-IR region with high extinction values, which allows PDT of deep-lying zones [5].

The most effective photosensitizers for APDT are molecules containing positively charged groups in their composition. In the 90s, it was shown that there is a difference in susceptibility to APDT between gram-positive and gram-negative bacteria, which is associated with their structure: gram-positive bacteria have a cytoplasmic membrane surrounded by a porous cell wall consisting of peptidoglycan and lipoteichoic acid, which allows the photosensitizer to easily bind with it, and the membrane of gram-negative bacteria consists of outer and inner cytoplasmic membranes separated by a layer of peptidoglycan [11-13]. Neutral, anionic and cationic photosensitizer molecules bind equally well to gram-positive bacteria, while only cationic or neutral photosensitizers can bind to gram-negative bacteria. At the moment, a large number of cationic derivatives of natural chlorins containing both alkylammonium groups

and quaternized heteroaromatic fragments have been synthesized [14-18].

Previously, our research group obtained a derivative of natural chlorin, into which a residue of nicotinic acid was introduced with its subsequent quaternization [19]. This compound had both high photoinduced toxicity towards bacterial cells, as well as biofilms based on them. However, the complexity of the synthesis of this compound complicates its further implementation in practice. In this work, we have proposed an approach that makes it possible to introduce a heterocyclic fragment into the chlorin molecule using one stage inverse electron demand Diels-Alder reaction click-reaction, and also studied the photoinduced toxicity of the resulting compound and its cationic derivative against gram-positive and gram-negative bacteria.

Materials and Methods

Chemistry

Solvents were purified and prepared according to standard procedures. Silica gel 40/60 (Merck, Germany) was used for column chromatography. Absorption spectra were obtained on a Shimadzu spectrophotometer UV 1800 UV/VIS in 10 mm thick quartz cuvettes in chloroform and water. The NMR spectrum was recorded on Bruker DPX 300 spectrometer in CDCl_3 . The synthesis of photosensitizers **1** and **2** was carried out according to a previously described method [20]. Cationic derivative **3** was obtained by reacting compound **2** (25 mg; 0.033 mmol) with methyl iodide (145.5 mg; 1.025 mmol) in acetonitrile (1 ml) at 60°C for 2 hours. The solvent was evaporated under reduced pressure. The target product was isolated using column chromatography (DCM/MeOH/AcOH, 450/10/1, v/v/v). The yield of compound **3** was 63.3% (19 mg). ^1H NMR (300 MHz, CDCl_3 , δ , ppm): 9.77 (H, s, 10-H), 9.60 (H, d, $J = 4.7$ Hz, 5'-H), 9.20 (H, s, 5-H), 8.71+8.72 (H, s, 20-H), 8.07 (H, d, $J = 4.7$ Hz, 6'-H), 7.62 (2H, m, o-Phe), 7.12 (H, m, p-Phe), 7.02 (H, m, o-Phe), 5.42 (H, d, $J = 18.8$ Hz, 15 1 -CH $_2^a$), 4.46 (2H, m, 18-H, 17-H), 4.30 (3H, s 13 2 -CH $_3$), 3.81 (3H, s, 15 3 -CH $_3$), 3.80 (2H, k, $J = 7.7$ Hz, 8 1 -CH $_2$), 3.71 (3H, s, 17 4 -CH $_3$), 3.62 (3H, s, 12-CH $_3$), 3.53 (3H, s, *N*-CH $_3$), 3.20 (3H, s, 7-CH $_3$), 2.95 (3H, s, 2-CH $_3$), 2.60 (H, m, 17 2 -CH $_2^a$), 2.28 (2H, m, 17 1 -CH $_2^a$, 17 1 -CH $_2^b$), 1.84 (H, m, 17 1 -CH $_2^b$), 1.75 (3H, d, $J = 18.1$ Hz, 18-CH $_3$), 1.74 (3H, t, $J = 7.7$ Hz, 8 2 -CH $_3$), -1.33 (H, s, I - NH), -1.72 (H, s, III - NH). ESI-MS: m/z calc. for $\text{C}_{46}\text{H}_{49}\text{N}_6\text{O}_6$: 781.37, found: $[\text{M}+\text{H}]^+$, 782.38, $[\text{M}+2\text{H}]^{2+}$ 391.69. UV/VIS (CHCl_3), λ_{max} , nm (ϵ , $\text{M}^{-1}\text{cm}^{-1}$): 395 (180000), 497 (17500), 686 (44000). To prepare a water-soluble form of compounds **2** and **3**, 4% Kolliphor ELP solution in water was used. A weighed portion of the corresponding chlorin (1 mg) was dissolved in dichloromethane (2 ml) and added to 4% Kolliphor solution in water (3 ml). The resulting mixture was stirred in a flow of argon at a temperature of 41°C until the organic phase was completely removed. The resulting emulsion was passed through a syringe filter with a pore diameter of 200 nm.

Microbiology

The source of non-monochromatic LED red radiation was a single-band laser ($\lambda = 660$ nm, $P_s = 70.73$ mW/cm 2). Exposure of the PS in the microbial suspension before irradiation is 30 min. The dose of light during irradiation is 20 J/cm 2 .

To assess the antibacterial activity of PS, we used suspensions of daily microbial cultures of *S. aureus* ATCC 25923 ($n = 15$), *K. pneumoniae* ATCC 13883 ($n = 15$), *E. faecalis* ATCC 29212 ($n = 15$), *P. aeruginosa* ATCC 27853 ($n = 15$), which are common causative agents of inflammatory processes in the ear and upper respiratory tract. The concentration of the microbial suspension in the experiment was 3×10^3 CFU/ml. Control – test strains that were under equal conditions, but were not exposed to PS and irradiation. 200 μl of a suspension of microorganisms was added to the wells of a microplate and 2, 8 and 12 μl of 0.4 mM solution of PS **2** and **3** were injected, respectively. After exposure and irradiation, the microplates were incubated for 24 hours at $T = 37^\circ\text{C}$. To determine the survival rate of microorganisms, the method of surface inoculation using a spatula on solid nutrient media (Koch plate method) was used. After thermostating the control crops, we calculated and expressed the results obtained on solid media.

Formulas for calculating the number of viable microorganisms:

1. If the number of colonies exceeds 10:

$$M = a * 10n/V,$$

where a is the average number of colonies grown after sowing from a given dilution; 10 – dilution factor; n is the serial number of the dilution from which the sowing was made; V – volume of suspension taken for sowing, cm 3 .

2. If the number of colonies is less than 10, but more than 4:

$$M = c/V * n,$$

where c is the number of colonies counted in the dish, V is the volume of the suspension taken for inoculation, cm 3 , n is the serial number of the dilution from which the inoculation was made.

3. If there are from 1 to 3 colonies, then we accept as – “microorganisms are present in quantities less than $1 \times V$ per cm 3 ” (V is the dilution factor).

The calculation data is included in Table 1. Statistical analysis of the obtained data was carried out using the SPSS application package Statistics 21.0 and Rstudio 4.2.2. Mean values, standard deviations, and medians were determined. When comparing groups, parametric (ANOVA) and nonparametric methods (Kruskal–Wallis, Mann–Whitney, Wilcoxon) estimates were used depending on the normality of the sample distribution, which was determined using the Shapiro–Wilk test. The results were considered statistically significant at a confidence level of at least 95%.

Results and discussion

Previously, we carried out a one-step functionalization of the chlorin e6 trimethyl ester molecule, which allowed us to introduce a pyridazine group into pyrrole A using the inverse electron demand Diels-Alder reaction (Fig. 1) [20]. It was shown that this reaction occurs in high yields without changing the properties of the original PS. In this work, the reaction of chlorin e6 trimethyl ester with 3-phenyl-1,2,4,5-tetrazine was carried out to obtain pyridazine-substituted derivative **2**. The resulting PS was reacted with methyl iodide to obtain quaternized derivative **3**. Thus, we

obtained chlorins containing heterocyclic fragments at the periphery of the macrocycle, in neutral and cationic form.

The resulting PS **2** and **3** are insoluble in water, so their water-soluble forms were prepared in the form of an emulsion in 4% Kolliphor ELP, which is a clinically approved solubilizer.

The antimicrobial effect of the obtained PS was assessed *in vitro* against bacteria *S. aureus*, *K. pneumoniae*, *E. faecalis* and *P. aeruginosa*. By counting the number of colonies, the probability of the effect of cationic and anionic PS on Gram “-” and “+” microorganisms were determined (Table 1).

Таблица 1
Таблица подсчета колоний

Table 1
Colony count table

Бактерия Bacteria	Концентрация ФС (мкМ) PS concentration (μM)	PS 2		PS 3		Контроль Control
		Среднее количество микроорганизмов Average number of microorganisms M±m	КОЕ/мл CFU/ml	Среднее количество микроорганизмов Average number of microorganisms M±m	КОЕ/мл CFU/ml	
<i>S. aureus</i>	4	77.5±16.9	7.6*10 ³	18.3±14.6	1.8*10 ³	Сливной рост Confluent growth 2*10 ⁶
	16	16.9±8.6	1.7*10 ³	3.7±4.4	4*10 ²	
	24	2.6±2.9	микроорганизмы присутствуют в количестве менее 1 на см ³ microorganisms are present in less than 1 per cm ³	0.8±1.4	микроорганизмы присутствуют в количестве менее 1 на см ³ microorganisms are present in less than 1 per cm ³	
<i>K. pneumoniae</i>	4	153.1±4.3	1.5*10 ⁴	114.4±17.8	1.1*10 ⁴	Сливной рост Confluent growth 6*10 ⁶
	16	20.1±2.5	2*10 ³	53.6±9.6	5.4*10 ³	
	24	0.4±1	микроорганизмы присутствуют в количестве менее 1 на см ³ microorganisms are present in less than 1 per cm ³	1.8±2.7	микроорганизмы присутствуют в количестве менее 1 на см ³ microorganisms are present in less than 1 per cm ³	
<i>E. faecalis</i>	4	149.3±4.2	1.5*10 ⁴	43.8±4.3	4.4*10 ³	Сливной рост Confluent growth 4*10 ⁶
	16	41.2±3.2	4.1*10 ³	9.1±1.6	9*10 ²	
	24	5.5±6.8	6*10 ²	0.5±1	микроорганизмы присутствуют в количестве менее 1 на см ³ microorganisms are present in less than 1 per cm ³	
<i>P. aeruginosa</i>	4	162.1±2.8	1.6*10 ⁴	114.4±7.81	1.4*10 ⁴	Сливной рост Confluent growth 5*10 ⁶
	16	17.6±4.8	1.8*10 ³	13.3±4.9	1.3*10 ³	
	24	1.8±2.5	микроорганизмы присутствуют в количестве менее 1 на см ³ microorganisms are present in less than 1 per cm ³	1.4±2.5	микроорганизмы присутствуют в количестве менее 1 на см ³ microorganisms are present in less than 1 per cm ³	

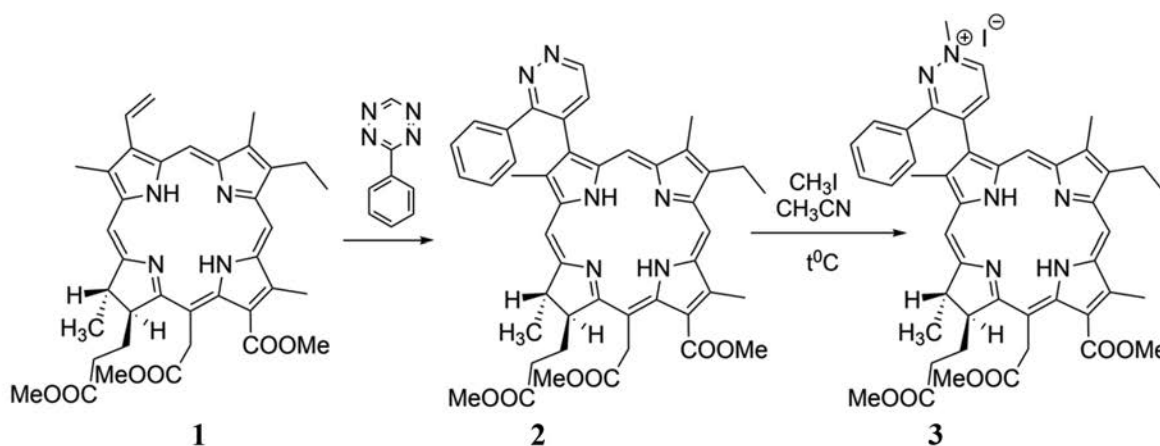


Рис. 1. Синтез пиридазин-замещенных производных хлорина.
Fig. 1. Synthesis of pyridazine-substituted chlorin derivatives.

Analysis of the data obtained showed that all PS have inhibitory properties towards the tested microorganisms. When a microbial suspension was incubated with 4 μM and 16 μM PS **2** and **3** followed by irradiation, a rather bacteriostatic effect was detected or a slight increase in microbial numbers from the initial concentration of microorganisms was observed, while in the control a stable confluent growth was observed. When using 24 μM PS, a noticeable bactericidal effect is observed. Negative dynamics of microorganisms is observed depending on the concentration of PS in the suspension of microorganisms. When comparing the difference between the use of PS **2** and **3**, a significant decrease in the number of colonies can be traced when exposed to cationic PS **3** compared to PS **2** in the case of gram-positive bacteria. When comparing the effectiveness against gram-negative bacteria, the cationic derivative **3** was more effective compared to the pyridazine-substituted derivative **2**, but the same significant difference in biological activity as in the case of gram-positive bacteria was not detected. The results obtained from the study of photoinduced cytotoxicity suggest the

high efficiency of PS **3** compared to similar chlorophyll A derivatives [21, 22].

Conclusions

Studies have shown that the proposed cationic photosensitizer, obtained using the tetrazine-alkene addition reaction starting from trimethyl ester of chlorin e6, has high photoinduced antimicrobial activity against both gram-positive and gram-negative bacteria. An additional advantage of the proposed PS is the ease of its preparation, and the raw materials for its synthesis are readily available. We are currently planning to conduct a study of the effectiveness of the resulting PS on bacteria in biofilms, as well as to carry out in vivo experiments on models of wound infections.

Acknowledgments

The work was carried out with the support of the Ministry of Science and Higher Education of the Russian Federation (government assignment №075-00701-24-07 dated 04/03/2024; FSFZ-2024-0013).

REFERENCES

- Macias J., Kahly O., Pattik-Edward R., Khan S., et al. Sepsis: A Systematic Review of Antibiotic Resistance and Antimicrobial Therapies, *Mod Res Inflamm*, 2022, vol. 11, no. 02, pp. 9–23. doi: 10.4236/mri.2022.112002.
- Murray C. J., Ikuta K. S., Sharara F., Swetschinski L., et al. Global burden of bacterial antimicrobial resistance in 2019: a systematic analysis, *Lancet*, 2022, vol. 399, no. 10325, pp. 629–655. doi: 10.1016/S0140-6736(21)02724-0.
- Hamblin M. R., Hasan T. Photodynamic therapy: A new antimicrobial approach to infectious disease?, *Photochem Photobiol Sci*, 2004, vol. 3, no. 5, pp. 436–450. doi: 10.1039/b311900a.
- Dai T., Huang Y. Y., Hamblin M. R. Photodynamic therapy for localized infections-State of the art, *Photodiagnosis Photodyn Ther*, 2009, vol. 6, no. 3–4, pp. 170–188. doi: 10.1016/j.pdpdt.2009.10.008.
- Suvorov N., Pogorilyy V., Diachkova E., Vasil'ev Y., et al. Derivatives of natural chlorophylls as agents for antimicrobial photodynamic

ЛИТЕРАТУРА

- Macias J., Kahly O., Pattik-Edward R., Khan S., Qureshi A., Shaik A., et al. Sepsis: A Systematic Review of Antibiotic Resistance and Antimicrobial Therapies // *Mod. Res. Inflamm.* – 2022. – Vol. 11, № 02. – P. 9–23. doi: 10.4236/mri.2022.112002.
- Murray C.J., Ikuta K.S., Sharara F., Swetschinski L., Robles Aguilar G., et al. Global burden of bacterial antimicrobial resistance in 2019: a systematic analysis // *Lancet*. – 2022. – Vol. 399, № 10325. – P. 629–655. doi: 10.1016/S0140-6736(21)02724-0.
- Hamblin M.R., Hasan T. Photodynamic therapy: A new antimicrobial approach to infectious disease? // *Photochem. Photobiol. Sci.* – 2004. – Vol. 3, № 5. – P. 436–450. doi: 10.1039/b311900a.
- Dai T., Huang Y.Y., Hamblin M.R. Photodynamic therapy for localized infections-State of the art // *Photodiagnosis Photodyn. Ther.* – 2009. – Vol. 6, № 3–4. – P. 170–188. doi: 10.1016/j.pdpdt.2009.10.008.
- Suvorov N., Pogorilyy V., Diachkova E., Vasil'ev Y., Mironov A., et al. Derivatives of natural chlorophylls as agents for antimicrobial photo-

- therapy, *Int J Mol Sci*, 2021, vol. 22, no. 12, p. 6392. doi: 10.3390/ijms22126392.
6. de Souza da Fonseca A., de Paoli F., Mencialha A. L. Photodynamic therapy for treatment of infected burns, *Photodiagnosis Photodyn Ther*, 2022, vol. 38, p. 102831. doi: 10.1016/j.pdpdt.2022.102831.
7. Huang L., Xuan Y., Koide Y., Zhiyentayev T., et al. Type I and Type II mechanisms of antimicrobial photodynamic therapy: An in vitro study on gram-negative and gram-positive bacteria, *Lasers Surg Med*, 2012, vol. 44, no. 6, pp. 490–499. doi: 10.1002/lsm.22045.
8. Bustamante V., Palavecino C. E. Effect of photodynamic therapy on multidrug-resistant *Acinetobacter baumannii*: A scoping review, *Photodiagnosis Photodyn Ther*, 2023, vol. 43, p. 103709. doi: 10.1016/j.pdpdt.2023.103709.
9. Jao Y., Ding S. J., Chen C. C. Antimicrobial photodynamic therapy for the treatment of oral infections: A systematic review, *J Dent Sci*, 2023, vol. 18, no. 4, pp. 1453–1466. doi: 10.1016/j.jds.2023.07.002.
10. Hamblin M. R. Antimicrobial photodynamic inactivation: a bright new technique to kill resistant microbes, *Curr Opin Microbiol*, 2016, vol. 33, pp. 67–73. doi: 10.1016/j.mib.2016.06.008.
11. Bertolini G., Rossi F., Valduga G., Jori G., et al. Photosensitizing activity of water- and lipid-soluble phthalocyanines on *Escherichia coli*, *FEMS Microbiol Lett*, 1990, vol. 71, no. 1–2, pp. 149–155. doi: 10.1111/j.1574-6968.1990.tb03814.x.
12. Nitzan Y., Gutterman M., Malik Z., Ehrenberg B. Inactivation of Gram-Negative Bacteria By Photosensitized Porphyrins, *Photochem Photobiol*, 1992, vol. 55, no. 1, pp. 89–96. doi: 10.1111/j.1751-1097.1992.tb04213.x.
13. Merchat M., Bertolini G., Giacomini P., Villanueva A., et al. Meso-substituted cationic porphyrins as efficient photosensitizers of gram-positive and gram-negative bacteria, *J Photochem Photobiol B Biol*, 1996, vol. 32, no. 3, pp. 153–157. doi: 10.1016/1011-1344(95)07147-4.
14. Kustov A. V., Kustova T. V., Belykh D. V., Khudyaeva I. S., et al. Synthesis and investigation of novel chlorin sensitizers containing the myristic acid residue for antimicrobial photodynamic therapy, *Dye Pigment*, 2020, vol. 173, p. 107948. doi: 10.1016/j.dyepig.2019.107948.
15. Ryazanova O., Voloshin I., Dubey I., Dubey L., et al. Fluorescent Studies on Cooperative Binding of Cationic Pheophorbide-a Derivative to Polyphosphate, *Ann NY Acad Sci*, 2008, vol. 1130, no. 1, pp. 293–299. doi: 10.1196/annals.1430.033.
16. Miyatake T., Hasunuma Y., Mukai Y., Oki H., et al. Assemblies of ionic zinc chlorins assisted by water-soluble polypeptides, *Bioorganic Med Chem*, 2016, vol. 24, no. 5, pp. 1155–1161. doi: 10.1016/j.bmc.2016.01.054.
17. Kustov A. V., Belykh D. V., Smirnova N. L., Venediktov E. A., et al. Synthesis and investigation of water-soluble chlorophyll pigments for antimicrobial photodynamic therapy, *Dye Pigment*, 2018, vol. 149, pp. 553–559. doi: 10.1016/j.dyepig.2017.09.073.
18. Morshnev P. K., Kustov A. V., Drondel E. A., Khlydeev I. I., et al. The interaction of chlorin photosensitizers for photodynamic therapy with blood transport proteins, *J Mol Liq*, 2023, vol. 390, p. 123116. doi: 10.1016/j.molliq.2023.123116.
19. Brusov S. S., Koloskova Y. S., Grin M. A., Tiganova I. G., et al. New cationic purpurinimide for photodynamic inactivation of *Pseudomonas Aeruginosa* biofilms, *Russ Biother J*, 2014, vol. 13, no. 4, pp. 59–63.
20. Suvorov N. V., Cheskov D. A., Mironov A. F., and Grin M. A. Inverse electron demand Diels–Alder reaction as a novel method for functionalization of natural chlorins, *Mendelev Commun*, 2019, vol. 29, no. 2, pp. 206–208. doi: 10.1016/j.mencom.2019.03.031.
21. Garcia de Carvalho G., Pacheco Mateo R., Costa e Silva R., Maquera Huacho P. M., et al. Chlorin-based photosensitizer under blue or red-light irradiation against multi-species biofilms related to periodontitis, *Photodiagnosis Photodyn Ther*, 2023, vol. 41, p. 103219. doi: 10.1016/j.pdpdt.2022.103219.
22. Yang W., Yoon Y., Lee Y., Oh H., et al. Photosensitizer-peptoid conjugates for photoinactivation of Gram-negative bacteria: structure-activity relationship and mechanistic studies, *Org Biomol Chem*, 2021, vol. 19, no. 29, pp. 6546–6557. doi: 10.1039/d1ob00926e.
- todynamic therapy // *Int. J. Mol. Sci.* – 2021. – Vol. 22, № 12. – P. 6392. doi: 10.3390/ijms22126392.
6. de Souza da Fonseca A., de Paoli F., Mencialha A.L. Photodynamic therapy for treatment of infected burns // *Photodiagnosis Photodyn Ther.* – 2022. – Vol. 38. – P. 102831. doi: 10.1016/j.pdpdt.2022.102831.
7. Huang L., Xuan Y., Koide Y., Zhiyentayev T., Tanaka M., et al. Type I and Type II mechanisms of antimicrobial photodynamic therapy: An in vitro study on gram-negative and gram-positive bacteria // *Lasers Surg. Med.* – 2012. – Vol. 44, № 6. – P. 490–499. doi: 10.1002/lsm.22045.
8. Bustamante V., Palavecino C.E. Effect of photodynamic therapy on multidrug-resistant *Acinetobacter baumannii*: A scoping review // *Photodiagnosis Photodyn Ther.* – 2023. – Vol. 43. – P. 103709. doi: 10.1016/j.pdpdt.2023.103709.
9. Jao Y., Ding S.J., Chen C.C. Antimicrobial photodynamic therapy for the treatment of oral infections: A systematic review // *J. Dent. Sci.* – 2023. – Vol. 18, № 4. – P. 1453–1466. doi: 10.1016/j.jds.2023.07.002.
10. Hamblin M.R. Antimicrobial photodynamic inactivation: a bright new technique to kill resistant microbes // *Curr. Opin. Microbiol.* – 2016. – Vol. 33. – P. 67–73. doi: 10.1016/j.mib.2016.06.008.
11. Bertolini G., Rossi F., Valduga G., Jori G., van Lier J. Photosensitizing activity of water- and lipid-soluble phthalocyanines on *Escherichia coli* // *FEMS Microbiol. Lett.* – 1990. – Vol. 71, № 1–2. – P. 149–155. doi: 10.1111/j.1574-6968.1990.tb03814.x.
12. Nitzan Y., Gutterman M., Malik Z., Ehrenberg B. Inactivation of Gram-Negative Bacteria By Photosensitized Porphyrins // *Photochem. Photobiol.* – 1992. – Vol. 55, № 1. – P. 89–96. doi: 10.1111/j.1751-1097.1992.tb04213.x.
13. Merchat M., Bertolini G., Giacomini P., Villanueva A., Jori G. Meso-substituted cationic porphyrins as efficient photosensitizers of gram-positive and gram-negative bacteria // *J. Photochem. Photobiol. B Biol.* – 1996. – Vol. 32, № 3. – P. 153–157. doi: 10.1016/1011-1344(95)07147-4.
14. Kustov A. V., Kustova T. V., Belykh D. V., Khudyaeva I.S., Berezin D.B. Synthesis and investigation of novel chlorin sensitizers containing the myristic acid residue for antimicrobial photodynamic therapy // *Dye. Pigment.* – 2020. – Vol. 173. – P. 107948. doi: 10.1016/j.dyepig.2019.107948.
15. Ryazanova O., Voloshin I., Dubey I., Dubey L., Zozulya V. Fluorescent Studies on Cooperative Binding of Cationic Pheophorbide-a Derivative to Polyphosphate // *Ann. N. Y. Acad. Sci.* – 2008. – Vol. 1130, № 1. – P. 293–299. doi: 10.1196/annals.1430.033.
16. Miyatake T., Hasunuma Y., Mukai Y., Oki H., Watanabe M., et al. Assemblies of ionic zinc chlorins assisted by water-soluble polypeptides // *Bioorganic Med. Chem.* – 2016. – Vol. 24, № 5. – P. 1155–1161. doi: 10.1016/j.bmc.2016.01.054.
17. Kustov A. V., Belykh D. V., Smirnova N.L., Venediktov E.A., Kudayarova T. V., et al. Synthesis and investigation of water-soluble chlorophyll pigments for antimicrobial photodynamic therapy // *Dye. Pigment.* – 2018. – Vol. 149. – P. 553–559. doi: 10.1016/j.dyepig.2017.09.073.
18. Morshnev P.K., Kustov A. V., Drondel E.A., Khlydeev I.I., Abramova O.B., et al. The interaction of chlorin photosensitizers for photodynamic therapy with blood transport proteins // *J. Mol. Liq.* – 2023. – Vol. 390. – P. 123116. doi: 10.1016/j.molliq.2023.123116.
19. Brusov S.S., Koloskova Y.S., Grin M.A., Tiganova I.G., Pagina O.E., et al. New cationic purpurinimide for photodynamic inactivation of *Pseudomonas Aeruginosa* biofilms // *Russ. Biother. J.* – 2014. – Vol. 13, № 4. – P. 59–63.
20. Suvorov N. V., Cheskov D.A., Mironov A.F., Grin M.A. Inverse electron demand Diels–Alder reaction as a novel method for functionalization of natural chlorins // *Mendelev Commun.* – 2019. – Vol. 29, № 2. – P. 206–208. doi: 10.1016/j.mencom.2019.03.031.
21. Garcia de Carvalho G., Pacheco Mateo R., Costa e Silva R., Maquera Huacho P.M., de Souza Rastelli A.N., et al. Chlorin-based photosensitizer under blue or red-light irradiation against multi-species biofilms related to periodontitis // *Photodiagnosis Photodyn Ther.* – 2023. – Vol. 41. – P. 103219. doi: 10.1016/j.pdpdt.2022.103219.
22. Yang W., Yoon Y., Lee Y., Oh H., Choi J., et al. Photosensitizer-peptoid conjugates for photoinactivation of Gram-negative bacteria: structure-activity relationship and mechanistic studies // *Org. Biomol. Chem.* – 2021. – Vol. 19, № 29. – P. 6546–6557. doi: 10.1039/d1ob00926e.

RESULTS OF MICROSURGICAL RESECTION OF GLIOBLASTOMAS UNDER ENDOSCOPIC AND FLUORESCENT CONTROL

Rynda A.Yu., Olyushin V.E., Rostovtsev D.M., Zabrodskaya Yu.M., Papayan G.V.

Russian Neurosurgical Institute named after prof. A.L. Polenov – a branch of the National Medical Research Center named after V.A. Almazov Ministry of Health of Russia, St. Petersburg, Russia

Abstract

Overall survival and recurrence-free survival (RFS) in patients with glioblastoma directly depend on the radicality of tumor resection. According to a number of literature sources, it is known that endoscopic surgeries under fluorescence control increase the rate of total resection. However, until now, there is little data on whether endoscopic resection with fluorescence control affects RFS and overall survival of patients with glioblastoma. The aim of our study was to investigate the effect of intraoperative endoscopic and fluorescence control on overall survival and RFS in patients with glioblastoma. A retrospective single-center analysis was performed in 20 patients with glioblastoma. Ten patients underwent tumor resection using an operating microscope with endoscopic and fluorescence control. In 5 patients, 5-aminolevulinic acid (5-ALA) (alasens) at a dose of 20 mg/kg was used as a photosensitizer, in 5 patients, chlorin e6 (photoditazine) at a dose of 1 mg/kg. Ten patients underwent resection under endoscopic control, but without fluorescence control. Both cohorts of patients were comparable in age, functional status, tumor localization, adjuvant treatment methods, and molecular status. The criteria for assessing the effectiveness of the study in the groups were: the radicality of the surgical intervention according to postoperative magnetic resonance imaging with contrast enhancement, as well as the median RFS and OS in patients. In the group of combined surgery under microscopic and fluorescence control with an endoscope, the rate of total tumor resection was higher than in the group of patients who underwent only surgery under a microscope and an endoscope without fluorescence control (100% versus 60%; $p = 0.002$). Median OS (20.2 months (95% CI 11.9–28.6) versus 16.3 months (95% CI 11.0–20.9); ($p = 0.003$)) and median RFS (11.7 months (95% CI 9.8–15.7) versus 9.8 months (95% CI 6.1–13.4) ($p = 0.04$)), were also statistically significantly higher compared to the group of patients who received treatment to the same extent, but without fluorescence control. As our experience has shown, the use of fluorescence control during tumor resection in patients with glioblastoma with endoscopic assistance is certainly necessary, given the technical capabilities available, as it has a positive effect on the treatment results for this category of patients.

Key words: glioblastoma, endoscopy, fluorescent resection, results, survival, 5-ALA, chlorin e6.

For citations: Rynda A.Yu., Olyushin V.E., Rostovtsev D.M., Zabrodskaya Yu.M., Papayan G.V. Results of microsurgical resection of glioblastomas under endoscopic and fluorescent control, *Biomedical Photonics*, 2024, vol. 13, no. 3, pp. 20–30. doi: 10.24931/2413–9432–2024–13–3–20–30

Contacts: Rynda A.Yu., e-mail: artemii.rynda@mail.ru

РЕЗУЛЬТАТЫ МИКРОХИРУРГИЧЕСКОЙ РЕЗЕКЦИИ ГЛИОБЛАСТОМ ПОД ЭНДОСКОПИЧЕСКИМ И ФЛУОРЕСЦЕНТНЫМ КОНТРОЛЕМ

А.Ю. Рында, В.Е. Олюшин, Д.М. Ростовцев, Ю.М. Забродская, Г.В. Папаян

Российский нейрохирургический институт им. проф. А.Л. Поленова – филиал ФГБУ «Национальный медицинский исследовательский центр имени В.А. Алмазова» Минздрава России, Санкт-Петербург, Россия

Резюме

Общая выживаемость (ОВ) и безрецидивная выживаемость (БРВ) у пациентов с глиобластомой напрямую зависит от радикальности резекции опухоли. Согласно данным ряда авторов эндоскопические операции под флуоресцентным контролем увеличивают частоту тотальной резекции. Однако до сих пор имеется мало данных о влиянии эндоскопической резекции с флуоресцентным контролем на показатели БРВ и ОВ пациентов с глиобластомой. Целью нашего исследования было изучение влияния интраоперационного эндоскопического и флуоресцентного контроля на показатели ОВ и БРВ у пациентов с глиобластомой. Проведен ретроспективный одноцентровый анализ у 20 пациентов с глиобластомой. 10 пациентам выполнена резекция опухоли с использованием операционного микроскопа с эндоскопическим и флуоресцентным контролем. У 5 пациентов в качестве фотосенсибилизатора использовали

5-аминолевулиновую кислоту (5-АЛК) в дозе 20 мг/кг, у 5 пациентов хлорин еб в дозе 1 мг/кг. 10 пациентам выполнена резекция под эндоскопическим контролем, но без флуоресцентного контроля. Обе когорты пациентов были сопоставимы по возрасту, функциональному состоянию, локализации опухоли, методам адьювантного лечения и молекулярному статусу. Критериями оценки эффективности проводимого исследования в группах были: радикальность проведенного оперативного вмешательства по данным послеоперационной магнитно-резонансной томографии с контрастным усилением, а также медианы БРВ и ОВ. В группе комбинированного хирургического вмешательства под микроскопическим и флуоресцентным контролем с эндоскопом частота тотальной резекции опухоли была выше, чем в группе пациентов, перенесших только хирургическое вмешательство под микроскопом и эндоскопом без флуоресцентного контроля (100% против 60%; $p=0,002$). Медиана ОВ в первой группе составила 20,2 мес (95% ДИ 11,9-28,6) против 16,3 мес во второй группе (95% ДИ 11,0-20,9) ($p=0,003$), медиана БРВ 11,7 мес. (95% ДИ 9,8-15,7) против 9,8 мес (95% ДИ 6,1-13,4) ($p=0,04$). соответственно. Как показал наш опыт, использование флуоресцентного контроля во время резекции опухоли у пациентов с глиобластомой при эндоскопической ассистенции положительно отражается на результатах лечения пациентов с глиобластомой и может быть рекомендовано для широкого внедрения в клиническую практику.

Ключевые слова: глиобластома, эндоскопия, флуоресцентная резекция, результаты, выживаемость, 5-АЛК, хлорин еб.

Для цитирования: Рында А.Ю., Олюшин В.Е., Ростовцев Д.М., Забродская Ю.М., Папаян Г.В. Результаты микрохирургической резекции глиобластом под эндоскопическим и флуоресцентным контролем // Biomedical Photonics. – 2024. – Т. 13, № 3. – С. 20–30. doi: 10.24931/2413–9432–2024–13–3–20–30

Контакты: Рында А.Ю., e-mail: artemii.rynda@mail.ru

Despite recent advances in neurooncology and the development of new treatment methods [1–5], the survival rate of patients with glioblastoma remains low [6, 7]. The median overall survival (OS) in this category of patients ranges from 11 to 17 months [6, 7]. Surgical resection is an important step in the treatment of patients with glioblastoma [8]. It has been proven that the use of fluorescence guidance during surgical intervention in patients with glioblastoma increases the OS and RFS rates, which is confirmed by convincing results of prospective randomized neurosurgical studies [9–15].

The main goal of surgical treatment is the complete removal of tumor tissue while maximally preserving the patient's neurological functions. A number of studies have shown that the totality of resection significantly increases the RFS and OS medians compared to subtotal resection in patients with glioblastoma [15–20]. In turn, visualization of fluorescence may be difficult due to the collapse of the edges of the post-resection cavity and a decrease in illumination with an increase in the depth of the resection cavity [10, 12, 14]. This may lead to limitations in microscopic resection under fluorescence control: visible fluorescence of tumor tissue depends on the cell density and cellular metabolism, as well as on adequate exposure of the tumor tissue to blue light [16, 18 – 20].

Several scientific papers have demonstrated that the use of an endoscope with fluorescence control made it possible to increase the degree of resection radicality, and according to data from individual publications, to improve the OS rates in patients with malignant brain tumors [21 – 26]. Information on the use of a combined approach (endoscope and fluorescence) is quite limited, which actualizes the significance of our study. There are also few literature data assessing the impact of fluorescence-guided and endoscope-guided resection of glioblastoma on OS and RFS rates in patients [22, 24–30].

Materials and methods

The study was a retrospective single-center analysis of the effectiveness of fluorescence endoscopic control in the removal of primary glioblastomas in patients [31] who underwent routine microscopic resection under endoscopic control in the period from 2014 to 2016 at the Russian Neurosurgical Research Institute named after prof. A.L. Polenov. The patients were assessed for resection totality, RFS, and OS rates.

Of the 20 patients in both groups, 13 (65%) were men and 7 (35%) were women. The average age was 56.0 years, 4 (20%) patients were over 65 years old.

All 20 patients underwent preoperative MRI with gadolinium contrast enhancement. All patients underwent a preoperative clinical and diagnostic examinations, including examination by specialists (neurologist, therapist, oncologist, ophthalmologist) and laboratory and instrumental research methods (blood and urine tests, electroencephalogram, electrocardiogram). Detailed clinical characteristics of patients in both groups are presented in Table 1.

The study protocol was reviewed by the local ethics committee (Protocol No. 4 dated 17/12/2013). All patients were informed about the course of the surgery. Written consent was obtained from all patients as part of the standard informed consent procedure for surgery.

Inclusion and Exclusion Criteria

Only patients with primary glioblastoma, the localization of which was clearly defined, were included in the study to ensure that the totality of resection could be achieved in all patients. Patients were over 18 years old. Patients who underwent biopsy or required intraoperative neuromonitoring were excluded. Patients without postoperative contrast-enhanced MRI of the brain, patients in severe condition, patients with signs of renal and hepatic insufficiency, chronic viral infections

(hepatitis C, B, HIV infection), and patients with endocrine diseases or metabolic disorders were also excluded.

Surgical stage

Of the 10 patients in the main group, 5 patients received 5-ALA (alasers) as a fluorescence inducer orally, manufactured by the Scientific Center "NIOPIK", Federal State Unitary Enterprise (Russia), at a dose of 20 mg/kg, 8 hours before the intraoperative stage of the operation.

Tumor removal was performed using an intraoperative microscope with fluorescence control (OPMI Pentero 800, Carl Zeiss, Germany).

Five patients of the main group received intravenous fluorescence inducer chlorin e6 (photoditazine), manufactured by OOO VETA-GRAND (Russia), at a dose of 1 mg/kg, dissolved in 200 ml of 0.9% sodium chloride solution, 2 hours before the expected stage of

Таблица 1
Клиническая характеристика пациентов

Table 1
Clinical characteristics of patients

Признак Sign	Эндоскопический контроль Endoscopic control	Эндоскопический и флуоресцентный контроль Endoscopic and fluorescent control	Значение p p value
Количество пациентов Number of patients	10	10	
Возраст / Age			
Границы / Age limits	33-73	41-68	0,8
Медиана / Median age	55,6	56,5	
Пол / Gender			
мужчины / men	7 (70%)	6 (60%)	0,7
женщины / women	3 (30%)	4 (40%)	
Предоперационный индекс Карновского / Preoperative Karnofsky index			
Границы / Index boundaries	70-100	70-100	0,9
Медиана / Median	85	83	
Предоперационный размер опухоли, см³ / Preoperative tumor size, cm³			
Медиана / Median	25,4	27,8	0,7
Границы / Size limits	3,4-37	4,2-44,5	
Преимущественная локализация опухоли / Predominant tumor location			
лобная доля / frontal lobe	3 (30%)	2 (20%)	0,6
теменная доля / parietal lobe	2(20%)	4 (40%)	
височная доля / temporal lobe	4(40%)	4 (40%)	
затылочная доля / occipital lobe	1 (10%)	0 (0%)	
Полушарие / Hemisphere			
правое / right	7 (70%)	4 (40%)	0,01
левое / left	3 (30%)	6 (60%)	
Характер опухоли по данным МРТ головного мозга с контрастным усилением гадолинием Character of the tumor according to MRI of the brain with gadolinium contrast enhancement			
кистозное / cystic	2 (20%)	1 (10%)	0,8
кистозно-солидное / cystic-solid	7 (70%)	8 (80%)	
солидное / solid	1 (10%)	1 (10%)	
MGMT метилирование после первой операции / MGMT methylation after first surgery			
положительный / positive	4 (40%)	3 (30%)	0,7
отрицательный / negative	6 (60%)	7 (70%)	

the operation. Tumor removal was performed using an operating microscope (LEICA OHS-1) with the D-Light AF System Karl Storz (Germany) and a fluorescence attachment manufactured by Russia Science Seoul, Korean Electrotechnology Research Institute (KERI), (Seoul, Republic of Korea) (developed by G.V. Papayan).

Tumor removal in the group without fluorescence control was performed under the control of an intraoperative microscope (OPMI Pentero, Carl Zeiss, Germany).

For endoscopic control, an endoscope (Karl Storz, Germany) with a special light source (D-light C; Karl Storz) and a camera system (Karl Storz) were used in all patients in both groups. The endoscope was used after complete microscopic removal of all visualized tissue.

For the fluorescence control group, the endoscope was set to the D-light mode, which allowed switching between white and blue light source modes using a corresponding bandpass filter in the light transmission path (Fig. 1). A long-pass filter on the endoscope eyepiece

blocked excitation light, which allowed detection of tumor cell fluorescence signals. The excitation and detection filter system allowed transmission of enough blue light so that the red fluorescence of endogenous fluorophores and non-specific fluorescence were suppressed, resulting in normal tissue being visualized as blue. Microscopic fluorescent tissue and endoscopic fluorescent tissue not visualized under the microscope were completely removed and used separately for histopathological examination (Fig. 2).

Postoperative evaluation

All patients underwent MRI within 24 h after surgery. Any residual enhancement greater than 0.2 cm³ was defined as residual tumor. Performance status was assessed using the Karnofsky scale at discharge. All included patients underwent regular clinical examination and contrast-enhanced MRI every 3 months. The presence of recurrence was assessed by subsequent MRI according to the Response Assessment in Neuro-Oncology (RANO) criteria [8].

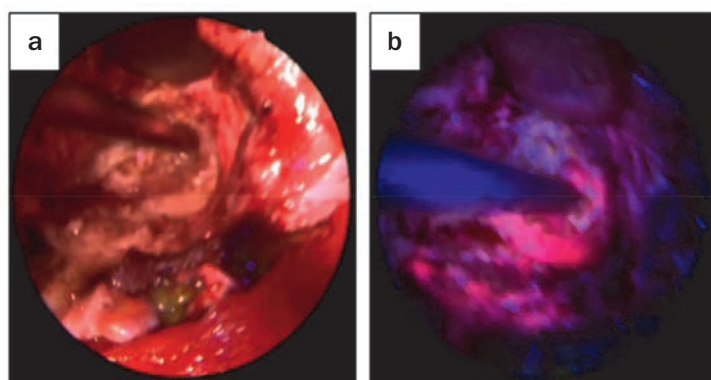


Рис. 1. Интраоперационная картина:
а – изображение в эндоскопе при обычном освещении, без флуоресценции;
б – изображение в эндоскопе в флуоресцентном режиме.
Fig. 1. Intraoperative picture:
a – endoscope view under normal lighting, without fluorescence;
b – endoscope view in fluorescent mode.

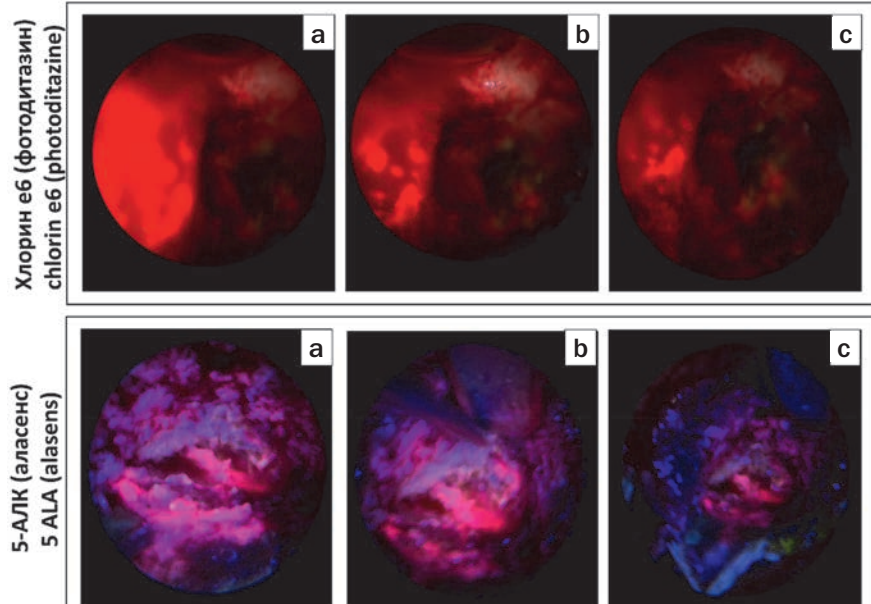


Рис. 2. Интраоперационная картина флуоресцентной диагностики в процессе резекции опухоли 5-АЛК и хлорином е6 (а, б, с – поэтапное удаление части опухолевой ткани накопившей флуоресцент).
Fig. 2. Intraoperative picture of fluorescent diagnostics during tumor resection with 5-ALA and chlorin e6 (a, b, c – step-by-step removal of part of the tumor tissue that has accumulated fluorescence).

Postoperative period

All patients received standard adjuvant therapy (chemotherapy and radiotherapy) in the postoperative period according to the Stupp protocol [32]. Radiotherapy included fractionated external beam therapy to the resected tumor bed with a total focal dose of 50-60 Gy in 25-30 fractions (1.8-2.0 Gy per fraction), for 5-6 weeks. As chemotherapy after the first operation, patients received temozolomide (at a dose of 150-200 mg/m² from the 1st to the 5th day every 28 days).

In the postoperative period, patients underwent control MRI of the brain every 3 months in the first 12 months or when symptoms appeared, then every 4 months.

If a relapse was detected based on MRI of the brain, if indicated, repeated surgical treatment was performed or the patient was referred for repeated adjuvant therapy (chemotherapy and radiation therapy). Chemotherapy

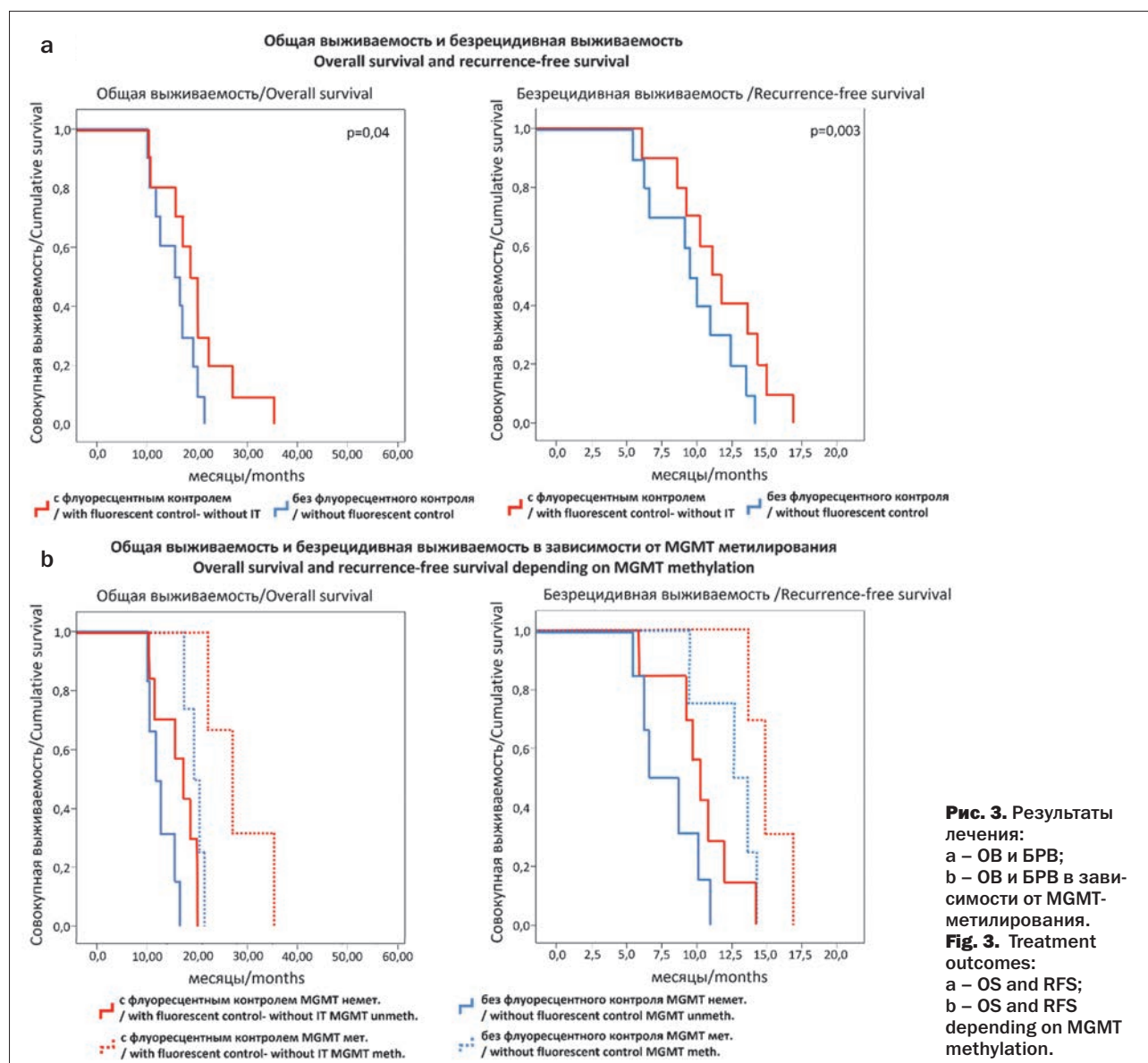
regimens for relapse were prescribed by oncologists based on the results of histological examination of the tumor material, after repeated surgeries, or according to generally accepted regimens. The following chemotherapy regimens were used: avastin + irinotecan; PCV (lomustine, vincristine, procarbazine); lomustine + vincristine; temozolomide + avastin.

Efficacy assessment criteria of the conducted study

The efficacy assessment criteria of the conducted study in the groups were: radicality of the performed surgical intervention according to the data of postoperative MRI with contrast enhancement and values of the OS and RFS medians.

Statistical analysis

All analyses were performed using SPSS (version 20, IBM Corp.). Continuous variables were measured as mean or median values and standard deviation. Differences between both cohorts were analyzed using the unpaired



t-test. Descriptive survival was analyzed using the Kaplan-Meier method, p-values < 0.05 were considered significant.

Results

In the early postoperative period, no patient experienced complications associated with endoscopic or fluorescence control during surgery. The Karnofsky index values in patients in each group after surgery were comparable with preoperative data (p=0.9).

Totality of resection, RFS, and OS

According to postoperative gadolinium-enhanced MRI of the brain, total resection was achieved in all 10 (100%) patients who underwent combined surgery under a microscope and fluorescence control with an endoscope, compared with 6 (60%) patients who underwent only surgery under a microscope and an endoscope without fluorescence control (p=0.002). The RFS median in the cohort of combined resection using fluorescence control with an endoscope and a microscope was 11.7 months. (CI 95% 9.8–15.7) versus 9.8 months (CI 95% 6.1–13.4; p=0.04) in the cohort of resections using a microscope and endoscope, but without fluorescence control (Fig. 3a).

The OS median in the cohort of combined resection with fluorescence and endoscopic control and a microscope was 20.2 months (CI 95% 11.9–28.6) compared with 16.3 months (CI 95% 11.0–20.9) in the cohort of resection using a microscope and endoscope, but without fluorescence control (p=0.003) (Table 2, Fig. 3a).

A direct connection was shown between the detection of a number of molecular markers, in particular the MGMT methylation index, and the RFS and OS rates. Thus, according to our study, patients in both groups with a methylated MGMT promoter had better OS and RFS rates compared with patients with an unmethylated MGMT promoter (Fig. 3b).

In our study, no relationship was found between age, gender, preoperative Karnofsky index, tumor location and size before surgery, volume of adjuvant therapy (chemotherapy and radiotherapy), and the values of RFS and OS. This is partly due to the fact that the patients who were selected for the study were maximally comparable in these characteristics, partly due to the small sample of patients.

Таблица 2
Результаты лечения пациентов в зависимости от клинических и гистологических данных
Table 2
Treatment results for patients depending on clinical and histological data

Пациент / Patient	Резекция с флуоресцентным контролем / Fluorescence-guided resection	Пол / Gender	Возраст / Age	Индекс Карновского / Karnofsky index KPS	Локализация опухоли (доля/сторона) / Tumor Location (lobe/side)	Характер опухоли по данным МРТ головного мозга с контрастным усилением гадолинием / Character of the tumor according to MRI of the brain with gadolinium contrast enhancement	Размер опухоли (см³) / Tumor volume (cm³)	MGMT метилирование / MGMT methylation	IDH мутация / IDH mutation	Тотальность резекции по данным МРТ / Totality of resection according to MRI data	Повторная резекция / Repeated resection	Общая доза ЛТ (Гр) / Total dose of RT (Gr)	Количество циклов ТМЗ / Number of TMZ cycles	Безрецидивная выживаемость, мес. / Recurrence-free survival, months	Вторая/третья линия лечения после рецидива / Second/third line of treatment after relapse	Общая выживаемость, мес. / Overall survival, months
1	да/yes	ж/f	45	90	лобная правая/ frontal right	кистозно-солидное/ cystic-solid	33,1	мет/ meth	нет/no	да/yes	да/yes	60	8	17,1	ТМЗ+авастин/ TMZ+avastin	36,5
2	да/yes	м/m	68	90	теменная левая/ parietal left	кистозно-солидное/ cystic-solid	4,2	мет/ meth	IDH1 (R132H)	да/yes	да/yes	60	6	13,5	ТМЗ/TMZ	22,4
3	да/yes	ж/f	61	100	лобная левая/ frontal left	солидное/ solid	29,6	немет/ unmeth	нет/no	да/yes	нет/no	60	5	8,8	авастин+ иринотекан/ avastin+ irinotecan	11,5
4	да/yes	м/m	57	80	височная левая/ temporal left	кистозно-солидное/ cystic-solid	10,8	немет/ unmeth	IDH1/ IDH2	да/yes	да/yes	60	7	14,5	ТМЗ/TMZ	20,3

5	да/ yes	ж/f	49	80	теменная правая/ parietal right	кистозно- солидное/ cystic-solid	37,1	немет/ unmeth	нет/no	да/yes	да/ yes	90	6	10,7	TM3+авастин/ TMZ+avastin	17,7
6	да/ yes	ж/f	58	80	теменная левая/ parietal left	кистозно- солидное/ cystic-solid	42	мет/ meth	нет/no	да/yes	да/ yes	60	6	15,3	TM3/TMZ	27,9
7	да/ yes	м/m	41	70	височная левая/ temporal left	кистозное/ cystic	38,7	немет/ unmeth	нет/no	да/yes	нет/ no	60	5	11,8	TM3/TMZ	20,3
8	да/ yes	ж/f	60	70	височная правая/ temporal right	кистозно- солидное/ cystic-solid	44,5	немет/ unmeth	нет/no	да/yes	нет/ no	60	3	9,3	ломустин + винкристин/ lomustine + vincristine	18,4
9	да/ yes	м/m	67	90	теменная правая/ parietal right	кистозно- солидное/ cystic-solid	20,6	немет/ unmeth	нет/no	да/yes	да/ yes	60	7	10,1	PCV (ломустин, винкристин, прокарбазин)/ PCV	16,6
10	да/ yes	ж/f	59	80	височная левая/ temporal left	кистозно- солидное/ cystic-solid	17,4	немет/ unmeth	нет/no	да/yes	да/ yes	90	5	5,8	ломустин + винкристин/ lomustine + vincristine	10,7
11	нет/ no	ж/f	58	70	лобная правая/ frontal right	кистозно- солидное/ cystic-solid	35,5	немет/ unmeth	нет/no	нет/no	нет/ no	60	3	6,4	TM3+авастин/ TMZ+avastin	11,9
12	нет/ no	ж/f	44	90	теменная правая/ parietal right	кистозно- солидное/ cystic-solid	29,7	мет/ meth	нет/no	нет/no	нет/ no	90	6	13,8	авастин+ иринотекан/ avastin+ irinotecan	22,3
13	нет/ no	м/m	46	90	височная правая/ temporal right	кистозно- солидное/ cystic-solid	37	немет/ unmeth	нет/no	да/yes	да/ yes	60	5	11,1	PCV (ломустин, винкристин, прокарбазин)/ PCV	17,6
14	нет/ no	м/m	69	90	теменная левая/ parietal left	солидное/ solid	18,8	немет/ unmeth	нет/no	да/yes	да/ yes	60	7	10,2	TM3/TMZ	16,9
15	нет/ no	ж/f	73	80	височная правая/ temporal right	кистозное/ cystic	28,5	немет/ unmeth	нет/no	нет/no	нет/ no	60	5	8,3	TM3+авастин/ TMZ+avastin	13,3
16	нет/ no	ж/f	61	90	лобная левая/ frontal left	кистозно- солидное/ cystic-solid	33,9	мет/ meth	нет/no	да/yes	нет/ no	60	7	9,8	TM3/TMZ	18,9
17	нет/ no	ж/f	55	70	височная правая/ temporal right	кистозно- солидное/ cystic-solid	29,8	немет/ unmeth	IDH1 (R132H)	нет/no	да/ yes	60	9	5,3	TM3/TMZ	11,1
18	нет/ no	ж/f	60	80	височная левая/ temporal left	кистозно- солидное/ cystic-solid	17,6	мет/ meth	нет/no	да/yes	да/ yes	60	5	14,6	авастин+ иринотекан/ avastin+ irinotecan	20,1
19	нет/ no	м/m	57	100	затыл- лочная правая/ occipital right	кистозное/ cystic	3,4	немет/ unmeth	нет/no	да/yes	да/ yes	45	6	6,1	TM3+авастин/ TMZ+avastin	10,5
20	нет/ no	ж/f	33	90	лобная правая/ frontal right	кистозно- солидное/ cystic-solid	19,4	мет/ meth	нет/no	да/yes	да/ yes	60	5	12,5	ломустин + винкристин/ lomustine + vincristine	17,7

Morphological analysis

Morphological examination of tumor areas depending on fluorescence intensity showed that there is a direct connection between tumor cell density, tumor anaplasia degree, and fluorescence intensity during surgery. The brighter the tumor tissue fluorescence, the higher the

tumor cell density, and the more malignant the tumor area according to morphology (Ki-67 and TP 53 index, VEGF expression level). In the tumor necrosis zone, either very weak fluorescence or no fluorescence was observed. The sensitivity of the fluorescence monitoring method during surgery (dependence of fluorescence intensity on

tumor anaplasia degree) was 100%, and the specificity (when comparing fluorescent and non-fluorescent tumor tissue areas) reached 85% (Fig. 4).

Comparison of the morphological data of biopsies obtained during surgery in patients for whom 5-ALA and chlorin e6 were used as fluorescence inducers did not show a significant difference in the specificity and sensitivity of detecting tumor tissue areas.

Morphological analysis of tumor tissue areas in patients in the group with endoscopic control, but without fluorescence control, showed that the sensitivity of the technique for detecting tumor tissue areas was 60% (analysis of possible areas perceived as tumor tissue, taken during surgery under visual endoscopic control), and the specificity was 40% (comparative analysis between tissue areas taken during surgery that were perceived under endoscopic control as tumor tissue, and areas that were perceived in the endoscopic picture as normal brain tissue).

Discussion

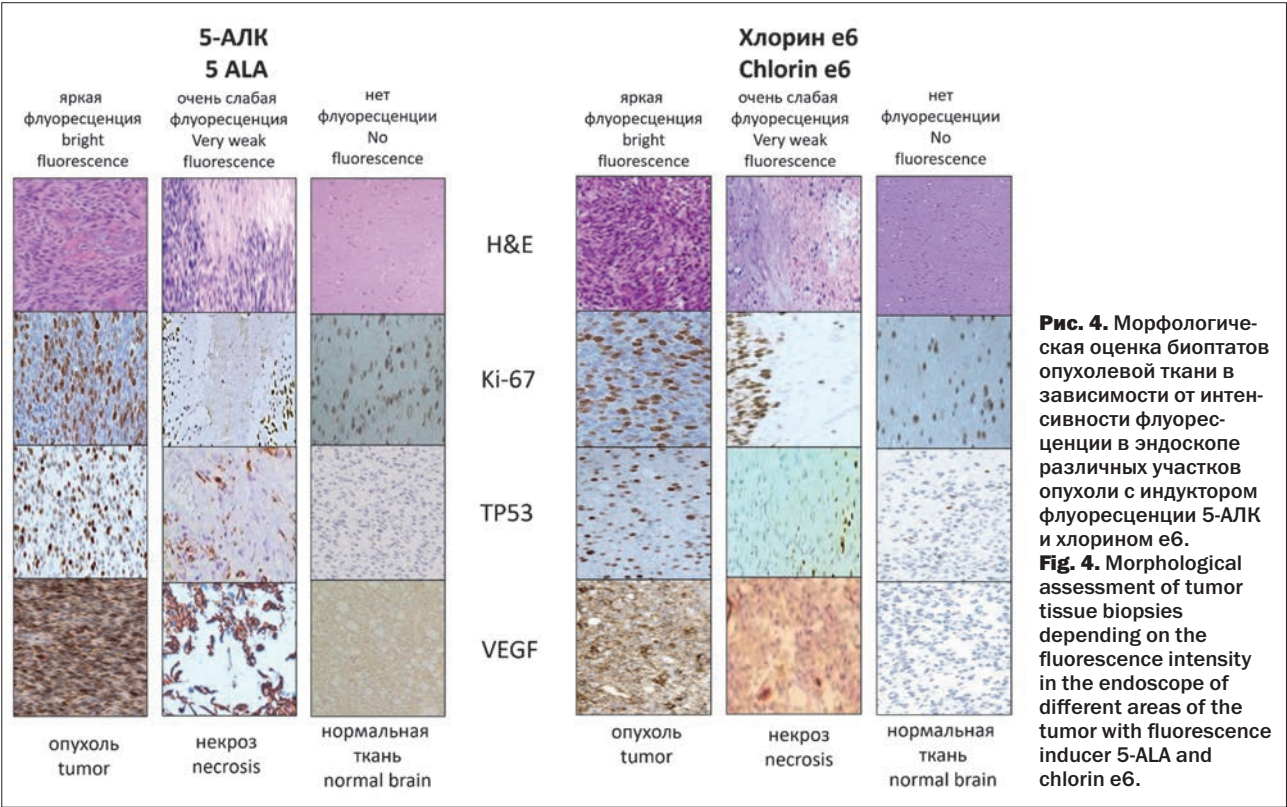
In this study, we assessed the effect of fluorescence guidance in combined microscopic and endoscopic resection on median RFS and OS medians in patients with glioblastoma. The sensitivity and specificity of the techniques were also assessed. Our results indicate that median RFS and OS were higher in patients with glioblastoma if endoscopic resection was supplemented with fluorescence guidance. Thus, the use of fluorescence

guidance allowed increasing the sensitivity of the technique from 60 to 100%, and the specificity from 40 to 85%.

Effect of a combined approach on resection radicality

Analysis of different works shows that the use of an endoscope during surgery allows the surgeon to significantly increase the frequency of total resections (95%) and achieve a significantly greater removal of tumor tissue volume, not limited to the contrasting parts of the tumor according to MRI data [18, 25]. And the use of fluorescence control in addition to the endoscope allows for the radicality of resection to be brought to a higher level [26–28, 30, 33]. In addition, the use of a combination of an endoscope and fluorescence control in glioblastoma removal appears to be a safe and feasible technique, since an endoscope in fluorescence mode allows for the identification of tumor tissue with high sensitivity (100%) and specificity (85%) [27, 28]. Due to a significant decrease in the distance between the light source and the tumor tissue, endoscopic control and fluorescence control make it possible to identify tumor tissue that is not sufficiently visualized microscopically (located at the edges of the tumor, in blind zones around the craniotomy area, and deep in the surgical field with poorer illumination). This, in turn, leads to an increase in the frequency of total resections and makes it possible to perform supratotal resection [26, 30].

Thus, in the work of A.A. Potapov et al. [23], 17 patients underwent microsurgical resection with fluorescence



endoscopy using 5-ALA and Karl Storz endoscopic equipment to determine tumor residues in the resection cavity. The primary diagnosis of the tumor included malignant gliomas, metastases, and malignant tumors of the skull base. In most cases, the possibility of monitoring the "out of the border" areas of the resection cavity using an angled endoscope was confirmed. Bright fluorescence was observed not only in grade IV gliomas, but also in 3 of 4 metastases. The authors concluded that the use of an endoscope to perform fluorescence navigation with 5-ALA increases the diagnostic efficiency for differentiating normal brain tissue from tumor tissue [23].

Our results further highlight the importance of endoscopic and fluorescence guidance in glioblastoma resection and demonstrate that the current limitations of standard endoscopically guided surgery can be overcome by adding fluorescence guidance.

Impact on overall survival

In the study by Bettag et al. [24], additional fluorescence and endoscopic guidance were used during surgery in 20 of 114 patients, while the remaining patients underwent tumor resection under the control of an operating microscope and fluorescence. Both cohorts were comparable in age, functional status, lesion location, adjuvant treatment methods, and molecular status. Complete total resection was achieved in all patients treated with the use of endoscopy, compared with approximately 75.9% of patients treated with the use of only a microscope ($p=0.003$). The RFS median in the cohort using an endoscope was 19.3 months (95% CI 10.8–27.7) compared with 10.8 months (95% CI 8.2–13.4; $p=0.012$) in the microscope-only cohort. The OS median in the endoscope group was 28.9 months (95% CI 20.4–34.1)

compared with 16.8 months (95% CI 14.0–20.9) in the microscope-only group ($p=0.001$) [24].

Our study showed that the use of endoscopic and fluorescence guidance increased the resection completeness rate and thereby improved RFS and OS rates in patients with glioblastoma.

Study Limitations

Our study has several limitations. First, it was a retrospective study and further prospective studies are needed to confirm our results. Second, the cohort in which the combined approach was used was small and selective. Third, the entire study population was selective since only patients with well-localized glioblastomas were included in the study. However, both cohorts were comparable in terms of potential confounding factors, which allows to suggest that the combined approach is superior to the standard microscopic approach with an endoscope in terms of the radicality rate of the performed surgery and survival in patients with glioblastoma.

Conclusion

This is one of the first studies in our country comparing fluorescence-guided glioblastoma resection using an endoscope with standard resection using an endoscope in addition to microscopic resection. The use of fluorescence guidance during tumor resection using an endoscope, as shown by our experience, increases the radicality of resection and the OS and RFS medians in patients with glioblastoma. At the same time, it should be noted that the observed effect contrasts with the limitations of the study design. Therefore, there is a need to continue conducting further research on a larger group of patients to confirm our findings.

REFERENCES

1. Rynda A.Yu., Olyushin V.E., Rostovtsev D.M., et al. Intraoperative photodynamic therapy in complex treatment of malignant gliomas. *Zhurnal Voprosy Neurokhirurgii Imeni N.N. Burdenko*, 2023, vol. 87(1), pp.25-34. (In Russian) doi:10.17116/neiro20238701125
2. Rynda A.Yu., Olyushin V.E., Rostovtsev D.M., et al. Intraoperative fluorescence control with chlorin E6 in resection of glial brain tumors. *Zhurnal Voprosy Neurokhirurgii Imeni N.N. Burdenko*, 2021, vol.85, no.4, pp. 20-28. (In Russian). doi:10.17116/neiro20218504120
3. Rynda A.Y., Rostovtsev D.M., Zabrodskaia Y.M., et al. Immunotherapy with autologous dendritic cells in the complex treatment of malignant gliomas – results. *J. Neurooncol.*, 2024, vol.166, pp.309-319. doi: 10.1007/s11060-023-04559-1
4. Rynda A.Y., Olyushin V., Rostovtsev D. Immunotherapy With Autologous Dendritic Cells in the Structure of Complex Treatment of Gliomas. *Neurosurgery*, 2024, vol.70 (1), pp.196. doi: 10.1227/neu.0000000000002809_1244
5. Rynda A.Yu., Rostovtsev D.M., Olyushin V.E., Zabrodskaia Yu.M. Therapeutic pathomorphosis in malignant glioma tissues after photodynamic therapy with chlorin e6 (reports of two clinical cases). *Biomedical Photonics*, 2020, vol.9(2), pp.45-54. (In Russian) doi: 10.24931/2413-9432-2020-9-2-45-54
6. Ostrom Q.T., Cioffi G., Waite K., et al. CBTRUS Statistical Report: primary Brain and Other Central Nervous System Tumors Diagnosed

ЛИТЕРАТУРА

1. Рында А.Ю., Олюшин В.Е., Ростовцев Д.М. и соавт. Применение интраоперационной фотодинамической терапии в структуре комплексного лечения злокачественных глиом // Журнал «Вопросы нейрохирургии» имени Н.Н. Бурденко. – 2023. – Т. 87, №1. – С. 25-34. doi: 10.17116/neiro20238701125
2. Рында А.Ю., Олюшин В.Е., Ростовцев Д.М. и соавт. Результаты использования интраоперационного флуоресцентного контроля с хлорином Е6 при резекции глиальных опухолей головного мозга // Журнал «Вопросы нейрохирургии» имени Н.Н. Бурденко. – 2021. – Т.85, №4. – С.20-28. doi: 10.17116/neiro20218504120.
3. Rynda A.Y., Rostovtsev D.M., Zabrodskaia Y.M. et al. Immunotherapy with autologous dendritic cells in the complex treatment of malignant gliomas – results. // *J. Neurooncol.* – 2024. – Vol.166. – P. 309-319. doi: 10.1007/s11060-023-04559-1
4. Rynda A.Y., Olyushin V., Rostovtsev D. Immunotherapy With Autologous Dendritic Cells in the Structure of Complex Treatment of Gliomas // *Neurosurgery*. – 2024. – Vol.70 (1). – P. 196. doi: 10.1227/neu.0000000000002809_1244
5. Rynda A.Yu., Rostovtsev D.M., Olyushin V.E. et al. Therapeutic pathomorphosis in malignant glioma tissues after photodynamic therapy with chlorin e6 (reports of two clinical cases) // *Biomedical Photonics*. – 2020. – Vol.9, №2. – P. 45–54. doi: 10.24931/2413-9432-2020-9-2-45-54
6. Ostrom Q.T., Cioffi G., Waite K. et al. CBTRUS Statistical Report: primary Brain and Other Central Nervous System Tumors Diagnosed

- in the United States in 2014-2018. *Neuro Oncol.*, 2021, vol.23, pp. III1-III105. doi: 10.1093/NEUONC/NOAB200
7. Poon M.T.C., Sudlow C.L.M., Figueroa J.D., Brennan P.M. Longer-term (≥ 2 years) survival in patients with glioblastoma in population-based studies pre- and post-2005: A systematic review and meta-analysis. *Sci Rep.*, 2020, vol.10, pp.11622. doi: 10.1038/s41598-020-68011-4
8. Karschnia P., Vogelbaum M.A., van den Bent M., et al. Evidence-based recommendations on categories for extent of resection in diffuse glioma. *Eur J Cancer.*, 2021, vol.149, pp.23-33. doi: 10.1016/j.ejca.2021.03.002
9. Rynda A.Yu., Olyushin V.E., Rostovtsev D.M., et al. Comparative analysis of 5-ALA and chlorin E6 fluorescence-guided navigation in malignant glioma surgery. *Pirogov Russian Journal of Surgery = Khirurgiya. Zhurnal im. N.I. Pirogova*, 2022, vol.1, pp.5-14. (In Russian) doi: 10.17116/hirurgia20220115
10. Goryaynov S.A., Potapov A.A., Okhlopov V.A., et al. Metabolic navigation during brain tumor surgery: analysis of a series of 403 patients. *Russian journal of neurosurgery*, 2022, vol.24(4), pp.46-58. doi:10.17650/1683-3295-2022-24-4-46-58
11. Rynda A.Yu., Zabrodskaya Yu.M., Olyushin V.E., et al. Morphological evaluation of the effectiveness of fluorescence navigation with chlorin e6 in surgery for malignant gliomas. *Arkhiv Patologii*, 2021, vol.83(5), pp.13-20. (In Russian) doi: 10.17116/patol20218305113
12. Goryaynov S.A., Buklina S.B., Khapov I.V., et al. 5-ALA-guided tumor resection during awake speech mapping in gliomas located in eloquent speech areas: Single-center experience. *Front. Oncol.*, 2022, vol.12, pp.940951. doi: 10.3389/fonc.2022.940951
13. Rynda A.Yu., Rostovtsev D.M., Olyushin V.E. Fluorescence-Guided Resection of Glioma – literature review. *Russian Neurosurgical Journal named after professor A.L. Polenov*, 2018, vol.X(1), pp. 97-110. (In Russian)
14. Batalov A.I., Goryaynov S.A., Zakharova N.E., et al. Prediction of Intraoperative Fluorescence of Brain Gliomas: Correlation between Tumor Blood Flow and the Fluorescence. *J. Clin. Med.*, 2021, vol.10, pp. 2387. doi: 10.3390/jcm10112387
15. Rynda A.Yu., Olyushin V.E., Rostovtsev D.M., et al. Fluorescent diagnostics with chlorin e6 in surgery of low-grade glioma. *Biomedical Photonics*, 2021, vol. 10, no. 4, pp. 35-43 (In Russian). doi: 10.24931/2413-9432-2021-10-4-35-43
16. Potapov A.A., Chobulov S.A., Nikitin P.V., et al. Intraoperative vascular fluorescence in cerebral glioblastomas and vascular histological features. *Zhurnal Voprosy Neurokhirurgii Imeni N.N. Burdenko*, 2019, vol.83(6), pp.21-34. (In Russian). doi: 10.17116/neiro20198306121
17. Rynda A.Yu., Rostovtsev D.M., Olyushin V.E., Zabrodskaya Yu.M. Fluorescence-guided resection of glioma using «photoditazin». *Grekov's Bulletin of Surgery*, 2017, vol.176(5), pp.10-15. (In Russian). doi: 10.24884/0042-4625-2017-176-5-10-15
18. Goryaynov S.A., Okhlopov V.A., Golbin D.A., et al. Fluorescence Diagnosis in Neurooncology: Retrospective Analysis of 653 Cases. *Front. Oncol.*, 2019, vol.9, pp.830. doi: 10.3389/fonc.2019.00830
19. Stummer W., Pichlmeier U., Meinel T., et al. ALA-Glioma Study Group. Fluorescence-guided surgery with 5-aminolevulinic acid for resection of malignant glioma: a randomised controlled multicentre phase III trial. *Lancet Oncol.*, 2006, vol.7(5), pp.392-401. doi: 10.1016/S1470-2045(06)70665-9
20. Goriainov S.A., Potapov A.A., Pitskhelauri D.I., et al. Intraoperative fluorescence diagnostics upon recurrent operations for brain gliomas. *Zhurnal Voprosy Neurokhirurgii Imeni N.N. Burdenko*, 2014, vol.78(2), pp.22-31. (In Russian).
21. Rynda A., Olyushin V., Rostovtsev D. Fluorescence navigation in glioma surgery using 5 ALA and chlorin E6. *Neuro-Oncology*, 2021, vol.23(2), pp. ii25. doi: 10.1093/neuonc/noab180.086
22. Rapp M., Kamp M., Steiger H.J., Sabel M. Endoscopic-assisted visualization of 5-aminolevulinic acid-induced fluorescence in malignant glioma surgery: a technical note. *World Neurosurg.*, 2014, vol.82, ppe277-e279. doi: 10.1016/j.wneu.2013.07.002
23. Potapov A.A., Usachev D.J., Loshakov V.A., et al. First experience in 5-ALA fluorescence-guided and endoscopically assisted microsurgery of brain tumors. *Medical Laser Application*, 2008, vol.23(4), pp. 202-208. doi: 10.1016/j.mla.2008.07.006
24. Bettag C., Schatlo B., Abboud T. et al. Endoscope-enhanced fluorescence-guided microsurgery increases survival in patients in the United States in 2014-2018. // *Neuro Oncol.* – 2021. – Vol. 23: – P. III1–III105. doi: 10.1093/NEUONC/NOAB200
7. Poon M.T.C., Sudlow C.L.M., Figueroa J.D., Brennan P.M. Longer-term (≥ 2 years) survival in patients with glioblastoma in population-based studies pre- and post-2005: A systematic review and meta-analysis // *Sci Rep.* – 2020. – Vol. 10. – P. 11622. doi: 10.1038/s41598-020-68011-4
8. Karschnia P., Vogelbaum M.A., van den Bent M. et al. Evidence-based recommendations on categories for extent of resection in diffuse glioma // *Eur. J. Cancer.* – 2021. – Vol.149. – P. 23-33. doi: 10.1016/j.ejca.2021.03.002
9. Рында А.Ю., Олюшин В.Е., Ростовцев Д.М. и соавт. Сравнительный анализ флуоресцентной навигации в хирургии злокачественных глиом с использованием 5-АЛА и хлорина Е6 // *Хирургия. Журнал им. Н.И. Пирогова.* – 2022. – №1. – С.5-14. doi: 10.17116/hirurgia20220115
10. Горайнов С.А., Потапов А.А., Охлопков В.А. и соавт. Метаболическая навигация в хирургии опухолей головного мозга: анализ серии 403 пациентов // *Нейрохирургия.* – 2022. – Т.24, №4. – С.46-58. doi: 10.17650/1683-3295-2022-24-4-46-58
11. Рында А.Ю., Забродская Ю.М., Олюшин В.Е. и соавт. Морфологическая оценка эффективности флуоресцентной навигации с хлорином е6 в хирургии злокачественных глиом // *Архив патологии.* – 2021. – Т.83, №5. – С.13-20. doi: 10.17116/patol20218305113
12. Goryaynov S.A., Buklina S.B., Khapov I.V. et al. 5-ALA-guided tumor resection during awake speech mapping in gliomas located in eloquent speech areas: Single-center experience // *Front. Oncol.* – 2022. – Vol.12. – P. 940951. doi: 10.3389/fonc.2022.940951
13. Рында А.Ю., Ростовцев Д.М., Олюшин В.Е. Флуоресцентно-контролируемая резекция астроцитарных опухолей головного мозга – обзор литературы // *Российский нейрохирургический журнал имени профессора А.Л. Поленова.* – 2018. – Т. X, №1. – С.97-110.
14. Batalov A.I., Goryaynov S.A., Zakharova N.E. et al. Prediction of Intraoperative Fluorescence of Brain Gliomas: Correlation between Tumor Blood Flow and the Fluorescence // *J. Clin. Med.* – 2021. – Vol.10. – P. 2387. doi: 10.3390/jcm10112387
15. Рында А.Ю., Олюшин В.Е., Ростовцев Д.М. и соавт. Флуоресцентная диагностика с хлорином е6 в хирургии глиом низкой степени злокачественности // *Biomedical Photonics.* – 2021. – Т. 10, № 4. – С. 35-43. doi: 10.24931/2413-9432-2021-10-4-35-43
16. Потапов А.А., Чобулов С.А., Никитин П.В. и соавт. Интраоперационная флуоресценция сосудов в структуре глиобластом головного мозга и их гистологическая характеристика // *Журнал «Вопросы нейрохирургии» имени Н.Н. Бурденко.* – 2019. – Т.83, №6. – С.21-34. doi: 10.17116/neiro20198306121
17. Рында А.Ю., Ростовцев Д.М., Олюшин В.Е., Забродская Ю.М. Флуоресцентно-контролируемая резекция глиальных опухолей с «Фотодитазин» // *Вестник хирургии имени И.И. Грекова.* – 2017. – Т.176, №5. – С.10-15. doi: 10.24884/0042-4625-2017-176-5-10-15
18. Goryaynov S.A., Okhlopov V.A., Golbin D.A. et al. Fluorescence Diagnosis in Neurooncology: Retrospective Analysis of 653 Cases // *Front. Oncol.* – 2019. – Vol.9. – P. 830. doi: 10.3389/fonc.2019.00830
19. Stummer W., Pichlmeier U., Meinel T. et al. ALA-Glioma Study Group. Fluorescence-guided surgery with 5-aminolevulinic acid for resection of malignant glioma: a randomised controlled multicentre phase III trial // *Lancet Oncol.* – 2006. – Vol.7(5). – P.392-401. doi: 10.1016/S1470-2045(06)70665-9
20. Горайнов С.А., Потапов А.А., Пицхеллаури Д.И. и соавт. Интраоперационная флуоресцентная диагностика и лазерная спектроскопия при повторных операциях по поводу глиом головного мозга // *Журнал «Вопросы нейрохирургии» имени Н.Н. Бурденко.* – 2014. – Т. 78, №2. – С.22-31.
21. Rynda A., Olyushin V., Rostovtsev D. Fluorescence navigation in glioma surgery using 5 ALA and chlorin E6 // *Neuro-Oncology.* – 2021. – Vol. 23, (2). – P. ii25. doi: 10.1093/neuonc/noab180.086
22. Rapp M., Kamp M., Steiger H.J., Sabel M. Endoscopic-assisted visualization of 5-aminolevulinic acid-induced fluorescence in malignant glioma surgery: a technical note. // *World Neurosurg.* – 2014. – Vol.82. – P.277-e279. doi: 10.1016/j.wneu.2013.07.002
23. Potapov A.A., Usachev D.J., Loshakov V.A. et al. First experience in 5-ALA fluorescence-guided and endoscopically assisted microsurgery of brain tumors // *Medical Laser Application.* – 2008. – Vol.23(4). – P. 202-208. doi: 10.1016/j.mla.2008.07.006
24. Bettag C., Schatlo B., Abboud T. et al. Endoscope-enhanced fluorescence-guided microsurgery increases survival in patients

- with glioblastoma. *Acta Neurochir (Wien)*, 2023, vol.165(12), pp.4221-4226. doi: 10.1007/s00701-023-05862-6
25. Bettag C., Schregel K., Langer P., et al. Endoscope-assisted fluorescence-guided resection allowing supratotal removal in glioblastoma surgery. *Neurosurg Focus*, 2021, vol.50: pp. E3. doi: 10.3171/2020.10.FOCUS20560.
 26. Strickland B.A., Zada G. 5-ALA Enhanced Fluorescence – Guided Microscopic to Endoscopic Resection of Deep Frontal Subcortical Glioblastoma Multiforme. *World Neurosurgery*, 2021, vol.148, pp. 65. doi: 10.1016/j.wneu.2020.12.168
 27. Sakata T., Tanikawa M., Yamada H. Minimally invasive treatment for glioblastoma through endoscopic surgery including tumor embolization when necessary: a technical note. *Front Neurol.*, 2023, vol.14, pp.1170045. doi: 10.3389/fneur.2023.1170045
 28. Ma R., Livermore L.J., Taylor L. et al. Endoscopic 5-Aminolevulinic Acid – Induced Fluorescence-Guided Intraparenchymal Brain Tumor Resection – Can the Endoscope Detect More Fluorescence Than the Microscope? *World Neurosurgery*, 2024, vol.185, pp. e1268-e1279. doi: 10.1016/j.wneu.2024.03.067
 29. Takeda J., Nonaka M., Li Y., et al. 5-Aminolevulinic acid fluorescence-guided endoscopic surgery for intraventricular tumors. *Surg Neurol Int.*, 2022, vol.13, pp. 302. doi: 10.25259/SNI_488_2022
 30. McKinnon C., Voets N., Livermore L., et al. Endoscopic ipsilateral interhemispheric approach for resection of selected deep medial brain tumors. *World Neurosurg.*, 2020, vol.144, pp.162-169. doi: 10.1016/j.wneu.2020.08.147
 31. Louis D.N., Perry A., Wesseling P., et al. The 2021 WHO classification of tumors of the central nervous system: a summary. *Neuro Oncol.*, 2021, vol.23(8), pp.1231-1251. doi: 10.1093/neuonc/noab106
 32. Stupp R., Mason W.P., van den Bent M.J., et al. Radiotherapy plus concomitant and adjuvant temozolomide for glioblastoma. *N Engl J Med.*, 2005, vol.352(10), pp. 987-996. doi: 10.1056/NEJMoa043330
 33. Rynda A.Yu., Olyushin V.E., Rostovtsev D.M., et al. Patients with long-term survival in malignant gliomas after photodynamic therapy. S.S. Korsakov *Journal of Neurology and Psychiatry.*, 2024, vol.124(6), pp. 54-61. (In Russian). doi: 10.17116/jnevro202412406154
 - with glioblastoma // *Acta Neurochir (Wien)*. – 2023. – Vol.165(12). – P. 4221-4226. doi: 10.1007/s00701-023-05862-6
 25. Bettag C., Schregel K., Langer P. et al. Endoscope-assisted fluorescence-guided resection allowing supratotal removal in glioblastoma surgery // *Neurosurg Focus*. – 2021. – Vol.50. – P. E3. doi: 10.3171/2020.10.FOCUS20560.
 26. Strickland B.A., Zada G. 5-ALA Enhanced Fluorescence–Guided Microscopic to Endoscopic Resection of Deep Frontal Subcortical Glioblastoma Multiforme // *World Neurosurgery*. – 2021. – Vol.148. – P.65. doi: 10.1016/j.wneu.2020.12.168
 27. Sakata T., Tanikawa M., Yamada H. Minimally invasive treatment for glioblastoma through endoscopic surgery including tumor embolization when necessary: a technical note // *Front Neurol*. – 2023. – Vol.14. – P. 1170045. doi: 10.3389/fneur.2023.1170045
 28. Ma R., Livermore L.J., Taylor L. et al. Endoscopic 5-Aminolevulinic Acid–Induced Fluorescence-Guided Intraparenchymal Brain Tumor Resection – Can the Endoscope Detect More Fluorescence Than the Microscope? // *World Neurosurgery*. – 2024. – Vol. 185. – P. e1268-e1279. doi: 10.1016/j.wneu.2024.03.067
 29. Takeda J., Nonaka M., Li Y. et al. 5-Aminolevulinic acid fluorescence-guided endoscopic surgery for intraventricular tumors // *Surg Neurol Int*. – 2022. – Vol.13. – P. 302. doi: 10.25259/SNI_488_2022
 30. McKinnon C., Voets N., Livermore L. et al. Endoscopic ipsilateral interhemispheric approach for resection of selected deep medial brain tumors // *World Neurosurg.* – 2020. – Vol.144. – P. 162-169. doi: 10.1016/j.wneu.2020.08.147
 31. Louis D.N., Perry A., Wesseling P. et al. The 2021 WHO classification of tumors of the central nervous system: a summary // *Neuro Oncol*. – 2021. – Vol.23(8). – P. 1231-1251. doi: 10.1093/neuonc/noab106
 32. Stupp R., Mason W.P., van den Bent M.J. et al. Radiotherapy plus concomitant and adjuvant temozolomide for glioblastoma // *N. Engl. J. Med.* – 2005. Vol. 352(10). – P. 987-996. doi: 10.1056/NEJMoa043330
 33. Рында А.Ю., Олюшин В.Е., Ростовцев Д.М. и соавт. Пациенты с длительной выживаемостью при злокачественных глиомах после фотодинамической терапии // *Журнал неврологии и психиатрии им. С.С. Корсакова*. – 2024. – Т.124, №6. – С.54-61. doi: 10.17116/jnevro202412406154

MORPHOLOGICAL EVALUATION OF THE EFFECTIVENESS OF TREATING INFECTED WOUNDS WITH HIGH-INTENSITY PULSED BROADBAND IRRADIATION

Egorov V.S.^{1,2}, Filimonov A.Yu.¹, Chudnykh S.M.^{1,2,3}, Abduvosidov Kh.A.^{1,3,4}, Chekmareva I.A.^{5,6}, Paklina O.V.^{1,5}, Baranchugova L.M.⁴, Kondrat'ev A.V.⁷

¹Moscow clinical scientific center n.a. A.S. Loginov, Moscow, Russia

²Russian university of medicine, Moscow, Russia

³Tver state medical university, Tver, Russia

⁴Russian biotechnological university, Moscow, Russia

⁵A.V. Vishnevsky national medical research center of surgery, Moscow, Russia

⁶Peoples' friendship university of Russia, Moscow, Russia

⁷Bauman Moscow state technical university, Moscow, Russia

Abstract

The objective of this study was to investigate the effectiveness of high-intensity pulsed broadband irradiation in treating infected wounds. A morphological study was conducted on wound specimens from 105 Wistar rats, in which infected wounds were experimentally induced (three groups). The first group was treated with high-intensity pulsed broadband irradiation, the second group received traditional ultraviolet irradiation, and the third group was treated only with antiseptics. Monitoring was performed before treatment, on the 7th, 14th, and 21st days of treatment. Non-parametric statistical methods were used for data analysis. Prior to treatment, the wounds exhibited signs of the acute inflammation phase. By the 7th day, the first group's wounds were in the proliferation phase. In the second and third groups, edema and infiltration persisted. By the 14th day, the first group's wounds showed signs of granulation tissue formation and transition to the regeneration stage. In the second group, there was a reduction in infiltration, the appearance of new capillaries, and an increase in fibroblasts. In the third group, inflammatory symptoms persisted. By the 21st day, the first group showed remodeling of connective tissue with signs of delicate scar formation. In the second group, signs of connective tissue remodeling were observed, while in the third group, there was reduced infiltration with slow formation of new vessels. Thus, the use of high-intensity pulsed broadband irradiation in the early stages effectively mitigates inflammation, activates local immune response, and accelerates reparative processes.

Keywords: infected wounds, wound healing process, high-intensity pulsed broadband irradiation, ultraviolet irradiation, infiltration, connective tissue remodeling.

For citations: Egorov V.S., Filimonov A.Yu., Chudnykh S.M., Abduvosidov Kh.A., Chekmareva I.A., Paklina O.V., Baranchugova L.M., Kondrat'ev A.V. Morphological evaluation of the effectiveness of treating infected wounds with high-intensity pulsed broadband irradiation, *Biomedical Photonics*, 2024, vol. 13, no. 3, pp. 31–41. doi: 10.24931/2413-9432-2024-13-3-31-41

Contacts: Abduvosidov Kh.A., e-mail: sogdiana99@gmail.com

МОРФОЛОГИЧЕСКАЯ ОЦЕНКА ЭФФЕКТИВНОСТИ ЛЕЧЕНИЯ ИНФИЦИРОВАННЫХ РАН ВЫСОКОИНТЕНСИВНЫМ ИМПУЛЬСНЫМ ШИРОКОПОЛОСНЫМ ОБЛУЧЕНИЕМ

В.С. Егоров^{1,2}, А.Ю. Филимонов¹, С.М. Чудных^{1,2,3}, Х.А. Абдувосидов^{1,3,4},
И.А. Чекмарева^{5,6}, О.В. Паклина^{1,5}, Л.М. Баранчугова⁴, А.В. Кондратьев⁷

¹Московский клинический научно-практический центр им. А.С. Логинова ДЗМ, Москва, Россия

²Российский университет медицины, Москва, Россия

³Тверской государственный медицинский университет, Тверь, Россия

⁴Российский биотехнологический университет, Москва, Россия

⁵НМИЦ Хирургии им. А.В. Вишневского, Москва, Россия⁶Российский Университет дружбы народов, Москва, Россия⁷Московский государственный технический университет имени Н.Э. Баумана, Москва, Россия

Резюме

Целью исследования явилось изучение эффективности высокоинтенсивного импульсного широкополосного облучения инфицированных ран. Проведено морфологическое исследование препаратов ран 105 крыс линии Wistar, которым в эксперименте моделировали инфицированные раны (три группы животных). В 1-й группе для лечения ран использовали высокоинтенсивное импульсное широкополосное облучение, во 2-й группе – традиционное ультрафиолетовое облучение, и в 3-й применяли только антисептик. Оценка эффективности производили до лечения, на 7-е, 14-е и 21-е сутки лечения. До начала лечения картина ран соответствовала фазе острого воспаления. На 7-й день в 1-й группе морфологическая картина соответствовала фазе пролиферации. Во 2-й и 3-й группах отек и инфильтрация к этому сроку сохранялись. К 14-му дню в 1-й группе наблюдали признаки формирования грануляционной ткани и переход ран в стадию регенерации. Во 2-й группе уменьшалась инфильтрация, появлялись новые капилляры, увеличивалось количество фибробластов. В 3-й группе, воспалительные явления сохранялись. К 21-му дню в первой группе наблюдалось ремоделирование соединительной ткани с признаками образования нежного рубца. Во 2-й группе животных наблюдались явления ремоделирования соединительной ткани. В препаратах ран 3-й группы инфильтрация уменьшена, новые сосуды образуются с замедлением. Таким образом, использование высокоинтенсивного импульсного широкополосного облучения инфицированных ран в более ранние сроки купирует воспаление, активизирует местную иммунную реакцию и ускоряет репаративные процессы.

Ключевые слова: инфицированные раны, раневой процесс, высокоинтенсивное импульсное широкополосное облучение, ультрафиолетовое облучение, инфильтрация, ремоделирование соединительной ткани.

Для цитирования: Егоров В.С., Филимонов А.Ю., Чудных С.М., Абдувосидов Х.А., Чекарева И.А., Паклина О.В., Баранчугова Л.М., Кондратьев А.В. Морфологическая оценка эффективности лечения инфицированных ран высокоинтенсивным импульсным широкополосным облучением // Biomedical Photonics. – 2024. – Т. 13, № 3. – С. 31–41. doi: 10.24931/2413-9432-2024-13-3-31-41

Контакты: Абдувосидов Х.А., e-mail: sogdiana99@gmail.com

Introduction

Nowadays, doctors of many specialties use various physical methods of influence in the treatment of a large number of diseases, including inflammatory ones. Thus, in surgery, phototherapy methods are widely used, which include laser and ultraviolet irradiation of tissues.

Due to the high drug resistance of microorganisms, some authors suggest looking for alternative ways to treat infected wounds using physical methods of influence [1, 2]. The sensitivity of many microorganisms to ultraviolet radiation is well known and thoroughly characterized. Over the past decade, antimicrobial therapy based on the use of optical radiation has achieved significant success against antibiotic resistance among various strains of microorganisms. Such kind of treatment includes methods using the antimicrobial properties of blue light, antimicrobial photodynamic therapy and bactericidal ultraviolet irradiation. Phototherapy has an advantage over traditional antibiotics, since it quickly destroys microbial cells and the likelihood of the development of photoresistance in microbes is low. As many authors claim, antimicrobial approaches based on optical radiation have great potential for the treatment of antibiotic-resistant infections and related diseases [3, 4, 5].

According to experimental and clinical studies, the use of technologies based on high-intensity continuous-

spectrum ultraviolet radiation allows for the shortest possible time to reduce the contamination of infected wounds, which makes it possible to recommend the use of such phototherapeutic devices for the treatment of severe infectious diseases occurring against the background of severe immunodeficiency and allergic phenomena [6]. The effect of pulsed high-intensity optical irradiation is a highly effective method with a powerful biocidal and immunostimulating effect [7].

Currently, there are many works devoted to the clinical, bactericidal and immunological effectiveness of various phototherapy methods, while studies are rarely found that describe in detail the morphological basis for the effectiveness of their use, including ultraviolet irradiation.

Our work is devoted to studying the effectiveness of high-intensity pulsed broadband irradiation in the treatment of infected wounds using morphological research methods.

Materials and Methods

A morphological study of wound specimens from 105 animals was conducted, which were experimentally modeled with infected wounds. The study was approved by the Interuniversity Ethics Committee (extract from protocol No. 06-23 dated 15.06.23) and was conducted in the vivarium of the Russian University of Medicine of

the Ministry of Health of the Russian Federation. Mature male Wistar rats weighing 200-250 g were used for the experiment. Infected wounds were modeled under aseptic conditions after anesthesia with a 2% solution of xylazine and zoletil 100. The skin in the withers area was cut with a diameter of 20 mm. Hemostasis was performed, after which a trigger was introduced into the wound in the form of a gauze ball moistened with a mixture of cultures from control strains of *Staphylococcus aureus*, *Pseudomonas aeruginosa*, *Klebsiella pneumoniae*, *Candida albicans* in equal volumes and dilutions, containing 10^9 microbial bodies in 1 ml. The wound with the trigger was sutured. On the next day, the sutures and the trigger were removed, and the animals were randomly divided into three groups. Every day, all animals of all groups without exception underwent wound toilet with 0.1% chlorhexidine solution.

Animals of the 1st (main) group ($n=30$) underwent high-intensity pulsed broadband irradiation during the treatment. This method was performed using a device based on a pulsed xenon lamp of the "pulsed for pumping lasers straight tube 5/60" type, operating in a pulse-periodic mode with a pulse frequency of 5 Hz and an average electric power of 100 W. The average radiation power of the lamp in the UV-C range of the spectrum (200-280 nm) was 3 W, the pulse power of UV-C radiation was 24 kW.

The software of the used device included the following therapy modes: 1st mode – 50 pulses with an irradiation cycle duration of 10 s; 2nd mode – 100 pulses for 20 s; 3rd mode – 200 pulses with a duration of 40 s. Taking into account the contamination and vastness of the modeled wounds, to combat infection and stop inflammation, wound irradiation in the first five days of treatment was carried out using mode 3 at a distance of 5 cm from the wound. Starting from the sixth day of treatment and for the next five days, mode 2 was used at a distance of 10 cm from the wounds.

On the wounds of animals of the 2nd group, daily, for 10 days, a 3-minute traditional ultraviolet irradiation with the "Solnyshko" ultraviolet quartz irradiator, based on a UV mercury bactericidal lamp of the arc compact bactericidal ultraviolet lamp of type 7, with an electric power of 7 W. The power of UV-C radiation (254 nm) of the lamp was 1.2 W.

And in the 3rd control group of animals, wound treatment was carried out only with the help of an antiseptic by daily toilet and applying a bandage with a 0.1% chlorhexidine solution to the wound.

All manipulations were performed in compliance with the requirements of the "European Convention for the Protection of Vertebrate Animals used for Experimental and other Scientific Purposes" (Strasbourg, 1986), the World Medical Association Declaration on the Humane

Treatment of Animals (Helsinki, 2000), and in accordance with the requirements of Order No. 267 of the Ministry of Health of the Russian Federation dated 19/06/2003 "Rules for the handling, maintenance, anesthesia and euthanasia of experimental animals".

To control the morphological picture before the start of treatment, 5 animals were withdrawn from the experiment in each group. On the 7th, 14th and 21st days, 10 animals were withdrawn from the experiment in each group. Animals were withdrawn using an overdose of intramuscular anesthesia (2% xylazine and zoletil 100). After euthanasia, soft tissues in the wound area were excised and fixed in 10% formalin solution, followed by specimens of paraffin blocks and histological specimens using standard methods. Morphological examination was performed on specimens stained with hematoxylin and eosin, with a section thickness of 5 μ m.

Electron microscopic examination was performed on a JEM 100 CX electron microscope (JEOL, Japan) in transmission mode at an accelerating voltage of 80 kV. For this purpose, biological material was fixed in a 2.5% glutaraldehyde solution, then in a 1% osmium oxide solution and embedded in a mixture of araldite resins. Semi-thin sections (1-1.5 μ m) were stained with toluidine blue. Ultra-thin sections were contrasted with uranyl acetate and lead citrate.

For qualitative and quantitative study, histological specimens were pre-scanned on a digital scanner PANNORAMIC 250 Flash (3DHISTECH Ltd. Hungary) and then studied using the program Pannoramic Viewier 1.15.4 (3DHISTECH Ltd. Hungary).

Statistical processing of the obtained results was carried out using the programs Microsoft Office Excel and Statistica 10.0.1011 (StatSoft, Tibco, USA). The analysis was carried out using nonparametric statistical methods, since the preliminary study showed unequal dispersion of the studied features. Descriptive statistics data are presented as a median and interquartile range of 25% and 75%. Comparison of three groups was performed by the Kruskal-Wallis test, where at $p < 0.05$ the sign was considered statistically significantly different in the three groups. Then, paired comparison between the groups was performed using the Mann-Whitney criterion and Bonferroni correction. The sign was considered statistically significantly different between the two groups at $p < 0.0167$. Preliminary comparison of the groups over time was performed using the Friedman test for related traits with calculation of the Kendall concordance coefficient (KC). The sign was considered statistically significantly different at $p < 0.05$. Then, sequential pairwise comparison of the sign within the groups was performed using the Wilcoxon test with the Bonferroni correction. The sign was considered statistically significantly different between the two groups at $p < 0.0167$.

Results

Neutrophilic and lymphocytic infiltration with hemorrhagic areas were observed in the wounds of animals of all groups before treatment (Fig. 1a). The vessels and capillaries found in the specimens were paralytically dilated or filled with erythrocytes. The

vascular endothelium was swollen. Collagen fibers present in the wounds were damaged and swollen. In the area of the wound bottom, among the fatty tissue, a large number of mast cells in varying degrees of degranulation were noted (Fig. 1b, c). Foci of hemorrhage were visible in the muscle tissue. The tissue was edematous and

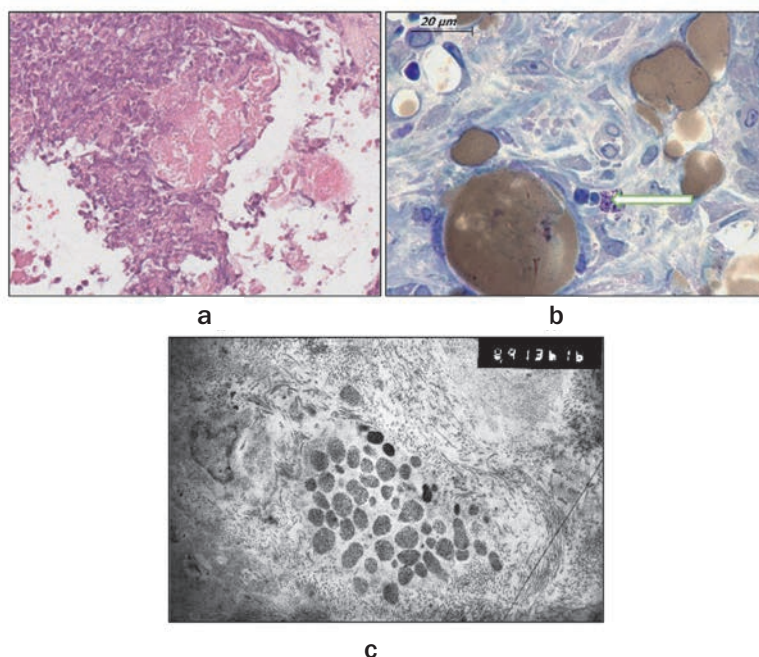


Рис. 1. Препараты ран животных до лечения: а – раневой дефект, некроз ткани, участки кровоизлияния; б – тучная клетка – стрелка; с – тучная клетка в состоянии дегрануляции; Увеличение: а – 200; б – 1000; с – электронограмма x8900. Окраска: а – гематоксилин-эозин; б – толуидиновый синий; с – уранил ацетат и цитрат свинца.

Fig. 1. Specimens of animal wounds before treatment: а – wound defect, tissue necrosis, areas of hemorrhage; б – mast cell – indicated by an arrow; с – mast cell in a state of degranulation. Magnification: а – 200x; б – 1000x; с – electron micrograph x8900. Staining: а – hematoxylin and eosin; б – toluidine blue; с – uranyl acetate and lead citrate.

Таблица 1

Количественный состав клеток в гистологических препаратах ран до начала лечения

Table 1

Quantitative composition of cells in histological wound specimens before treatment

Клеточный состав Cell composition	1-я группа Group 1	2-я группа Group 2	3-я группа Group 3	p – между исследуемыми группами p – between groups
Нейтрофилы Neutrophils	316 (274;346)	303 (276;345)	314 (261;364)	p=0,88
Лимфоциты Lymphocytes	62 (59;68)	59 (57;66)	65 (60;68)	p=0,051
Макрофаги Macrophages	0	0	0	
Дегранулирующие базофилы Degranulating basophils	11 (10;12)	12 (11;13)	11 (10;13)	p=0,049
Базофилы Basophils	0	0	0	
Плазмocyты Plasmacells	1 (1;1)	1 (1;1)	1 (1;1)	p=0,47
Фибробласты Fibroblasts	0	0	0	
Сравнение клеточного состава внутри групп в динамике Comparison within groups over time	p(H/N)<0.0001, KK=1; p(L/L)<0.0001, KK=1; p(M/M)<0.0001, KK=1; p(ДБ/DB)<0.0001, KK=0,98; p(Б/В)<0.0001, KK=1; p(П/Р)<0.0001, KK=0,58; p(Ф/Ф)<0.0001, KK=0,98	p(H/N)<0.0001, KK=1; p(L/L)<0.0001, KK=0,9; p(M/M)<0.0001, KK=0,78; p(ДБ/DB)<0.0001, KK=1; p(Б/В)<0.0001, KK=0,92; p(П/Р)<0.0001, KK=0,92; p(Ф/Ф)<0.0001, KK=1	p(H/N)<0.0001, KK=1; p(L/L)<0.0001, KK=0,93; p(M/M)<0.0001, KK=0,93; p(ДБ/DB)<0.0001, KK=0,98; p(Б/В)<0.0001, KK=0,93; p(П/Р)<0.0001, KK=0,81; p(Ф/Ф)<0.0001, KK=1	

contained damaged vessels with swollen endothelium. The edges of the wound were bordered by thickened epidermis, with signs of edema.

Statistical analysis of the quantitative composition of cells before the treatment revealed no significant difference between the groups (Table 1).

By the 7th day of treatment, edema persisted in the specimens of animals of all groups. A tendency toward a decrease and transformation of the infiltrate was noted. In the 1st group, the infiltration areas acquired the appearance of a layered structure, and hemosiderin granules appeared. The pigment granules were located freely in the intercellular space and macrophages, staining the latter brown (Fig. 2a, b). In other groups, the decrease in infiltrate was less significant. Thus, in the 2nd group of animals, infiltration in the form of rosettes around small vessels was observed. In the wound specimens of animals of the 3rd group, thrombosed blood vessels were noted, both small and larger. Neutrophils in the wound had signs of NETosis. In all groups, degranulation of mast cells was noted (Fig. 2c). In the specimens of the 1st and 2nd

groups of animals, young fibroblasts appeared, which in the 1st group of animals were lined up in strands oriented parallel to the wound surface (Fig. 2d). In the 2nd group of animals such orientation of cells was not determined (Fig. 2e).

In all groups, by the 7th day of treatment, the number of neutrophils was significantly reduced compared to the previous day of control (Tables 1, 2). Differences in the number of neutrophils in wound specimens between the groups (Table 2) were statistically significant. Thus, in the 1st group their number was significantly less compared to the 2nd and 3rd groups ($p < 0.0001$ for both groups), and in the 2nd group the number of neutrophils was significantly less compared to the 3rd group ($p < 0.0001$).

Also, in the specimens of animals of the 1st group, the number of lymphocytes was reduced compared to the previous day of control and compared to other groups (Tables 1, 2). In animals of all groups, macrophages appeared in the wounds, which were significantly more in the wound specimens of animals of the 1st group ($p < 0.0001$ compared to the 2nd and 3rd groups) and the

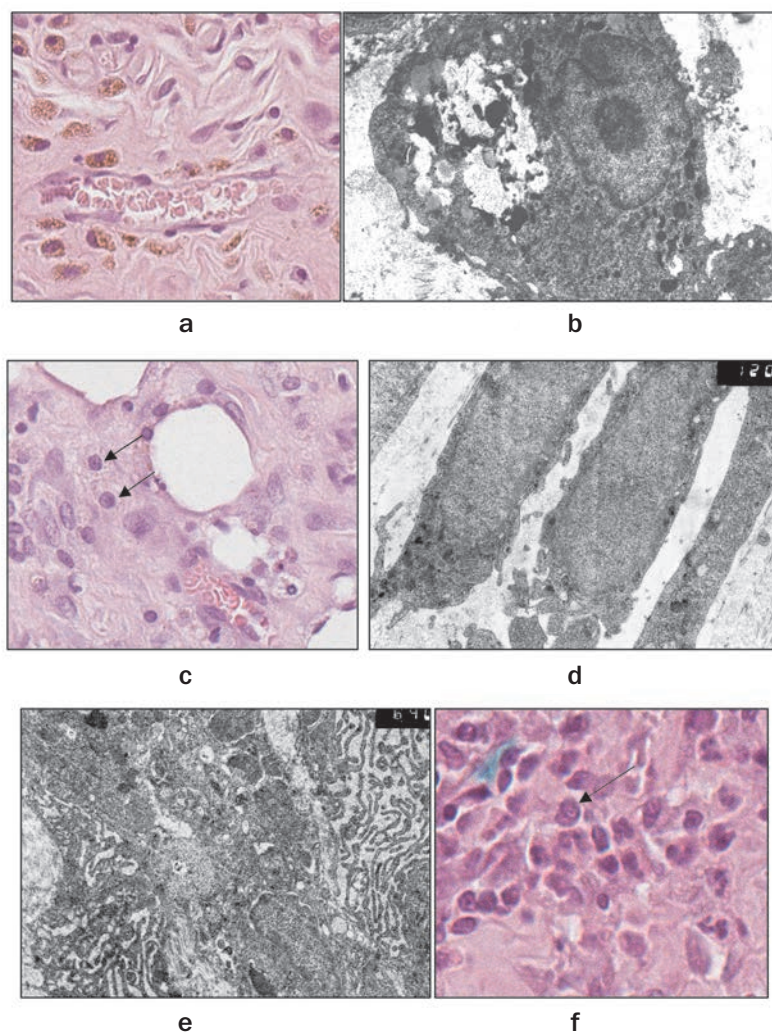


Рис. 2. Препараты ран животных на 7-й день лечения (a-d – 1-я группа; e-f – 2-я группа): а – в соединительной ткани гранулы гемосидерина коричневого цвета; б – функционально активный макрофаг, в центре клетки крупная фагосома с клеточным детритом; с – тучные клетки в состоянии полной дегрануляции; д – фибробласты ориентированные параллельно поверхности раны; е – функционально активные фибробласты без выраженной пространственной ориентации; ф – в поле зрения плазмочит.
а, с, ф увеличение: – 400, окраска – гематоксилин-эозин; б, д, е – электронограммы, увеличение – 12000, окраска – уранил ацетат и цитрат свинца.
Fig. 2. Specimens of animal wounds on the 7th day of treatment (a-d: Group 1; e-f: Group 2): а – brown hemosiderin granules in connective tissue; б – functionally active macrophage. Large phagosome with cellular debris in the center; с – mast cells in a state of complete degranulation; д – fibroblasts aligned parallel to the wound surface; е – functionally active fibroblasts without distinct spatial orientation; ф – plasma cell in the field of view.
Magnification: а, с, ф – staining – hematoxylin and eosin, 400x; б, д, е – electron micrographs, staining – uranyl acetate and lead citrate, magnification – 12000x.

Таблица 2

Количественный состав клеток в гистологических препаратах ран на 7 день лечения

Table 2

Quantitative composition of cells in histological wound specimens on the 7th day of treatment

Клеточный состав Cell composition	1-я группа Group 1	2-я группа Group 2	3-я группа Group 3	р – между исследуемыми группами p – between groups
Нейтрофилы Neutrophils	64 (59;67)	82 (77;86)	176,5 (167;188)	p<0,0001 p(1-2) <0,0001 p(1-3) <0,0001 p(2-3) <0,0001
Лимфоциты Lymphocytes	13 (12;14)	60 (53;67)	73 (72;74)	p<0,0001 p(1-2) <0,0001 p(1-3) <0,0001 p(2-3) <0,0001
Макрофаги Macrophages	34 (30;36)	17 (16;18)	4 (2;6)	p<0,0001 p(1-2) <0,0001 p(1-3) <0,0001 p(2-3) <0,0001
Дегранулирующие базофилы Degranulating basophils	1 (1;1)	4 (3;5)	7 (6;8)	p<0,0001 p(1-2) <0,0001 p(1-3) <0,0001 p(2-3) <0,0001
Базофилы Basophils	6 (5;8)	1 (1;1)	0	p<0,0001 p(1-2) <0,0001 p(1-3) <0,0001 p(2-3) <0,0001
Плазмоциты Plasma cells	3,5 (2;6)	2 (2;2)	1 (1;1)	p<0,0001 p(1-2) <0,0001 p(1-3) <0,0001 p(2-3) <0,0001
Фибробласты Fibroblasts	13,5 (12;17)	2,5 (2;4)	0	p<0,0001 p(1-2) <0,0001 p(1-3) <0,0001 p(2-3) <0,0001
р – внутри каждой исследуемой группы между 7-ым днем контроля и днем до начала лечения p – within each group between Day 7 and pre-treatment	p(H/N)<0.0001 p(L/L)<0.0001 p(M/M)<0.0001 p(ДБ/ДБ)<0.0001 p(Б/Б)<0.0001 p(П/П)<0.0001 p(Ф/Ф)<0.0001	p(H/N)<0.0001 p(L/L)=0,62 p(M/M)<0.0001 p(ДБ/ДБ)<0.0001 p(Б/Б)<0.0001 p(П/П)<0.0001 p(Ф/Ф)<0.0001	p(H/N)<0.0001 p(L/L)<0.0001 p(M/M)<0.0001 p(ДБ/ДБ)<0.0001 p(П/П)=0,69	

2nd group ($p < 0.0001$ compared to the 3rd group). On the 7th day of wound treatment, in response to the therapy, the number of plasma cells in the wound specimens of animals of the 1st and 2nd groups increased (Tables 1, 2; Fig. 2f).

Morphological examination of wound specimens on the 14th day of treatment showed that in specimens of the 1st group of animals, inflammatory tissue infiltration was minimal. Fibroblasts oriented parallel to the wound surface were in a state of high functional activity (as confirmed by ultrastructural analysis), synthesized proteins, including collagen (Fig. 3a). New vessels grew toward the wound center and perpendicular to the wound surface (Fig. 3b). Fibroblasts were grouped along the vessels (Fig. 3c). Mast cells were single, in a state of partial degranulation. (Fig. 3d,e). In the 2nd group, infiltration decreased, in some specimens, formation of new capillaries was noticeable. In the 3rd group, a scab

still remained, infiltrate and edema under the scab, neutrophils and macrophages were visible (Fig. 3f). In some areas, infiltration extended to muscle and adipose tissue. There were no histological signs of connective tissue remodeling.

Quantitative analysis showed that the number of neutrophils and lymphocytes on the 14th day of treatment became significantly lower than on the 7th day (Tables 2, 3). The dynamics of the number of macrophages in each group was different. Thus, in the 1st group, their number compared to the 7th day of treatment and compared to other groups was statistically significantly lower ($p < 0.0001$ for all the above indicators). In the 2nd group of animals, the number of macrophages remained at the same level compared to the previous day of control ($p = 0.89$), but was significantly lower than in the 3rd group ($p < 0.0001$). In the wound specimens of the 3rd group, the macrophage indicators increased compared to the

7th day of treatment, which indicated a later response of the body to the treatment. At the same time, a significant decrease in the number of degranulating basophils was

detected in all groups ($p < 0.0001$ for all groups), while their content was increased in groups 1 and 2 ($p < 0.0001$). The mast cell population of groups 1 and 2 restored their

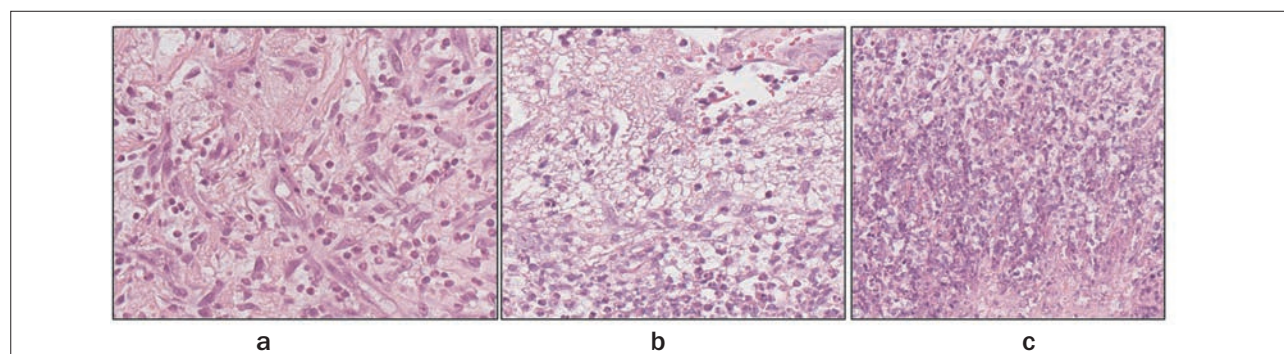
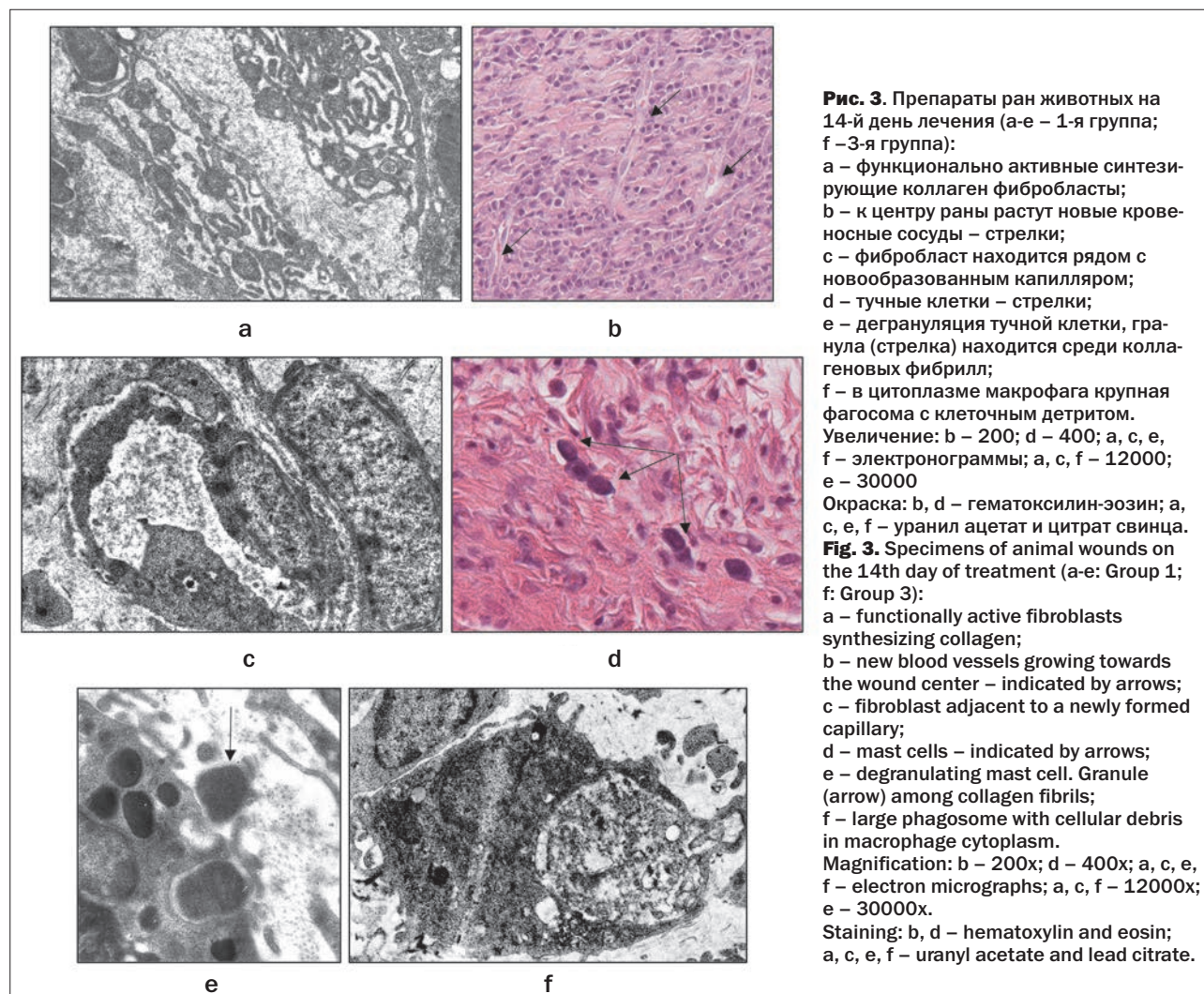


Таблица 3

Количественный состав клеток в гистологических препаратах ран на 14-й день лечения

Table 3

Quantitative composition of cells in histological wound specimens on the 14th day of treatment

Клеточный состав Cell composition	1-я группа Group 1	2-я группа Group 2	3-я группа Group 3	p – между исследуемыми группами p – between groups
Нейтрофилы Neutrophils	10,5 (7;14)	27 (25;34)	56 (49;61)	p<0,0001 p(1-2)<0,0001 p(1-3)<0,0001 p(2-3)<0,0001
Лимфоциты Lymphocytes	2 (2;2)	27 (25;29)	55 (51;60)	p<0,0001 p(1-2)<0,0001 p(1-3)<0,0001 p(2-3)<0,0001
Макрофаги Macrophages	6 (5;7)	17 (14;21)	33 (25;42)	p<0,0001 p(1-2)<0,0001 p(1-3)<0,0001 p(2-3)<0,0001
Дегранулирующие базофилы Degranulating basophils	0	1 (1;1)	2 (2;2)	p<0,0001 p(1-2)<0,0001 p(1-3)<0,0001 p(2-3)<0,0001
Базофилы Basophils	13 (12;15)	6 (5;8)	1 (1;1)	p<0,0001 p(1-2)<0,0001 p(1-3)<0,0001 p(2-3)<0,0001
Плазмоциты Plasmacells	2 (2;2)	1 (1;1)	1 (1;1)	p<0,0001 p(1-2)<0,0001 p(1-3)<0,0001 p(2-3)=0,7
Фибробласты Fibroblasts	45 (33;52)	17 (15;19)	5 (4;6)	p<0,0001 p(1-2) <0,0001 p(1-3) <0,0001 p(2-3) <0,0001
p – внутри каждой исследуемой группы между 14-ым и 7-ым днями p – within each group between Day 14 and Day 7	p(H/N)<0.0001 p(L/L)<0.0001 p(M/M)<0.0001 p(ДБ/DB)<0.0001 p(Б/В)<0.0001 p(П/Р)<0.0001 p(Ф/Ф)<0.0001	p(H/N)<0.0001 p(L/L)<0.0001 p(M/M)=0,89 p(ДБ/DB)<0.0001 p(Б/В)<0.0001 p(П/Р)<0.0001 p(Ф/Ф)<0.0001	p(H/N)<0.0001 p(L/L)<0.0001 p(M/M)<0.0001 p(ДБ/DB)<0.0001 p(Б/В)<0.0001 p(П/Р)=0,53 p(Ф/Ф)<0.0001	

functional activity. On the part of the connective tissue component, an increase in the content of fibroblasts was noted in groups 1 and 2 (Tables 2, 3). Single basophils and fibroblasts appeared in the wound specimens of group 3.

By the 21st day of treatment, there was a significant dynamics of morphological signs. Thus, when examining wound specimens of animals in group 1, in which high-intensity pulsed broadband irradiation was used in the treatment, connective tissue remodeling was observed in favor of complete restoration of the structure. In group 2 animals, in which traditional ultraviolet irradiation was used in the treatment of wounds, the macrophage reaction persisted. In the connective tissue under the scab, capillaries were present, although in smaller quantities than in group 1. In wound specimens of animals in groups 1 and 2, there

is a large number of inactive mast cells in the connective tissue (Table 4). In group 3, an admixture of neutrophils (Table 4) and thrombosis of small vessels are preserved. Edema persists, which is expressed in connective and adipose tissue.

Discussion

Wound healing is a complex biological process with successively overlapping physiological and morphological phases. To restore the barrier function of damaged skin, coordination of cellular and molecular processes is necessary. At the beginning of the wound healing process, in the first phase of inflammation, cellular elements such as neutrophils and macrophages migrate to the wound, mobilizing local and systemic defense. In the next phase, proliferation, connective tissue cells, fibroblasts and keratinocytes, begin to

Таблица 4
Количественный состав клеток в гистологических препаратах ран на 21-й день лечения

Table 4
Quantitative composition of cells in histological wound specimens on the 21st day of treatment

Клеточный состав Cell composition	1-я группа Group 1	2-я группа Group 2	3-я группа Group 3	р – между исследуемыми группами p – between groups
Нейтрофилы Neutrophils	0	6,5 (5;9)	23 (19;26)	p<0,0001 p(1-2) <0,0001 p(1-3) <0,0001 p(2-3) <0,0001
Лимфоциты Lymphocytes	0	3 (2;4)	14 (12;18)	p<0,0001 p(1-2) <0,0001 p(1-3) <0,0001 p(2-3) <0,0001
Макрофаги Macrophages	2 (2;2)	10 (8;13)	25 (23;27)	p<0,0001 p(1-2) <0,0001 p(1-3) <0,0001 p(2-3) <0,0001
Дегранулирующие базофилы Degranulating basophils	0	0	0	p<0,0001 p(1-2) <0,0001 p(1-3) <0,0001 p(2-3) <0,0001
Базофилы Basophils	19 (18;20)	9 (7;11)	2 (2;2)	p<0,0001 p(1-2) <0,0001 p(1-3) <0,0001 p(2-3) <0,0001
Плазмоциты Plasmacells	2 (2;2)	0	0	p<0,0001 p(1-2) <0,0001 p(1-3) <0,0001
Фибробласты Fibroblasts	66 (59;77)	34 (27;40)	14 (12;16)	p<0,0001 p(1-2) <0,0001 p(1-3) <0,0001 p(2-3) <0,0001
р – внутри каждой группы между 21-ым и 14-ым днем p – within each group between Day 21 and Day 14	p(H/N)<0.0001; p(L/L)<0.0001; p(M/M)<0.0001; p(B/B)<0.0001; p(П/Р)=1 p(Ф/Ф)<0.0001	p(H/N)<0.0001 p(L/L)<0.0001 p(M/M)<0.0001 p(ДБ/ДБ)<0.0001 p(Б/Б)<0.0002 p(П/П)<0.0001 p(Ф/Ф)<0.0001	p(H/N)<0.0001 p(L/L)<0.0001 p(M/M)<0.0001 p(ДБ/ДБ)<0.0001 p(Б/Б)<0.0001 p(П/П)<0.0001 p(Ф/Ф)<0.0001	

actively proliferate, triggering the process of connective tissue remodeling. The third phase of the wound healing process is the phase of regeneration or epithelialization, when fibroblasts begin to synthesize collagen, and the organization of a new matrix begins [8].

Various methods are used to analyze and evaluate wound healing, including planimetry and morphological examination. Planimetry allows clinical evaluation of the visible characteristics of the wound and, due to the presence of a scab, often does not correlate with the healing indices visualized by morphology, which makes morphological examination the “gold standard” for assessing wound healing [9].

There are data on the effectiveness of phototherapy in the treatment of wounds, including infected ones, however the studies mainly concern laser or photodynamic therapy, and the authors point out the

clinical, bactericidal and morphological effectiveness of their use [10, 11, 12]. There are few works devoted to studying the effectiveness of ultraviolet irradiation in the treatment of infected wounds, moreover they show only bactericidal effectiveness [13, 14].

K. Narita *et al.* in an experiment on mice, having modeled a wound infected with St. Aureus (MRSA), irradiated it with two types of lamps with radiation in the range of 222 nm and 254 nm. The authors performed bacteriological, histological and immunohistochemical studies. In the morphological study, the authors found a decrease in the inflammatory response to ultraviolet irradiation of infected wounds in the 222 nm range. In the study, histological analysis was performed only on the 5th and 8th days, and only neutrophilic infiltration was assessed without a statistical assessment of the full morphological picture [15].

V.V. Bagrov *et al.* showed the bactericidal, clinical and morphological effectiveness of antibacterial therapy in combination with high-intensity optical irradiation of infected wounds compared to the traditional use of Levomekol ointment (dioxomethyltetrahydropyrimidine (methyluracil), chloramphenicol). Histological analysis showed an earlier transition of the wound process (day 14) to the granulation phase in animals whose wounds were exposed to high-intensity optical irradiation, compared to the wounds of animals in the control group [16].

Thus, the data on the use of ultraviolet irradiation of infected wounds is limited and is presented mainly by a description of bactericidal effectiveness. In the existing studies, morphological signs of tissue regeneration are presented only at the initial stages of the wound process, at the stages of inflammation and proliferation, and there is no data on the full morphological picture occurring in the wound during treatment with ultraviolet irradiation until the completion of regenerative processes.

In our study, we present a qualitative and quantitative analysis of the morphological picture using high-intensity pulsed broadband irradiation, traditional ultraviolet irradiation and classical local application of an antiseptic.

Our experimental study of the treatment of infected wounds showed that before the treatment, the morphological picture of the wounds corresponded to

the acute inflammation phase. On the 7th day in the 1st group, the morphological picture corresponded to the proliferation phase. In the 2nd and 3rd groups, edema and infiltration persisted. By the 14th day, signs of granulation tissue formation and the transition of wounds to the regeneration stage were observed in the 1st group. In the 2nd group, infiltration decreased, new capillaries appeared, and the number of fibroblasts increased.

In the 3rd group, inflammatory phenomena persisted. By the 21st day, there were no signs of inflammation in the wound specimens of the 1st group, connective tissue remodeling with signs of formation of a delicate scar was observed. In the specimens of the 2nd group, signs of infiltration were minimal, connective tissue remodeling phenomena were observed, in which new capillaries were present. In the wound specimens of the 3rd group of animals, infiltration was reduced, new vessels were formed with a slowdown.

Conclusion

The morphological study showed that the use of high-intensity pulsed broadband irradiation of infected wounds, in contrast to traditional ultraviolet irradiation and treatment of wounds with antiseptics at an earlier stage, stops the inflammatory reaction of tissues, activates the local immune response and accelerates the processes of connective tissue remodeling.

REFERENCES

1. Alcolea J.M., Hernández E., Martínez-Carpio P.A., et al. Treatment of Chronic Lower Extremity Ulcers with A New Er:Yag Laser Technology. *Laser Ther.* 2017, vol. 26(3), pp. 211-222. <https://doi.org/10.5978/islm.17-OR-17>;
2. Aleksandrowicz H., Owczarczyk-Saczonek A., Placek W. Venous Leg Ulcers: Advanced Therapies and New Technologies. *Biomedicines*, 2021, vol. 9(11), pp. 1569. <https://doi.org/10.3390/biomedicines9111569>
3. Gupta A., Avci P., Dai T., et al. Ultraviolet Radiation in Wound Care: Sterilization and Stimulation. *Adv Wound Care (New Rochelle)*, 2013, vol. 2(8), pp. 422-437. <https://doi.org/10.1089/wound.2012.0366>;
4. Wang D., Kuzma M.L., Tan X., et al. Phototherapy and optical waveguides for the treatment of infection. *Adv Drug Deliv Rev.* 2021, vol. 179, pp. 114036. <https://doi.org/10.1016/j.addr.2021.114036>;
5. Szigeti R., Kellermayer R. Tying the past to the present: time tested knowledge with state-of-the-art technology in the fight against emerging and drug resistant microbes. *Ther Adv Infect Dis.* 2021, vol. 8, pp. 2049936121989552. <https://doi.org/10.1177/2049936121989552>
6. Arkhipov V.P., Bagrov V.V., Byalovsky Yu.Yu., et al. Organization of preclinical studies of the bactericidal and wound healing effects of the pulsed phototherapy apparatus «Zarya». *Problems of social hygiene, healthcare and the history of medicine*, 2021, vol. 29(5), pp. 1156-1162. <https://doi.org/10.32687/0869-866X-2021-29-5-1156-1162>.
7. Davydov A.I., Lipatov D.V., Kamrukov A.S., et al. The use of pulsed high-intensity optical irradiation and exogenous nitrogen monoxide in the complex treatment of patients with purulent inflammation of the uterine appendages. *Issues of gynecology, obstetrics and perinatology*, 2007, vol. 6 (1), pp. 14-17.

ЛИТЕРАТУРА

1. Alcolea J.M., Hernández E., Martínez-Carpio P.A., et al. Treatment of Chronic Lower Extremity Ulcers with A New Er:Yag Laser Technology // *Laser Ther.* – 2017. – Vol. 26(3). – P. 211-222. <https://doi.org/10.5978/islm.17-OR-17>;
2. Aleksandrowicz H., Owczarczyk-Saczonek A., Placek W. Venous Leg Ulcers: Advanced Therapies and New Technologies // *Biomedicines*. – 2021. – Vol. 9(11). – P. 1569. <https://doi.org/10.3390/biomedicines9111569>
3. Gupta A., Avci P., Dai T., et al. Ultraviolet Radiation in Wound Care: Sterilization and Stimulation // *Adv Wound Care (New Rochelle)*. – 2013. – Vol. 2(8). – P. 422-437. <https://doi.org/10.1089/wound.2012.0366>;
4. Wang D., Kuzma M.L., Tan X., et al. Phototherapy and optical waveguides for the treatment of infection // *Adv Drug Deliv Rev.* – 2021. – Vol. 179. – P. 114036. <https://doi.org/10.1016/j.addr.2021.114036>;
5. Szigeti R., Kellermayer R. Tying the past to the present: time tested knowledge with state-of-the-art technology in the fight against emerging and drug resistant microbes // *Ther Adv Infect Dis.* – 2021. – Vol. 8. – P. 2049936121989552. <https://doi.org/10.1177/2049936121989552>
6. Архипов В.П., Багров В.В., Бяловский Ю.Ю. и др. Организация доклинических исследований бактерицидного и ранозаживляющего действия импульсного фототерапевтического аппарата «Заря» // *Проблемы социальной гигиены, здравоохранения и истории медицины.* – 2021. – Т. 29, № 5. – С. 1156-1162. <https://doi.org/10.32687/0869-866X-2021-29-5-1156-1162>.
7. Давыдов А.И., Липатов Д.В., Камруков А.С. и др. Использование импульсного высокоинтенсивного оптического облучения и экзогенного монооксида азота в комплексном лечении больных гнойным воспалением придатков матки // *Вопросы гинекологии, акушерства и перинатологии.* – 2007. – Т. 6, № 1. – С. 14-17.

8. Rhea L., Dunnwald M. Murine Excisional Wound Healing Model and Histological Morphometric Wound Analysis. *J Vis Exp*, 2020, vol. 162, pp. 10.3791/61616. <https://doi.org/10.3791/61616>
9. Ansell D.M., Campbell L., Thomason H.A., et al. A statistical analysis of murine incisional and excisional acute wound models. *Wound Repair Regen*, 2014, vol. 22(2), pp. 281-287. <https://doi.org/10.1111/wrr.12148>
10. Chepurная Y.L., Melkonyan G.G., Gulmuradova N.T., Sorokin A.A. The effect of photodynamic therapy on the dynamics of the wound process in patients with purulent diseases of the fingers and hand. *Biomedical Photonics*, 2021, vol. 10(2), pp. 4-17. <https://doi.org/10.24931/2413-9432-2021-10-2-4-17>
11. Soltan H.H., Afifi A., Mahmoud A., Refaat M., Al Balah O.F. Effects of silver nanoparticle and low-level laser on the immune response and healing of albino mice skin wounds. *Biomedical Photonics*, 2024, vol. 13(1), pp. 16-27.
12. Zaitsev A. E., Asanov O. N., Chekmareva I. A. Analysis of the effectiveness of an erbium laser in the treatment of trophic purulent wounds in an experiment. *Medical Bulletin of the North Caucasus*, 2023, vol.8(4), pp. 394-397. <https://doi.org/10.14300/mnnc.2023.18093>
13. Dai T., Kharkwal G.B., Zhao J., et al. Ultraviolet-C light for treatment of *Candida albicans* burn infection in mice. *Photochem Photobiol*, 2011, vol. 87(2), pp. 342-349. <https://doi.org/10.1111/j.1751-1097.2011.00886.x>
14. Dai T., Murray C.K., Vrahas M.S., Baer D.G., Tegos G.P., Hamblin M.R. Ultraviolet C light for *Acinetobacter baumannii* wound infections in mice: potential use for battlefield wound decontamination? *J Trauma Acute Care Surg*, 2012, vol. 73(3), pp. 661-667. <https://doi.org/10.1097/TA.0b013e31825c149c>
15. Narita K., Asano K., Morimoto Y., et al. Disinfection and healing effects of 222-nm UVC light on methicillin-resistant *Staphylococcus aureus* infection in mouse wounds. *J Photochem Photobiol B*, 2018, vol. 178, pp. 10-18. <https://doi.org/10.1016/j.jphotobiol.2017.10.030>
16. Bagrov V.V., Bukhtiyarov I.V., Volodin L.Y. et al. Preclinical Studies of the Antimicrobial and Wound-Healing Effects of the High-Intensity Optical Irradiation "Zarnitsa-A" Apparatus. *Applied Sciences (Switzerland)*, 2023, vol. 13(19), pp. 10794. <https://doi.org/10.3390/app131910794>
8. Rhea L., Dunnwald M. Murine Excisional Wound Healing Model and Histological Morphometric Wound Analysis // *J Vis Exp*. – 2020. – Vol. 162. – P. 10.3791/61616. <https://doi.org/10.3791/61616>
9. Ansell D.M., Campbell L., Thomason H.A., et al. A statistical analysis of murine incisional and excisional acute wound models // *Wound Repair Regen*. – 2014. – Vol. 22(2). – P. 281-287. <https://doi.org/10.1111/wrr.12148>
10. Чепурная Ю.Л., Мелконян Г.Г., Гульмурадова Н.Т., Сорокин А.А. Влияние фотодинамической терапии на динамику раневого процесса у пациентов с гнойными заболеваниями пальцев и кисти // *Biomedical Photonics*. – 2021. – Vol. 10(2). – P. 4-17. <https://doi.org/10.24931/2413-9432-2021-10-2-4-17>
11. Soltan H.H., Afifi A., Mahmoud A., Refaat M., Al Balah O.F. Effects of silver nanoparticle and low-level laser on the immune response and healing of albino mice skin wounds // *Biomedical Photonics*. – 2024. – Vol. 13(1). – P. 16-27.
12. Зайцев А. Е., Асанов О. Н., Чекарёва И. А. Анализ эффективности эрбиевого лазера при лечении трофических гнойных ран в эксперименте // *Медицинский вестник Северного Кавказа*. – 2023. – Т.8, №4. – С. 394-397. <https://doi.org/10.14300/mnnc.2023.18093>
13. Dai T., Kharkwal G.B., Zhao J., et al. Ultraviolet-C light for treatment of *Candida albicans* burn infection in mice // *Photochem Photobiol*. – 2011. – Vol. 87(2). – P. 342-349. <https://doi.org/10.1111/j.1751-1097.2011.00886.x>
14. Dai T., Murray C.K., Vrahas M.S., Baer D.G., Tegos G.P., Hamblin M.R. Ultraviolet C light for *Acinetobacter baumannii* wound infections in mice: potential use for battlefield wound decontamination? // *J Trauma Acute Care Surg*. – 2012. – Vol. 73(3). – P. 661-667. <https://doi.org/10.1097/TA.0b013e31825c149c>
15. Narita K., Asano K., Morimoto Y., et al. Disinfection and healing effects of 222-nm UVC light on methicillin-resistant *Staphylococcus aureus* infection in mouse wounds // *J Photochem Photobiol B*. – 2018. – Vol. 178. – P. 10-18. <https://doi.org/10.1016/j.jphotobiol.2017.10.030>
16. Bagrov V.V., Bukhtiyarov I.V., Volodin L.Y. et al. Preclinical Studies of the Antimicrobial and Wound-Healing Effects of the High-Intensity Optical Irradiation "Zarnitsa-A" Apparatus // *Applied Sciences (Switzerland)*. – 2023. – Vol. 13(19). – P. 10794. <https://doi.org/10.3390/app131910794>

PHOTODYNAMIC THERAPY IN THE PREVENTION OF HPV-INDUCED RECURRENCES OF PRECANCER AND INITIAL CANCER OF THE CERVIX

Trushina O.I., Filonenko E.V., Novikova E.G., Mukhtarulina S.V.

P.A. Herzen Moscow Oncology Research Center – branch of FSBI NMRRС of the Ministry of Health of the Russian Federation, Moscow, Russia

Abstract

Photodynamic therapy (PDT) has antiviral activity and is an effective method for preventing cervical HPV-associated relapses. In our study, we assessed the effectiveness of prophylactic anti-relapse PDT of the cervical stump at the second stage after high amputation of the cervix in 65 patients with a clinical diagnosis of carcinoma in situ and 35 with a diagnosis of cervical cancer stage 1A1. As a photosensitizer, a drug based on 5-aminolevulinic acid (5-ALA) in the form of a 12% gel at a dose of 0.1 mg/cm² was used. Irradiation was performed after 4 hours (light dose – 150 J/cm²). Complete eradication of HPV DNA was achieved in 94% of patients. In the remaining 6% of observations, the antiviral effect was registered as eradication of one or two types in case of multiple HPV infection with dominance of strains 16 and 18, or a significant decrease in the viral load. The observation periods ranged from 3 to 10 years. A persistent antiviral effect was maintained throughout the observation period in 93 (93%) women. Thus, PDT of the cervical stump with 5-ALA provides a pronounced antiviral effect at the second stage of treatment of precancerous and initial tumor pathology of the cervix due to the selective accumulation of the photosensitizer in infected cells with their subsequent direct phototoxic and photochemical destruction to the basal and parabasal layers of the epithelium, in which virus replication occurs.

Key words: cervical cancer, photodynamic therapy, human papillomavirus, 5-aminolevulinic acid.

For citations: Trushina O.I., Filonenko E.V., Novikova E.G., Mukhtarulina S.V. Photodynamic therapy in the prevention of HPV-induced recurrences of precancer and initial cancer of the cervix, *Biomedical Photonics*, 2024, vol. 13, no. 3, pp. 42–46. doi: 10.24931/2413–9432–2024–13–3–42–46

Contacts: Trushina O.I., e-mail: o.trushina@list.ru

ФОТОДИНАМИЧЕСКАЯ ТЕРАПИЯ В ПРОФИЛАКТИКЕ ВПЧ-ИНДУЦИРОВАННЫХ РЕЦИДИВОВ ПРЕДРАКА И НАЧАЛЬНОГО РАКА ШЕЙКИ МАТКИ

О.И. Трушина, Е.В. Филоненко, Е.Г. Новикова, С.В. Мухтарулина

«Московский научно-исследовательский онкологический институт им. П.А. Герцена – филиал ФГБУ «Национальный медицинский исследовательский центр радиологии» Министерства здравоохранения Российской Федерации, Москва, Россия

Резюме

Фотодинамическая терапия (ФДТ) обладает противовирусной активностью и является эффективным методом профилактики цервикальных ВПЧ-ассоциированных рецидивов. В нашем исследовании была оценена эффективность профилактической противорецидивной ФДТ культи шейки матки на втором этапе после высокой ампутации шейки матки у 65 пациенток с клиническим диагнозом carcinoma in situ и 35 – с диагнозом РШМ 1A1 ст. В качестве фотосенсибилизатора использовали аппликационно препарат на основе 5-аминолевулиновой кислоты (5-АЛК) в виде 12%-го геля в дозе 0,1 мг/см². Облучение проводили через 4 ч (световая доза – 150 Дж/см²). Полная эрадикация ДНК ВПЧ была достигнута у 94% пациенток. В остальных 6% наблюдениях противовирусный эффект зарегистрирован в виде эрадикации одного или двух типов при множественном инфицировании ВПЧ с доминированием 16 и 18 штаммов, или значительном снижении вирусной нагрузки. Сроки наблюдения составили от 3 до 10 лет. Стойкий противовирусный эффект в течение всего периода наблюдения сохранялся у 93 (93%) женщин. Таким образом, ФДТ культи шейки матки с 5-АЛК обеспечивает выраженный противовирусный эффект на втором этапе лечения предопухолевой и начальной опухолевой патологии шейки матки за счет селективного накопления фотосенсибилизатора в инфицированных клетках с последующим их прямым фототоксическим и фотохимическим разрушением до базальных и парабазальных слоев эпителия, в которых происходит репликация вируса.

Ключевые слова: рак шейки матки, фотодинамическая терапия, вирус папилломы человека, 5-аминолевулиновая кислота.

Для цитирования: Трушина О.И., Филоненко Е.В., Новикова Е.Г., Мухтарулина С.В. Фотодинамическая терапия в профилактике ВПЧ-индуцированных рецидивов предрака и начального рака шейки матки // *Biomedical Photonics*. – 2024. – Т. 13, № 3. – С. 42–46. doi: 10.24931/2413–9432–2024–13–3–42–46

Контакты: Трушина О.И., e-mail: o.trushina@list.ru

Introduction

The problem of cervical cancer (CC) has been the focus of attention of leading oncologists from all over the world for many decades. The steady increase in the number of women with malignant neoplasms of the cervix and the pronounced trend towards "rejuvenation" of the disease undoubtedly indicate the relevance of the search, development and implementation of new approaches to the prevention, diagnosis and treatment of cervical precancerous and tumor pathology. In the successful implementation of these tasks, an important role is given to the etiological factor of cervical carcinogenesis – the human papillomavirus (HPV). The DNA of this viral agent has a high oncogenic potential and is found in 99.7% of CC [1,2].

Over the past two decades, much attention has been paid to the issues of progression of papillomavirus infection (PVI) to invasive CC, while an equally important direction in the prevention of relapses of the disease after organ-preserving treatment of initial cervical oncopathology remains poorly studied. Recurrence of the tumor process in the cervix indicates to a greater extent the persistence of HPV, the leading factor in stimulating epithelial proliferation [3,4]. This viral agent is capable of initiating relapses of cervical intraepithelial neoplasia II-III (CIN) and initial CC (carcinoma in situ, CC stage 1A1) during the first three years after electrosurgical conization, the frequency of which, according to a number of authors, is variable and amounts to 15-75% [5,6]. Relapses of the disease in women under 40 years are more common (57.9%) than at an older age [7]. The frequency of relapses increases with involvement of the cervical canal in the process or in the case of mixed localization of the process, especially at the age of 30-39 years – 83.3% [8].

The causes of recurrence of precancer and initial cervical cancer of the uterine in the presence of a negative morphological resection margin are: preservation and persistence of latent and subclinical forms of HPV in unchanged tissues at the border with resection or destruction, necrosis zone, multifocal lesions; deposition of HPV DNA along with smoke on the mucous membranes of the cervix and vagina; the presence of additional foci of HPV infection in the vagina and perineum in every fourth woman with cervical neoplasia; reinfection; the inability to prevent the expression of papillomaviruses in the surrounding tissues [9,10,11,12,13].

The ineffectiveness of antiviral drug therapy aimed at regulating and normalizing the immune system is due to the effect only on episomal forms of HPV activity without destroying the virus strains integrated into the cellular genome [14,15]. Ablation methods (radiofrequency, electro-cryo-laser, argon-plasma) do not ensure HPV eradication due to insufficient

destruction depth, when only the superficial epithelium is destroyed without sanitizing the actively multiplying viral strains located in the basal layer [16]. Physical treatment methods also do not have the ability to precisely destroy papillomaviruses and do not affect the squamous-cylindrical junction of the epithelia and foci of metaplasia in the cervical canal [17,18]. In addition, the persistence of HPV leads to reactivation of latent infection to subclinical and clinical forms. Patients with a latent form of infection represent a risk group for the development of cervical relapses [19].

Thus, antitumor treatment measures do not have a targeted pathogenetically determined effect on HPV, since they do not take into account the features of the life cycle and physical status of the viral genome, respectively, and the risk of HPV-associated relapses of CIN and initial CC remains quite high.

The viral concept of cervical cancer dictates the need to revise traditional approaches to improving the results of treatment of precancerous and initial tumor pathology of the cervix, to search for new effective pathogenetically substantiated methods of influencing the risk factors of malignant progression of PVI, which will significantly reduce the risk of cervical relapses.

Materials and Methods

One of the promising methods of antiviral therapy and, accordingly, prevention of cervical HPV-associated relapses is photodynamic therapy (PDT). The method is based on the selective accumulation of a photosensitizer (PS) in virus-containing cells and the interaction of this drug with light radiation of a certain wavelength, which initiates a series of photophysical processes leading to the destruction of these cells that have accumulated the drug [20]. In connection with the above-described mechanism, it is advisable to supplement surgical treatment of virus-associated precancer and early cervical cancer with one or more courses of antiviral PDT.

PDT of the cervical stump was performed at the second stage after high amputation of the cervix in 65 patients with a clinical diagnosis of carcinoma in situ and 35 with a diagnosis of CC stage 1A1. The average age of the women was 35.6 ± 3.7 years. A drug based on 5-aminolevulinic acid (5-ALA) was used as a photosensitizer. The risk factors for HPV infection included young age, onset of sexual activity before the age of 16 (40%), more than 5 sexual partners (53.5%), infection with bacterial and other viral flora (18.2%), long-term use of oral contraceptives (5%), smoking and unprotected sex (50%).

Identification and differentiation of HPV DNA in all studies were performed using qualitative (PCR) and quantitative (RT PCR, Hybrid Capture II, competitive PCR) methods of detecting the viral genome. The

qualitative method identified virus-positive women, established the frequency of various types of PVI, determined the number of observations with mono- and mixed infection, identified age-related changes, and was also used to assess the antiviral efficacy of PDT. Quantitative research methods were performed to study the activity of the viral genome in stimulating epithelial proliferation, comparing the values of virus concentration with the severity of morphological changes, assessing and monitoring the antiviral efficacy of PDT depending on the genotype, mono- or mixed infection.

The unit of measurement for PCR RT was the logarithm of HPV DNA copies per 10^5 epithelial cells ($\lg/10^5$ cells), Hybrid Capture II – exceeding the clinically significant threshold level (this threshold was estimated as a concentration of 100 thousand genocopies/ml or 1 mg/ml), competitive PCR – the viral load of the 16th type of HPV in various concentrations from 101 to 106 copies per test tube.

A diagnostic test for HPV DNA identification was performed before surgical treatment by collecting not only cervical scrapings, but also material from the mucous membranes of the dome and vaginal walls, in which HPV, a powerful carcinogen and a key factor in disease recurrence, can also persist.

Infection with highly oncogenic HPV genotypes was an indication for PDT of the cervical stump after organ-preserving treatment with 5-ALA, an inducer of endogenous protoporphyrin IX (PPIX) synthesis. Treatment was performed on the 6th-8th day of the menstrual cycle. The time interval between the surgical stage of treatment and PDT was 3-4 weeks and depended on the timing of epithelialization in the treatment area.

Testing for HPV DNA was performed during the first year of observation 3-6-12 months after PDT, the second year – 6-12 months and in subsequent years (upon achieving complete eradication) – once every 3 years.

The antiviral efficacy of PDT was assessed by the following criteria:

- complete effect – complete eradication of HPV DNA, absence of viral load;
- no effect – absence of eradication of all types of HPV DNA and/or decrease in viral load values.

When developing the technique of antiviral PDT of the cervical stump, the need for irradiation of not only the integumentary epithelium of the cervical stump, but also the remaining part of the cervical canal, as well as the vaults and walls of the vagina was taken into account. This approach ensures an effect not only on the resection zone, but also on externally unchanged adjacent tissues.

5-ALA in the form of a 12% gel at a dose of 0.1 mg/cm² was applied topically to the cervical stump,

capturing the vaults and the upper third of the vagina, 4 hours before irradiation. Light regime is not required with this technology.

The diode laser "LFT-630-01-BIOSPEC" (Russia) was used as a source of light radiation. The radiation wavelength was 635 nm, the energy density was 150 J/cm².

PDT of the cervical canal was performed using a flexible mono-fiber quartz light guide with a cylindrical diffuser providing a 360° light matrix and a length corresponding to the length of the endocervix (from 1 to 2 cm). Photodynamic exposure to the vaginal portion of the cervical stump was performed remotely using a light guide with a lens and a light spot diameter of 2-3.5 cm. Irradiation was performed from one position.

The reaction of the cervical epithelium in the photodynamic exposure zone was minor edema and mild tissue hyperemia with the development of film necrosis on days 2-3 without a significant increase in these phenomena in the following days. Epithelialization processes were completed by the 12th-13th day of treatment.

Local administration of 5-ALA gel did not cause adverse or local allergic reactions in any clinical observation; the tolerability of the pharmaceutical was satisfactory. Cutaneous phototoxicity in the form of photodermatitis did not occur in any observation.

Results

A study of the overall prevalence of HPV types, which consists of the sum of the frequency of occurrence of the virus as a monotype and its association with other types, revealed a significant proportion of women (58.9%) infected with type 16 ($p < 0.05$). The remaining types were distributed by frequency of prevalence as follows: 18 – 12.8%, 31 – 10%, 45 – 7%, 33 – 4.5%, 35 – 3.8%, 56 – 2.6%, 58 – 0.2%. In a small number of cases, types 39, 48, 51, 52 were identified (0.1%). The data obtained coincide with large-scale epidemiological studies, which established the leading role in the development of cervical cancer of highly oncogenic HPV genotypes, among which types 16 and 18 are found in 70% of cases.

The number of patients infected with two or more HPV types was significantly higher (62.8%) than with one type (37.2%) ($p = 0.000006$), while the frequency of multiple types of the viral genome did not depend on the severity of pathological changes in the cervix ($p < 0.01$).

In the age category up to 40 years, there were more patients infected with several HPV types (75.6%) than in the group of older women (24.4%). This fact can be associated with higher sexual activity in reproductive age. The frequency of HPV type 16 was almost identical in the group of women of reproductive, premenopausal and postmenopausal ages in 88.2%, 86.7% and 86.3% of observations, respectively, which indicates the leading

etiologic role of HPV type 16 in inducing malignant transformation in the cervical epithelium, regardless of age characteristics.

The antiviral efficacy of PDT of the cervical stump was assessed in all clinical observations (n=100). Complete eradication of HPV DNA was achieved in 94% of patients. In the remaining 6% of observations, the antiviral effect was recorded as eradication of one or two types in case of multiple HPV infection with the dominance of strains 16 and 18, or a significant decrease in the viral load.

The observation periods ranged from 3 to 10 years. Complete eradication of HPV DNA after PDT of the cervical stump was established in 94 (94%) women. A persistent antiviral effect was maintained throughout the observation period in 93 women (93%).

In all clinical observations where there was no complete eradication of HPVt, a 2nd course of PDT was performed with a positive treatment result.

Relapse of the disease was recorded in only one patient (1%) 2 years after completion of treatment for preinvasive cervical cancer, where there was reinfection with HPV type 16 from a sexual partner.

Thus, PDT of the cervical stump with 5-ALA provides a pronounced antiviral effect at the second stage of

treatment of precancerous and initial tumor pathology of the cervix due to the selective accumulation of the photosensitizer in infected cells with their subsequent direct phototoxic and photochemical destruction to the basal and parabasal layers of the epithelium, in which virus replication occurs. Higher rates of eradication of oncogenic HPV types in comparison with methods of therapeutic, surgical and physical effects on the viral genome, the absence of reactivation of infection over a long observation period can be associated with the accumulation of endogenous PPIX by HPV-infected cells with subsequent photodynamic destruction of not only clinical and subclinical, but also latent forms of PVI activity. Targeted "point" destruction of multifocal foci of viral infection, irradiation of not only the vaginal portion of the cervical stump, but also the transition zone with the cervical canal along its entire length, destruction of cells with an integrated form of HPV when antiviral drugs are ineffective, impact on the physical status of the virus and viral load, also minimize the risk of activation of the viral process, which predetermines the success of treatment.

The obtained data on the antiviral effectiveness of PDT are of great interest in light of the proven etiological role of HPV in the development of cervical cancer.

REFERENCES

1. Sung H., Ferlay J., Siegel R.L., Laversanne M., Soerjomataram I., Jemal A. Global cancer statistics 2020: GLOBOCAN estimates of incidence and mortality worldwide for 36 cancers in 185 countries. *CA Cancer J Clin*, 2021, vol.7.
2. Klinyshkova T.V. Strategies of cervical screening: a modern view. *Russian bulletin of obstetrician-gynecologist*, 2023, vol. 23(4), pp. 20-26.
3. Gosvig C.F., Huusom L.D., Andersen K.K., Duun-Henriksen A.K., Frederiksen K., Iftner A. et al. Long-term follow-up of the risk for cervical intraepithelial neoplasia grade 2 or worse in HPV-negative women after conization. *Int J Cancer*, 2015, vol. 137(12), pp. 2927-2933.
4. Belotserkovtseva L.D., Davydov A.I., Shakhlamova M.N., Pankratov V.V. Modern concepts of treatment of patients with cervical intraepithelial neoplasia associated with papillomavirus infection. *Issues of gynecology, obstetrics and perinatology*, 2018. – vol. 17(4), pp. 120-124.
5. Zarochentseva N.V., Djijikhiya L.K., Nabieva V.N. Recurrence of cervical intraepithelial neoplasia after the use of excision treatment methods. *Issues of gynecology, obstetrics and perinatology*, 2020, vol. 19(2), pp. 68-77.
6. Kalliala I., Athanasiou A., Veroniki A.A., Salanti G., Efthimiou O., Raftis N. et al. Incidence and mortality from cervical cancer and other malignancies after treatment of cervical intraepithelial neoplasia: a systematic review and meta-analysis of the literature. *Ann Oncol*, 2020, vol. 31(2), pp. 213-27.
7. Bruno M.T., Cassaro N., Garofalo S., Boemi S. HPV16 persistent infection and recurrent disease after LEEP. *Virology*, 2019, vol. 16(1), pp. 148.
8. Chen L.M., Liu L., Tao X., He Y., Guo L.P., Zhang H.W. et al. Analysis of recurrence and its influencing factors in patients with cervical HSIL within 24 months after LEEP. *Zhonghua Fu Chan Ke Za Zhi*, 2019, vol. 54(8), pp. 534-40.
9. Kulakov V.I., Prilepskaya V.I., Minkina G.N., Rogovskaya S.I. Prevention of cervical cancer. *Handbook for doctors – Kulakov V.I.*, 2007, p. 57.

ЛИТЕРАТУРА

1. Sung H., Ferlay J., Siegel R.L., Laversanne M., Soerjomataram I., Jemal A. Global cancer statistics 2020: GLOBOCAN estimates of incidence and mortality worldwide for 36 cancers in 185 countries // *CA Cancer J Clin*. – 2021. – Vol.7.
2. Клинышкова Т.В. Стратегии цервикального скрининга: современный взгляд // *Российский вестник акушера-гинеколога*. – 2023. – Т.23, № 4. – С. 20-26.
3. Gosvig C.F., Huusom L.D., Andersen K.K., Duun-Henriksen A.K., Frederiksen K., Iftner A. et al. Long-term follow-up of the risk for cervical intraepithelial neoplasia grade 2 or worse in HPV-negative women after conization // *Int J Cancer*. – 2015. – Vol. 137(12). – P. 2927-2933.
4. Белоцерковцева Л.Д., Давыдов А.И., Шахламова М.Н., Панкратов В.В. Современные концепции лечения пациенток с цервикальной интраэпителиальной неоплазией, ассоциированной с папилломавирусной инфекцией // *Вопросы гинекологии, акушерства и перинатологии*. – 2018. – Т.17, №4. – С. 120-124.
5. Зароченцева Н.В., Джиджихия Л.К., Набиева В.Н. Рецидивы цервикальных интраэпителиальных неоплазий после применения эксцизионных методов лечения // *Вопросы гинекологии, акушерства и перинатологии*. – 2020. – Т.19, №2. – С. 68-77.
6. Kalliala I., Athanasiou A., Veroniki A.A., Salanti G., Efthimiou O., Raftis N. et al. Incidence and mortality from cervical cancer and other malignancies after treatment of cervical intraepithelial neoplasia: a systematic review and meta-analysis of the literature // *Ann Oncol*. – 2020. – Vol. 31(2). – P. 213-27.
7. Bruno M.T., Cassaro N., Garofalo S., Boemi S. HPV16 persistent infection and recurrent disease after LEEP // *Virology*. – 2019. – Vol. 16(1). – P. 148.
8. Chen L.M., Liu L., Tao X., He Y., Guo L.P., Zhang H.W. et al. Analysis of recurrence and its influencing factors in patients with cervical HSIL within 24 months after LEEP // *Zhonghua Fu Chan Ke Za Zhi*. – 2019. – Vol. 54(8). – P. 534-40.
9. Кулаков В.И., Прилепская В.И., Минкина Г.Н., Роговская С.И. Профилактика рака шейки матки // *Руководство для врачей – Кулаков В.И.* – 2007. – С. 57.

10. Wu J., Jia Y., Luo M., Duan Z. Analysis of Residual/Recurrent Disease and Its Risk Factors after Loop Electrosurgical Excision Procedure for High-Grade Cervical Intraepithelial Neoplasia. *Gynecol Obstet Invest*, 2016, vol. 81(4), pp. 296-301.
11. Palmer J.E., Raveenscroft S., Eccles K., Crossley J., Dudding N., Smith J.H. et al. Does Hoffman S.R., Le T., Lockhart A., Sanusi A., Dal Santo L., Davis M. et al. Patterns of persistent HPV infection after treatment for cervical intraepithelial neoplasia (CIN): A systematic review. *Int J Cancer*, 2017, vol. 141(1), pp. 8-23.
12. Kong T.W., Son J.H., Chang S.J., Paek J., Lee Y., Ryu H.S. Value of endocervical margin and high-risk human papillomavirus status after conization for high-grade cervical intraepithelial neoplasia, adenocarcinoma in situ, and microinvasive carcinoma of the uterine cervix. *Gynecol Oncol*, 2014, vol. 135(3), pp. 468-73.
13. Zhang H., Zhang T., You Z., Zhang Y. Positive Surgical Margin, HPV Persistence and Expression of Both TPX2 and PD-L1 Are Associated with Persistence/Recurrence of Cervical Intraepithelial Neoplasia after Cervical Conization. *PLoS One*, 2015, vol. 10(12).
14. Poomtavorn Y., Tanprasertkul C., Sammor A., Suwannarurk K., Thaweekul Y. Predictors of Absent High-grade Cervical Intraepithelial Neoplasia (CIN) in Loop Electrosurgical Excision Procedure Specimens of Patients with Colposcopic Directed Biopsy-Confirmed High-Grade CIN. *Asian Pac J Cancer Prev*, 2019, vol. 20(3), pp. 849-54.
15. Uijterwaal M.H., Kocken M., Berkhof J., Bekkers R.L., Verheijen R.H., Helmerhorst T.J., Meijer C.J. Posttreatment assessment of women at risk of developing high-grade cervical disease: proposal for new guidelines based on data from the Netherlands. *J Low Genit Tract Dis*, 2014, vol. 18(4), pp. 338-43.
16. Velentzis L.S., Brotherton J.M.L., Canfell K. Recurrent disease after treatment for cervical pre-cancer: determining whether prophylactic HPV vaccination could play a role in prevention of secondary lesions. *Climacteric*, 2019, vol. 22(6), pp. 596-602.
17. Santesso N., Mustafa R.A., Wiercioch W., Kehar R., Gandhi S., Chen Y., et al. Systematic reviews and meta-analyses of benefits and harms of cryotherapy, LEEP, and cold knife conization to treat cervical intraepithelial neoplasia. *Int J Gynaecol Obstet*, 2016, vol. 132(3), pp. 266-71.
18. D'Alessandro P., Arduino B., Borgo M., Saccone G., Venturella R., Di Cello A. et al. Loop Electrosurgical Excision Procedure versus Cryotherapy in the Treatment of Cervical Intraepithelial Neoplasia: A Systematic Review and Meta-Analysis of Randomized Controlled Trials. *Gynecol Minim Invasive Ther*, 2018, vol. 7(4), pp. 45-51.
19. Fernández-Montolí M.E., Tous S., Medina G., Castellarnau M., García-Tejedor A., de Sanjosé S. Long-term predictors of residual or recurrent cervical intraepithelial neoplasia 2-3 after treatment with a large loop excision of the transformation zone: a retrospective study. *BJOG*, 2020, vol. 127(3), pp. 377-87.
20. «Fluorescent diagnostics and photodynamic therapy in oncology». Edited by V.I. Chissov V.I., Filonenko E.V. Moscow, 2012, pp. 160-173.
10. Wu J., Jia Y., Luo M., Duan Z. Analysis of Residual/Recurrent Disease and Its Risk Factors after Loop Electrosurgical Excision Procedure for High-Grade Cervical Intraepithelial Neoplasia // *Gynecol Obstet Invest*. – 2016. – Vol. 81(4). – P. 296-301.
11. Palmer J.E., Raveenscroft S., Eccles K., Crossley J., Dudding N., Smith J.H. et al. Does Hoffman S.R., Le T., Lockhart A., Sanusi A., Dal Santo L., Davis M. et al. Patterns of persistent HPV infection after treatment for cervical intraepithelial neoplasia (CIN): A systematic review // *Int J Cancer*. – 2017. – Vol. 141(1). – P. 8-23.
12. Kong T.W., Son J.H., Chang S.J., Paek J., Lee Y., Ryu H.S. Value of endocervical margin and high-risk human papillomavirus status after conization for high-grade cervical intraepithelial neoplasia, adenocarcinoma in situ, and microinvasive carcinoma of the uterine cervix // *Gynecol Oncol*. – 2014. – Vol. 135(3). – P. 468-73.
13. Zhang H., Zhang T., You Z., Zhang Y. Positive Surgical Margin, HPV Persistence and Expression of Both TPX2 and PD-L1 Are Associated with Persistence/Recurrence of Cervical Intraepithelial Neoplasia after Cervical Conization // *PLoS One*. – 2015. – Vol. 10(12).
14. Poomtavorn Y., Tanprasertkul C., Sammor A., Suwannarurk K., Thaweekul Y. Predictors of Absent High-grade Cervical Intraepithelial Neoplasia (CIN) in Loop Electrosurgical Excision Procedure Specimens of Patients with Colposcopic Directed Biopsy-Confirmed High-Grade CIN // *Asian Pac J Cancer Prev*. – 2019. – Vol. 20(3). – P. 849-54.
15. Uijterwaal M.H., Kocken M., Berkhof J., Bekkers R.L., Verheijen R.H., Helmerhorst T.J., Meijer C.J. Posttreatment assessment of women at risk of developing high-grade cervical disease: proposal for new guidelines based on data from the Netherlands // *J Low Genit Tract Dis*. – 2014. – Vol. 18(4). – P. 338-43.
16. Velentzis L.S., Brotherton J.M.L., Canfell K. Recurrent disease after treatment for cervical pre-cancer: determining whether prophylactic HPV vaccination could play a role in prevention of secondary lesions // *Climacteric*. – 2019. – Vol. 22(6). – P. 596-602.
17. Santesso N., Mustafa R.A., Wiercioch W., Kehar R., Gandhi S., Chen Y., et al. Systematic reviews and meta-analyses of benefits and harms of cryotherapy, LEEP, and cold knife conization to treat cervical intraepithelial neoplasia // *Int J Gynaecol Obstet*. – 2016. – Vol. 132(3). – P. 266-71.
18. D'Alessandro P., Arduino B., Borgo M., Saccone G., Venturella R., Di Cello A. et al. Loop Electrosurgical Excision Procedure versus Cryotherapy in the Treatment of Cervical Intraepithelial Neoplasia: A Systematic Review and Meta-Analysis of Randomized Controlled Trials // *Gynecol Minim Invasive Ther*. – 2018. – Vol. 7(4). – P. 45-51.
19. Fernández-Montolí M.E., Tous S., Medina G., Castellarnau M., García-Tejedor A., de Sanjosé S. Long-term predictors of residual or recurrent cervical intraepithelial neoplasia 2-3 after treatment with a large loop excision of the transformation zone: a retrospective study // *BJOG*. – 2020. – Vol. 127(3). – P. 377-87.
20. «Флуоресцентная диагностика и фотодинамическая терапия в онкологии». Под редакцией В.И. Чиссова, Е.В. Филоненко. Москва. – 2012. – С. 160-173.


ФОТОСЕНСИБИЛИЗАТОРЫ НОВОГО ПОКОЛЕНИЯ ДЛЯ ФОТОДИНАМИЧЕСКОЙ ТЕРАПИИ



«ФОТОДИТАЗИН®» концентрат для приготовления раствора для инфузий — лекарственное средство (ПУ № ЛС 001246 от 18.05.2012 г.)
«ФОТОДИТАЗИН®» гель — изделие медицинского назначения (ПУ № ФСР 2012/13043 от 03.02.2012 г.)
«ФОТОДИТАГЕЛЬ®» — косметическое средство (ДС ЕАЭС № RU Д-RU.HB42.B.06108/20 от 24.09.2020 г.)

Препараты применяются для флуоресцентной диагностики и фотодинамической терапии злокачественных новообразований, а также патологий неонкологического характера в следующих областях медицины:

- | | |
|------------------------|--------------------|
| ✓ гинекология | ✓ ортопедия |
| ✓ урология | ✓ комбустиология |
| ✓ нейрохирургия | ✓ гнойная хирургия |
| ✓ торакальная хирургия | ✓ дерматология |
| ✓ офтальмология | ✓ косметология |
| ✓ травматология | ✓ стоматология |

 www.fotoditazin.com
www.фотодитазин.рф

ООО «ВЕТА-ГРАНД»

123056, г. Москва, ул. Красина, д. 27, стр. 2
Тел.: +7 (499) 250-40-00, +7 (929) 971-44-46
E-mail: veta-grand@mail.ru



@FOTODITAZIN



@FOTODITAGEL_FDT

